Interplay between mitochondrial dysfunction and epigenetic alterations in environmental linked Parkinson's Disease

by

Adhithiya Charli Manohar Charle

A dissertation submitted to the graduate faculty

in partial fulfillment of the requirements for the degree of

DOCTOR OF PHILOSOPHY

Major: Toxicology

Program of Study Committee:
Anumantha G. Kanthasamy, Major Professor
Arthi Kanthasamy
Guru Rao
Aileen Keating
Eric Underbakke
Dennis Lavrov

The student author, whose presentation of the scholarship herein was approved by the program of study committee, is solely responsible for the content of this dissertation. The Graduate College will ensure this dissertation is globally accessible and will not permit alterations after a degree is conferred.

Iowa State University

Ames, Iowa

2018

To my father V.T.M. Charle and mother Antonyammal,

thank you for being my biggest source of support and inspiration.

Thank you God for all the blessings and for making me who I am.

TABLE OF CONTENTS

LIST OF FIGURES

LIST OF TABLES

ACKNOWLEDGEMENTS

viii

My deepest gratitude goes to my parents V.T.M Charle and A.Antonyammal for their unconditional love, care, support, strength and for being my backbone throughout my academic career and life. I would also like to thank my brother Ajai for being there for me always. They have always stood by my side supporting and encouraging me.

Finally, my complete gratutide and thanks is to God. He has been on my side at very moment in my life providing with the best opportunities, happiness, family and friends. This doctoral diploma has been truly possible only through his blessings and kindness.

ABSTRACT

Parkinson's disease (PD) is a chronic age progressive neurodegenerative disease that affects about 1% of people over the age of 60. The hallmark pathological features of PD is characterized by the loss of 60-70% dopaminergic neurons, formation of Lewy bodies and aggregation of α-synuclein in the *substantia nigra* of the midbrain region. There are multiple factors that contribute to the origin of the disease and also these factors further trigger multiple pathways, thus prominently increasing the risk of incurring PD. Although the etiopathogenesis of PD is not very well understood, growing evidences suggest that mitochondrial dysfunction and oxidative stress play a central role in pathophysiological processes of PD. Many years of research has shown that incessant chronic exposure to several pesticides lead to mitochondria dysfunction and degeneration of dopaminergicc neuronal cells leading to PD. The primary target and goal of my Ph.D thesis was to particularly understand the specific role of mitochondrial complex I class of pesticides in causing dopaminergic neuronal damage. Our recently published study demonstrate that the green house pesticides, tebufenpyrad and pyridaben exposure cause a major adverse effect on mitochondrial function in cell based models of Parkinson's disease. These pesticides are classified as mitochondrial complex I inhibitors and are functionally analogous to the Parkinsonian neurotoxicant rotenone, in terms of target and mode of action. Herein, we demonstrate that acute exposure of tebufenpyrad or pyridaben to the N27 neuronal cells, induced a time dependent loss of mitochondrial function and structural integrity by significant impairment of mitochondrial respiration, ATP production and redox status,suggesting that the pesticides neurotoxicity is associated with mitochondrial dysfunction oxidative damage in dopaminergic neuronal cells. In an effort to understand the molecular mechanisms underlying mitochondria dysfunction mediated apoptotic cell death, we examined the role of PKCδ a pro-apoptotic signaling kinase and

its downstream target of phosphorylation. Our results show that tebufenpyrad exposure to the dopaminergic neuronal cells, lead to the activation of PKCδ in a caspase-3 dependent manner, which was marked by the cleavage of PKCδ and phosphorylation of PKCδ at T505. Importantly, we identified that activated PKCδ further phosphorylateslaminB1 at T575, leading to damage of the nuclear membrane integrity. Moreover the activation of PKCδ, phosphorylation of laminB1 at T575 and laminB1 loss was also observed in the PD substantia nigra brain tissues, but not in the control brains, thereby providing translational relevance to our mechanistic findings. .

To further understand the functional interplay between mitochondrial dysfunction and nuclear events, we examined epigenetic modification mediated acetylation of core histones in dopaminergic neurons.. Exposure of N27 dopaminergic cells to pyridaben induced a dose and time-dependent increase in acetylation of histones H3 and H4. Also, further analysis performed using immuno-fluorescence staining and confocal microscopy revealed the site specific AcH3(K23) and AcH4(K5) up-regulation following rotenone or pyridaben exposure in the N27 neuronal cells. Interestingly, pyridaben or rotenone treated nuclei also demonstrate a nuclear structural defect in the form of topological alteration or chromatin declustering. Furthermore , nuclear morphological change was marked by a time dependent loss of HP-1α, a very well studied marker of heterochromatin, suggesting the mitochondrial dysfunction initiates chromatin remodeling in dopaminergic neuronal cells. . Transgenic dopaminergic neuronal cells generated by TFAM CRISPR/Cas9 knockdown also phenocopy the hyperacetylation of histones H3 and H4 induced mitochondrial pesticides, further providing a stronger evidence for mitochondria driven nuclear architectural changes during neurotoxic pesticide exposure. . Furthermore, the Mitopark transgenic animal model of PD demonstrated progressive acetylation of histones H3 and H4 in a age-dependent manner as well as AcH3(K23) and AcH4(K5)

up-regulation and nuclear declustering morphology. Finally, our data was conclusively confirmed by the analysis of post-mortem human *substantia nigra* tissues, which demonstrated hyperacetylation of H3 and H4 and formation of nuclear declustering in the PD brains. The collecgtive interpretation of these results suggests that histone hyperacetylation is a key epigenetic mechanism in the nigral dopaminergic neuronal cells following mitochondrial dysfunction and neurotoxicity in the neuronal models of PD. Overall, our results suggests that exposure of dopaminergic neuronal cells to mitochondrial complex I inhibiting pesticides leads to accentuated PKCδ kinase activity, nuclear membrane damage and histone hyperacetylation, resulting in apoptotic dopaminergic neuronal cell death. Thus, intervening such molecular mechanisms, merits the development of strategies for diagnosis and drug based treatments for PD.

CHAPTER I : INTRODUCTION

Dissertation Organization

This dissertation is written by following an alternative thesis format and consists of manuscripts in the form of each individual chapters that are being prepared for submission and one of them has been already published. The dissertation thesis flows in an order as given - general introduction, three research papers, general conclusion that will predominantly focus and discuss the overall findings and novel concepts from all the chapters, and finally will end with an acknowledgment. After each corresponding chapter, its corresponding references are listed. But, with respect to the general introduction section, its corresponding references are listed following the general conclusions. Chapter I is general introduction and it provides background information on PD and the role mitochondrial dysfunction and damage and oxidative stress in the pathogenesis of PD. The literature review summarizes the different theories established and studied in PD, focussing the susceptibility of dopamingeric neurons to oxidative stress and cell death. These concepts will be discussed from the perspective of mitochondria and the energy requirements needed for the survival and regular homeostatic functioning of the dopaminergic neuronal cells. Also in this literature review, a completely novel concept related to dopaminergic neuronal susceptibility to mitochondrial complex 1 inhibiting toxicants will be brainstormed and introduced for the first time by following a heuristic approach backed by literature and published evidences.

Chapter II, underlines the neurotoxic potential of tebufenpyrad and pyridaben in causing alterations in mitochondrial dynamics (functional and structural) in the dopaminergic neuronal cell culture model of PD. This manuscript from this chapter

has been published in *Neurotoxicology*. Chapter III, highlights a unique signalling pathway that involves the role of PKCδ functioning as a LaminB1 kinase and mediating apoptotic dopaminergic neuronal cell death post tebufenpyrad exposure. Chapter IV, explores the hyperacetylation of H3 and H4 histones induced by mitochondrial inhibiting pesticides pyridaben and rotenone exposure in dopaminergic neuronal *in vitro* , *ex vivo* and *in vivo* models of PD. Chapter III and IV will be shortly communicated to the *Journal of Cell Biology* and *Nature Neuroscience,* respectively.

This dissertation contains the experimental results obtained by the author during his Doctoral studies under the supervision and guidance of his major professor and principal investigator, Dr. Anumantha G. Kanthasamy at Iowa State University.

Introduction

Parkinson's disease (PD) is identified as a progressive, chronic, age-dependent, neurodegenerative disorder that affects as many as 1.5 million people in the United States. It has also statistical predicted and shown that there about 60,000 newly diagnosed cases each year and than that more than 23,000 die from the disease every year (as reported by the Parkinson's Disease Action Network, National Centre for Disease Statistics).

In this current world with ever increasing population, the occurrence of PD has been predicted to increase by two-fold by the year 2040. PD was first identified and described by James Parkinson in 1817 as the "shaking palsy", and it is the second most common neurodegenerative disorder after Alzheimer's disease (Figure 1.1) (Lees et al., 2009; Shulman et al., 2011). Studies have suggested that men are more prone to develop PD than women (Baldereschi et al., 2000; Van Den Eeden et al., 2003; Wooten et al., 2004). This difference in variation of incurrence of disease

between the two sexes could be attributed to a number of reasons and factors, the main ones surmised could be occupational differences and presence of Estrogen hormone in women.
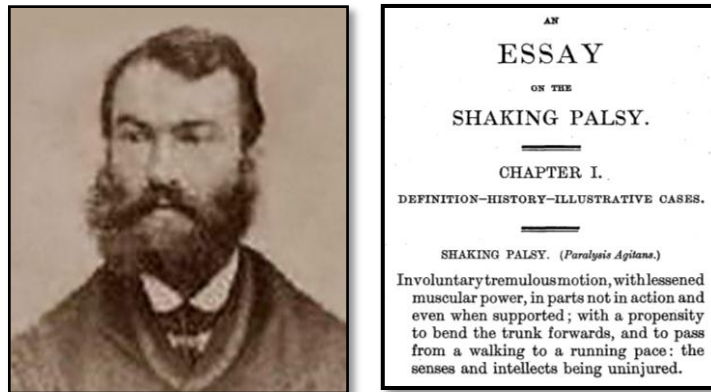
Figure 1.1 Dr. James Parkinson and his book essay on 'Shaking Palsy'.

PD was originally for the very first time identified in Ancient India (4500-1000 B.C) medical system of Ayurveda and it was called as *Kampavata* (literally translated means, tremors due to position or movements). The names for PD in ancient ayurvedic texts are vepathu (shaking, off track or being out of alignment), prevepana (excessive shaking), sirakampa (head tremor), spandin (quivering) and kampana (tremors)(Gourie-Devi et al., 1991; Ovallath and Deepa, 2013).

Pathological hallmarks of PD is vividly identified and declared as the gradual loss of dopaminergic neurons in the *substantia nigra pars compacta* (SNpc) and the formed existence of Lewy bodies which primarily constitutes the aggregated form of α-synuclein and other degradation proteins substances (Dauer and Przedborski, 2003; Werner et al., 2008). By the time the symptoms of the disease begin manifest and reveal itself, around 80% of striatal dopamine is depleted and 60-70% of dopaminergic neurons in the SNpc have already been degenerated and dead. The main clinical feature of PD is severe impairment in motor function such as tremors,

bradykinesia, rigidity, gait difficulty, and postural instability (Thomas and Beal, 2007). These are referred as the classical clinical symptoms of PD. Recently, non-motor symptoms have also been associated with PD. Non-motor symptoms of PD include speech abnormalities, sleep difficulties, constipation, olfactory dysfunction, depression, and cognitive impairment (Beitz, 2014; Chaudhuri and Schapira, 2009; Lotharius and Brundin, 2002).

Given below is the correlative plot comparing clinical symptoms and time progression of PD as taken from (Kalia and Lang, 2015) (Figure 1.2).
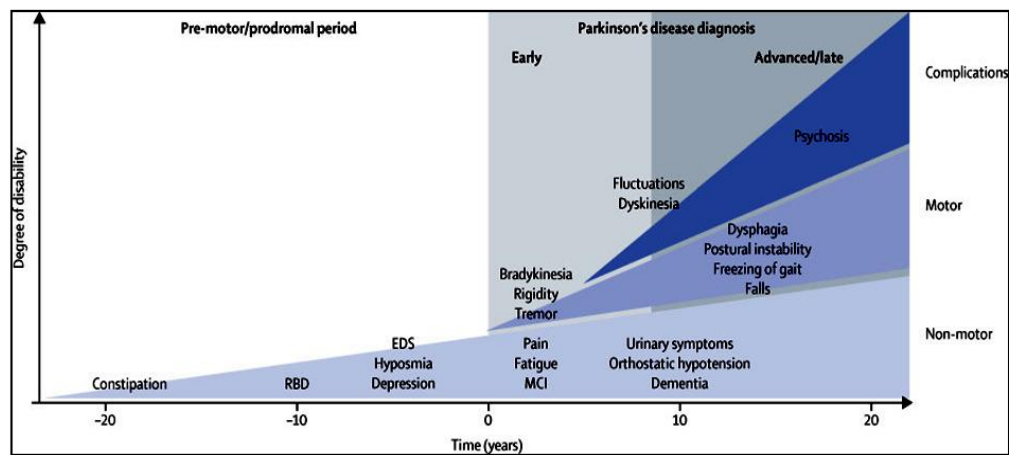
Figure 1.2 Clinical symptoms and time progression of PD.

Although there are many studies and evidences indicating and identifying neuroprotective medications for treatment of PD, each of those are for mitigation of the symptoms of the disease, but there is no permanent cure for complete eradication and stopping of disease progression. The most well accepted and known contributors for the etiopathogenesis of PD are environmental exposures and genetic factors. Some of the major environmental exposures associated with PD are persistent exposure to pesticides and metals, well water and herbicides (Dick et al., 2007; Kanthasamy et al., 2005; Miller, 2007; Priyadarshi et al., 2001; Richardson et al., 2006; Richardson et al., 2005). A few very well studied genetic factors linked to PD are genes such as α-

synuclein, DJ-1, Parkin, LRRK2, PINK1, Uch-L1, FBX07 and ATP13A2. These are also classified commonly as PARK genes (Klein and Westenberger, 2012).

One of the most well characterized causes associated with several neurodegenerative diseases such as PD, are mitochondrial dysfunction and oxidative stress (Banerjee et al., 2009; Bose and Beal, 2016; Lin and Beal, 2006; Thomas and Beal, 2007). The inhibition of complex I by the action and persistent exposures to complex I inhibiting pesticides such as 1-methyl-4-phenylpyridinium (MPP^+) or rotenone is associated with PD pathology and symptoms (Betarbet et al., 2000; Duchen, 2004; Greenamyre et al., 2001; Przedborski and Jackson-Lewis, 1998; Schapira, 2007). Another side of research in PD that is driving a lot of traction in recent years is the aspect of epigenetic changes, in particularly the histone modifications. It has been shown in several studies that epigenetic modifications are believed to be involved in pathogenesis of chronic neurodegenerative diseases such as AD and PD (Klionsky et al., 2016; Mattson, 2003; Migliore and Coppedè, 2009; Song et al., 2010). Hence, identifying a critical signalling mechanism which runs a union and accounts for the interplay between mitochondrial dysfunction and epigenetic modifications, would essentially pave way for a novel line of drug target discovery and treatment strategies for PD.

Our present study seeks to understand and unravel the linked synergism of molecular mechanisms such as pro-apoptotic signalling kinase activation and epigenetic changes involved in the neurotoxic effects induced by the action of mitochondrial targeted complex I inhibiting toxicants exposures in the dopaminergic neuronal cells, thereby implicating etiopathogeneis of PD.

Literature Review

Parkinson's Disease - A mitochondria and gene based investigation

This section of the review will cover the mitochondrial dysfunction mediated susceptibility of dopaminergic neurons to oxidative stress and apoptosis induced by chronic pesticides exposures and the genetics of Parkinson's disease (PD) focussing on the PARK genes.

Why are dopaminergic neurons susceptible to oxidative stress ?

Many years of molecular and epidemiological research shows the validated importance of chronic persistent exposure to environmental toxicants and its is association in causing PD. Even limited exposures have been reported to have initiated self perpetuating cascade of events leading to the death of dopamingeric neurons. One of the first serendipitous cases reported was of the MPTP intoxication, which lead to the development of PD like clinical and pathological features (Langston et al., 1983). The oxidized metabolite of MPTP is MPP^+, is a functionally analogous to paraquat (herbicide) and rotenone (mitochondrial poison used to control fish population in lakes). Also, paraquat and rotenone exposures have shown development of PD in animal models and also in epidemiological studies (Tanner, 1992; Tanner et al., 2011). Epidemiologic studies have also brought out an unusual side which states that drinking coffee and cigarette smoking minimizes the risk of development of PD (Hernán et al., 2002).

One version of the answer to the question of why dopaminergic neurons are susceptible to oxidative stress, is present in one of the most fundamental elements on the planet. Oxygen is the most essential component of eukaryotic organism's

existence, sustenance, growth and development. One of its important biological relevance is linked to redox potential. The human brain composes of 2% of the total body weight but still uses 20% of the total oxygen consumed. Majorly the neurons, specifically the dopaminergic neurons require a big load of the oxygen for its regular homeostatic function (Gandhi and Abramov, 2012; Halliwell, 2006). It has been shown in PD cases and also in animals models of PD post environmental pesticides exposure, that is a tremendous increase in the levels of reactive oxygen species such as superoxides, peroxynitrites, hydrogen peroxides and hydroxyl radicals. Also, there reported cases of rapidly increased free radicals such as O_3, H_2O_2, $^1O_2$ (Anantharam et al., 2002; Cantu et al., 2009; Caudle et al., 2012; Dranka et al., 2010; Hatcher et al., 2007; Kitazawa et al., 2001; Miller, 2007; Przedborski and Ischiropoulos, 2005; Richardson et al., 2006; Sherer et al., 2003). These components of reactive oxygen species interfere violently with the dopamingeric neuronal system of cells post their generation due to pesticides exposure, thereby affecting the neurons in an oxidative stress mediated manner. Another reason for such susceptibility has been theorized based on the phenotypic and functional importance of the dopamingeric neuronal cells, as given below.

- Dopaminergic neurons exhibit high oxygen consumption compared to other cells of the body. They requires 10X more oxygen than a regular bodily cell.

- The size of a dopaminergic neuron is around 1000μm of length on an average with millions of synaptic connections. Thus making a very strong interconnected network using incomparable amounts of energy for neurotransmitter release and signal communications.

- These neurons also have a longer life range as they are non-dividing.

Mitochondrial targeted pesticides and mitochondrial dysfunction

Mitochondrial dysfunction and damage is one of the most critical trigger of pathological and molecular evidences involved in many neurodegenerative disease including Parkinon's disease (PD), Alzheimer's disease (AD), Huntington's disease (HD), Amyotrophic lateral sclerosis (ALS), and many others. The degree and levels of impact on mitochondrial dysfunction depends varies between each diseases. The most common mitochondrial dysfunction factors are as follows.

- Inhibition of mitochondrial respiration

- Loss of ATP production and calcium dysregulation

- Mitochondria membrane damage and potential reduction

- Impaired mitochondrial clearance

- Structural damage of mitochondria

- Imbalance in mitochondrial fission and fusion process

In the pathogenesis of PD, oxidative stress has been strongly implicated in the process of neurodegeneration. Oxidative stress can result from either excessive production of ROS or insufficient antioxidant defense and can potentially damage cellular lipids, proteins, and DNA (Miller et al., 2009). One of the primary targets of the oxidative stress within the cell, is the mitochondria. Postmortem studies have consistently revealed high levels of oxidation of lipids, proteins, and nucleic acids in the SNpc of sporadic PD brains (Alam et al., 1997; Jenner, 2003; Tsang and Chung, 2009). Mitochondrial respiratory chain is the main source of ROS, in particular the hydrogen peroxide and superoxide anions. These ROS can be converted to even more potent ROS, such as the hydroxyl radical and hydroxyl anion in the presence of ferrous iron (Winterbourn, 2008). It is worth mentioning that the level of iron is

significantly increased in the SNpc of PD brains (Dexter et al., 1989). In addition to mitochondria, auto-oxidation of dopamine, a reaction generates superoxide and hydrogen peroxide, as well as reactive dopamine quinones, specifically contributes to the cellular ROS in dopaminergic neurons (Hastings, 2009). This dopamine-dependent oxidative stress could at least partially explain the selective vulnerability of dopaminergic neurons in PD. Another important contributor of oxidative stress is nitric oxide (NO), which is generated by nitric oxide synthase (NOS) (Jenner, 2003). Reaction of ROS with NO produces highly toxic reactive nitrogen species (RNS), such as the peroxynitrite and nitro-tyrosyl radicals (Zhang et al., 2000).

The toxicants or pesticides models of PD demonstrate significant importance of mitochondrial dysfunction mediated by the accentuated generation of oxidative stress factors such as superoxides and reactive oxygen species. The process of oxidative phosphorylation is the key supplier of energy for the dopamingeric neurons, so inhibiting this process triggers loss of mitochondrial function and also leads to the death of these population of neurons. Impairment of complex I activity of the mitochondrial electron transport chain has been detected in the SNpc, skeletal muscle, lymphocytes, and platelets of patients with PD (Barroso et al., 1993; Haas et al., 1995; Mizuno et al., 1989; Schapira et al., 1989). Moreover, inhibition of complex 1 has also lead to initiating further downstream pro-apoptotic signaling cascades such as alterations in mitochondria membrane potential, calcium dysregulation, impaired mitochondrial and other protein clearance, imbalance in mitochondrial fission and fusion process.

MPTP is one of the well studied mitochondrial complex I inhibitor, which has a proven ability to selective degenerate dopamingeric neuronal cells in brain leading

to PD (Langston, 2017; Nicklas et al., 1987; Przedborski and Jackson-Lewis, 1998; Stern et al., 1990). Studies with rotenone another neurotoxic complex I inhibitor, shows significant loss of dopaminergic neurons in cell culture, animal models of PD and epidemiological studies (Betarbet et al., 2000; Greenamyre et al., 2001; Sherer et al., 2007; Testa et al., 2005). On a general perspective, exposure to complex I inhibiting pesticides such as MPTP and rotenone lead to PD and this effect is not confined only to the brain, but also could be seen in platelets (Parker et al., 1989; Schapira et al., 1990a; Schapira et al., 1990b). The action of such complex I inhibitors markedly reduces the production of ATP particularly in the striatum and ventral midbrain (regions that are most sensitive to complex I inhibition). Furthermore, complex 1 inhibition impairs the mitochondrial potential and mitochondrial membrane transport. Thereby, increasing the risk of PD is associated with the exposure to mitochondrial target pesticides such as MPTP and rotenone (Dauer and Przedborski, 2003; Davey and Clark, 1996; Sherer et al., 2003).

Overwhelming evidence suggests that mitochondrial dysfunction is an important contributor to the neurodegenerative process observed in PD (Onyango, 2008; Thomas and Beal, 2007). This section of the review highlights the role and mechanistic action of complex 1 inhibition mediated intracellular signaling perturbation, post exposure to complex 1 inhibitors such as rotenone and MPTP.

Mitochondrial Complex 1 inhibiting pesticides signaling disruption in Parkinson's disease

In the past several years, we and many other labs have shown the neurotoxic potential of complex 1 inhibiting pesticides in dopamingeric neuronal models of PD (Anantharam et al., 2007; Charli et al., 2016; Ghosh et al., 2010; Greenamyre et al.,

2001; Kaul et al., 2003; Parker et al., 1989; Schapira et al., 1989; Sherer et al., 2003). Also earlier studies show that in non-familiar sporadic PD, there is a definite reduction of 15%−30% in the complex I activity (Schapira et al., 1990a).

Rotenone

Among the pesticides associated with PD, rotenone is a well-characterized inhibitor of mitochondrial complex I that occurs naturally in tropical legumes (Cabeza-Arvelaiz and Schiestl, 2012; Greenamyre et al., 2001). Experimentally, in a number of animal models of PD, rotenone has been proven to recapitulate PD pathological features and neurochemical hallmarks (Betarbet et al., 2000; Choi et al., 2011; Greenamyre et al., 2010; Johnson and Bobrovskaya, 2015; Sherer et al., 2003; Testa et al., 2005). In addition to the animal models, recent epidemiological evidence has linked pivotally the chronic rotenone exposure in humans with PD (Spivey, 2011; Tanner et al., 2011).

The pathogenic mechanisms underlying rotenone-induced Parkinsonism are not fully understood, but possibly involve inhibition of mitochondrial respiratory chains and induction of oxidative damage (Johnson and Bobrovskaya, 2015; Sherer et al., 2003). Past couple decades of research has gained traction related to the rotenone-rat model of PD. It has been shown that rotenone treated rats recapitulated several characteristics of PD including hallmark features such as selective loss of dopaminergic neuronal cells in the *substantia nigra* of the mid-brain region, α-synuclein aggregation, Lewy body formation, reduced levels of dopamine and motor deficits (Alam and Schmidt, 2002; Betarbet et al., 2000; Sherer et al., 2003). Recently it was shown that α-synuclein aggregation was promoted upon rotenone exposure in the PC12 cells, in a calcium-dependent manner. In a general circumstance, aggregated α-synuclein gets degraded by autophagy, but exposure to rotenone impaired this

process. Thereby by exacerbating phosphorylation of α-synuclein, leading to aggregation. Also, in this studied rotenone attenuated the phosphorylation of AKT and GSK3β, hence demonstrating rotenone-induced α-synuclein aggregation is mediated by the calcium/GSK3β signaling pathway (Yuan et al., 2015). Recently it has been shown that there is significant biophysical interaction between rotenone and α-synuclein. Using state of the art electron microscopy and Fourier transform infrared spectroscopy, it was confirmed that the direct interaction of α-synuclein and rotenone accentuates the fibrillation of α-synuclein leading to PD like pathology (Silva et al., 2013). Being a complex 1 inhibitor by function, rotenone dysregulates a number of mitochondrial functions that is involved in its maintenance. A recent study in neurons shows that rotenone induced LC3 activation triggers delivery of the damaged mitochondria to autophagosomes and lysosomes, resulting is a mitophagy mechanism. This process is mediated through an direct-interaction between LC3 and externalized cardiolipin (Chu et al., 2014). A similar study by the same group, Charleen Chu, et al., reiterated the importance of cardiolipin and LC3 interaction post rotenone exposure in the SH-SY5Y human cells as a signal for mitophagy (Chu et al., 2013). Another study shows chronic exposure of rotenone to rats induced mitophagy marked by hallmark features of autophagy such as beclin-1 cleavage, LC3 II activation and formation of autophagic vacuoles. This phenomena was protected against by the stereotaxic injection of DJ-1 expression in the *substantia nigra* of the rats. Thereby demonstrating the role of DJ-1 Protecting against Rotenone-Induced Dopaminergic Neuronal toxicity and Apoptosis by Enhancing ERK-Dependent Mitophagy (Gao et al., 2012).

There are a number of studies in past several years that has clearly established the understanding of rotenone toxicity and its relevance to PD. Rotenone (10-50 nM)

exposure on to the postnatal midbrian organotypic slice cultures for weeks of time lead to the demonstration of a dose- and time - dependent loss of the substantia nigra pars compacta neuron processes, significant reduction in complex 1 activity and neuronal loss and decreased expression of the dopaminergic neurons marked by the reduction in the expression of Tyrosine Hydroxylase (TH) protein (Testa et al., 2005). Another study demonstrated in the SK-N-MC human neuroblastoma cells exposed to rotenone (10 nM to 1 μM), established a dose-dependent ATP depletion, oxidative stress, and oxidative damage and hence mediated neuronal cell death (Sherer et al., 2003). Rats treated with rotenone demonstrated a significant behavioural impairment, loss of TH expression in the substantia nigra, decreased parkin, Hsp70 and DJ1 expression. Adding on the initiator and executioner caspases 3 and 9 had a accentuated increase in the rotenone treated rats. These factors were pronounced as a responsible contributors of oxidative damage and neuronal death (Sonia Angeline et al., 2012). rotenone also induces decreases in proteasome activity in the HEK and SK-N-MC cells, due to increased degradation of 20S proteasome components secondary to oxidative damage. The free radicals nitric oxide and peroxynitrites were proven to be the suspected contributors to this proteosome inhibition process (Chou et al., 2010).

MPTP

MPTP is a well known and studied complex 1 inhibitor and its exposure leads to systemically affecting the dopaminergic neuronal cells population in the midbrain region. MPTP first is metabolized by the enzyme MAO-B (monoamine oxidase) to 1-methyl-4-phenyl-2, 3-dihydropyridium ($MPDP^+$), which upon deprotonation generates correspondingly the oxidized product of MPP^+. This makes MPP^+ smoothly

ass through the blood brain barrier and directing it to the mitochondria (Przedborski and Jackson-Lewis, 1998; Smeyne and Jackson-Lewis, 2005). The molecular mechanism of MPTP and its oxidized form of MPP$^+$ has been very well characterized. It plays a very highlighting role in mediating or triggering dopaminergic neuron specific toxicity and apoptotic cell death.

MPTP causes damage to substantia nigra pars compacta dopaminergic neurons as seen in Parkinson's disease (PD). Exposure to MPTP results in its oxidative product MPP$^+$. The MPP$^+$ then accumulates inside the dopaminergic neurons. This process exacerbates the generation of free radicals and superoxides leading to the inhibition of intracellular ATP production. Also the generated superoxides react with nitric oxide resulting in peroxynitrite. Tyrosine hydroxylase is one such proteins that get nitrated by this raction and gets inactive, thereby restricting dopamine production in these neurons. In addition, the peroxynitrites damages the DNA leading to action of PARP (ADP-ribose polymerase), which further contributes to the energy depletion by using up the available ATP. This one of the hallmark mechanistic action of MPTP, making it a potential toxin mitigating the etiology of PD (Langston, 2017; Langston et al., 1983; Langston and Ballard, 1983; Przedborski et al., 2000; Stern et al., 1990). These functional insights and specific action on dopaminergic neuronal cells has been extensively studied using the MPTP animal models of PD.

Recent years of research has hinted a strong linearity between MPTP toxicity and α-synuclein. It has been shown that α-synuclein knock down human neuronal cells and mouse neurons have a resistance developed for the MPTP or its active metabolite MPP$^+$ (Fountaine et al., 2008; Fountaine and Wade-Martins, 2007). A similar trend of protective response against MPTP toxicity and dopaminergic neuronal

cell death is observed in the α-synuclein knockout mice. The negative effect of knocking down α-synuclein is that it results in significant reduction of synaptic vesicles, thereby inhibiting neurotransmitter release and capture (Abeliovich et al., 2000; Murphy et al., 2000). MPTP mediated α-synuclein aggregation formations is also hallmark effect observed in primate and mouse models, eliciting the pathology of PD (Anantharam et al., 2007; Ballard et al., 1985; Dauer and Przedborski, 2003; Kowall et al., 2000; Meredith and Rademacher, 2011; Przedborski and Vila, 2003).

Toxicity induced by MPTP plays a crucial role in triggering downstream events in the apoptotic cell death process. One such signaling is autophagy. It has been observed accumulation of autophagosomes in the post mortem PD brains, which primarily suggested that role of autophagy in the apoptosis of dopaminergic neurons. A similar feature of accumulation of autophagosomes, which significantly contributed to the pathology of PD and was observed in the MPTP mouse model of PD. Adding on it was alos demonstrated that there was an an early decrease in lysosome number in dopaminergic neurons as a result of lysosomal membrane destabilization and cytosolic release of cathepsins (Dehay et al., 2010; Nixon, 2013). One of the very recent interesting findings related to MPTP toxicity and selective loss of midbrain dopaminergic neurons, highlights the importance of MicroRNA-124. levels are found to be decreased in the MPTP treated mice mid brain region tissues. Adding on, MicroRNA-124 regulates apoptosis and autophagy processes by targeting Bcl-2 like protein 11 (Bim) in the mice injected with MPTP, marking its importance in eliciting PD (Wang et al., 2016). The same group also demonstrated that MicroRNA-124 regulates neuronal cellular apoptosis and autophagy in the SH-SY5Y cells treated my MPP$^+$ (100 μM) by protecting the neurons against MPP$^+$ toxicity by the reguilation of

the AMPK/mTOR pathway. This is observed by the increased p-AMPK but decreased p-mTOR levels, post supression of MicroRNA-124 prior to MPP^+ exposure in the dopaminergic neurons (Gong et al., 2016).

Pyridaben

Pyridaben (IUPAC name: 2-tert-butyl-5-[(4-tert-butylphenyl)methylsulfanyl]-4-chloropyridazin-3-one) is a commonly used acaricide for killing populations of mites or ticks in commercial greenhouses (Lümmen, 1998; Schuler et al., 1999). Chemically it is classified as a pyridazinone, whose major application is confined for usage in greenhouses and vineyards (EPA PC Code- 129105). Similar to rotenone, pyridaben has been shown to function as mitochondrial complex I inhibitors (classified by the IRAC-Insecticide Resistance Action Committee). as a mitochondrial complex I inhibitor.

Like rotenone, pyridaben is highly lipophilic and can thus easily cross the blood-brain barrier (Gendelman et al.). Considering the link between complex I dysfunction and PD, pyridaben likely poses a disease risk, but the epidemiological evidence is lacking. We and others have demonstrated that exposure to lower concentrations (nano and micromolar doses) of pyridaben induces significant neurotoxicity in cultured neuronal cells and midbrain organotypic slices (Charli et al., 2015; Sherer et al., 2007). Adding on, the trend in SK-N-MC human neuroblastoma cells has previously been shown as pyridaben has a greater and more potent cytotoxicity than that of rotenone (Sherer et al., 2007). Not just in a neuronal model system, but also in *C. elegans* exposed to rotenone (50 μM, 1 hr) or pyridaben (25 μM, 1 hr) resulted in significant redcution in the mitochondrial respiration , this reinstating the ability of these two pesticides to function as a

mitochndrial functional disruptor (Schuler et al., 1999). Another study of pyridaben-treated C57BL mice found a strong correlations between pyridaben exposure and both DAergic neuron loss and increased α-synuclein immunoreactivity. The authors also performed an RNAseq analysis and reported that mice exposed to certain pesticides exhibited gene expression patterns bearing significant correspondence to pathways that were well-known in human PD cases (Gollamudi et al., 2012). The Washington State Department of Agriculture documented neurological, ocular and gastrointestinal symptoms in farm workers poisoned by an off-target exposure to pyridaben (Calvert et al., 2015). Besides mitochondrial complex I impairment, thus far only a limited number of putative pathogenic mechanisms have been proposed to explain the underlying rotenone- and pyridaben-induced neurotoxicity, including oxidative stress and UPS dysfunction (Chou et al., 2010; Hoglinger et al., 2003; Shamoto-Nagai et al., 2003), which are highly interrelated molecular pathways that could synergistically culminate in neuronal death (Branco et al., 2010; Malkus et al., 2009; Mounsey and Teismann, 2010; Park et al., 2009; Winklhofer and Haass, 2010).

Genetics of PD - A brief walk with the PARK genes

The common approach in understanding the pathology of sporadic PD is focussed on studying about the disease incurred by the influence of exposure to environmental pesticides. But around 5-10 % of PD cases are due to genetic changes or mutations. There are have been many cell and animal based studies that highlights and focusses on the contributions of genetic factors leading to the devlopment of PD. Also, there have been a number of epidemological studies, which has helped in unraveling the role of gene alterations and their association to PD. Some of the PD

genes also known as PARK genes are listed in the figure below as illustrated in (Klein and Westenberger, 2012; Pankratz and Foroud, 2007) (Figure 1.3).

Symbol	Gene locus	Disorder	Inheritance	Gene	Status and remarks	Mode of identification
PARK1	4q21-22	EOPD	AD	SNCA	Confirmed	Linkage analysis
PARK2	6q25.2–q27	EOPD	AR	Parkin	Confirmed	Linkage analysis
PARK3	2p13	Classical PD	AD	Unknown	Unconfirmed; may represent a risk factor; gene not found since first described in 1998	Linkage analysis
PARK4	4q21–q23	EOPD	AD	SNCA	Erroneous locus (identical to PARK1)	Linkage analysis
PARK5	4p13	Classical PD	AD	UCHL1	Unconfirmed (not replicated since described in 1998)	Functional candidate gene approach
PARK6	1p35–p36	EOPD	AR	PINK1	Confirmed	Linkage analysis
PARK7	1p36	EOPD	AR	DJ-1	Confirmed	Linkage analysis
PARK8	12q12	Classical PD	AD	LRRK2	Confirmed; variations in LRRK2 gene include risk-conferring variants and disease-causing mutations	Linkage analysis
PARK9	1p36	Kufor-Rakeb syndrome; atypical PD with dementia, spasticity, and supranuclear gaze palsy	AR	ATP13A2	Confirmed; but complex phenotype that would not be mistaken for early-onset or classical parkinsonism	Linkage analysis
PARK10	1p32	Classical PD	Risk factor	Unknown	Confirmed susceptibility locus; gene unknown since first described in 2002	Linkage analysis
PARK11	2q36-27	Late-onset PD	AD	Unknown; not GIGYF2	Not independently confirmed; possibly represents a risk factor; gene not found since first described in 2002	Linkage analysis
PARK12	Xq21–q25	Classical PD	Risk factor	Unknown	Confirmed susceptibility locus; possibly represents a risk factor; gene not found since first described in 2003	Linkage analysis
PARK13	2p12	Classical PD	AD or risk factor	HTRA2	Unconfirmed	Candidate gene approach
PARK14	22q13.1	Early-onset dystonia-parkinsonism	AR	PLA2G6	Confirmed	Linkage analysis (homozygosity mapping)
PARK15	22q12–q13	Early-onset parkinsonian-pyramidal syndrome	AR	FBX07	Confirmed	Linkage analysis
PARK16	1q32	Classical PD	Risk factor	Unknown	Confirmed susceptibility locus	Genome-wide association studies
PARK17	16q11.2	Classical PD	AD	VPS35	Confirmed	Exome sequencing
PARK18	3q27.1	Classical PD	AD	EIF4G1	Unconfirmed; recently published (Chartier-Harlin et al. 2011)	Linkage analysis

AD, autosomal dominant; AR, autosomal recessive.

Figure 1.3 Summary of PD-associated genes (PARK genes)

First gene that was identified and associated with PD was *SNCA* (PARK 1) which codes for the α-synuclein protein. α-synuclein is one of the major components in the Lewy bodies in patients with familial and sporadic PD (Spillantini et al., 1997). *SNCA* gene is a autosomal dominant contributor of the disease. There have been three identified mutations in the SNCA namely, A53T, A30P and E46K, these were discovered in three distinctly different familial PD patients (Kruger et al., 1998; Polymeropoulos et al., 1997; Zarranz et al., 2004). The affected members of the A53T mutation in the SNCA have similar clinical and pathologic findings to those

with idiopathic PD, including a response to levodopa and the presence of Lewy bodies (Pankratz and Foroud, 2007). Despite many information related to the three mutations of SNCA gene was associated with PD, precise mechanism by which this occurs has not been very well understood.

The next autosomal dominant gene is *LRRK2* gene. This gene is called known as PARK8 and codes for the protein which is a kinase called as Leucine rich repeat kinase 2 (Mata et al., 2006). Many mutations on this gene have been identified in all of its five domains and although size wise it is big, many other additional studies have been performed and more mutations have been identified (Deng et al., 2005; Hulihan et al., 2008; Orr-Urtreger et al., 2007). One of the most common mutations on *LRRK2* that is well studied is the G2019S, this is accounted in almost 1-2% sporadic and 5-6% of familial PD reported cases. The mutations studied on *LRRK2* so far at the molecular level all seem to up-regulate kinase activity and increase autophosphorylation (Smith et al., 2005; West et al., 2005).

First in the list of autosomal recessive PD genes is *parkin.* The mutations in the *parkin* gene was reported with autosomal recessive juvenile parkinsonism in Japanese families (Hattori et al., 1998). Patients with *parkin* mutations have the usual classical PD features and symptoms, but the progression of the disease is slower. The response to levodopa is very well observed and characterised for patients with the *parkin* gene mutations (Lohmann et al., 2003). The parkin protein functions primarily as an E3 ubiquitin ligase and enables the disposal of damaged or misfolded proteins via the ubiquitin-proteosomal system (Leroy et al., 1998; Shimura et al., 2000). Parkin also has a potential role in maintenance of mitochondrial health

and functionally interacts with PINK1 during mitophagy (Deng et al., 2008; Narendra et al., 2008; Rothfuss et al., 2009).

PINK1 is identified in early onset and autosomal recessive cases of PD. The muattions in *PINK1* accounts for 1-7% of early onset or autosomal recessive PD. Patients diagonsed and tested with *PINK1* mutations appear to have clinical features that resemble late onset PD (Hatano et al., 2004; Valente et al., 2004). Many *PINK1* mutations are loss-of-function mutations that affect the kinase domain of the protein, suggesting the important role of the kinase activity of PINK1 in the pathogenesis of PD (Abou-Sleiman et al., 2006). Recent studies have shown that PINK1 functions targeting the upstream of parkin in a common pathway which regulates the selective elimination of damaged mitochondria through mitophagy (Youle and Narendra, 2011). PINK1 localizes to outer membrane of depolarized mitochondria and recruits parkin to initiate mitophagy. In recent years this pathway of PNK1 involved in mitophagy has been well characterized. Also, it has been shown that PINK1 protects against oxidative stress-induced apoptosis (Petit et al., 2005).

Autosomal recessive, early onset PD due to mutations in *DJ-1* has been identified only seven families worldwide. The reported mutations consist of missense mutations, whole exon deletions, a frameshift mutation, and a splice site mutation found in either a homozygous or compound heterozygous state. Through extensive molecular screening, it is estimated that mutations in *DJ-1* account for <1% of all cases of early onset PD (Bonifati et al., 2003a; Bonifati et al., 2003b).

An unseen dimension through the chromosomes

It all started more than three decades ago, when Dr. Langston attended a patient who was identified as a drug abuse case, with excessive use of a drug which was a meperidine analog. This was a by product of 1-methyl-4-phenyl-4-propionoxypiperidine (MPPP) called as 1-methyl-4-phenyl-1,2,3,6-tetrahydropyridine (MPTP). Through many research studies and heuristic and scientific evidences by his group and a few others, it was shown that MPTP was a potent causer of PD, upon chronic exposure (Ballard et al., 1985; Langston et al., 1983; Langston and Ballard, 1983; Lewin, 1984; Stern et al., 1990). A detailed prologue of this cases situation and the behavioural details has also been published recently in Dr. Langston's paper titled, "The MPTP Story" (Langston, 2017). Over the past couple of decades, plethora of groups have almost completely unravelled the mechanistic importance of MPTP exposures that leads to the death of dopamingeric neuronal cells in the *substantia nigra* region of the brain leading to PD (Anantharam et al., 2007; Blesa et al., 2012; Dauer and Przedborski, 2003; Jin et al., 2015; Kanthasamy et al., 1997; Kaul et al., 2003; Nicklas et al., 1987; Przedborski and Jackson-Lewis, 1998; Przedborski and Vila, 2003; Schmidt and Ferger, 2001).

Previously it has been studied and demonstrated that MPTP acts predominantly on the D1 and D2 receptors. It has been also noted that the D1 and D2 receptors are the most susceptible during methamphetamine drug abuse. D1 and D2 receptors are well established and are majorly expressed in the *striatum* and *substantia nigra* region of the brain and are functionally 50% homologous. It has also been characterised that the gene encoding for D1 and D2 receptors are housed in chromosome 5 and 11 respectively (Ares-Santos et al., 2013; Betarbet and

Greenamyre, 2004; Chang et al., 2007; Goulet and Madras, 2000; Grandy et al., 1989; Grandy et al., 1990; Higuchi et al., 1995; Hisahara and Shimohama, 2011; Zhang et al., 2016). MPTP is well known as a mitochondria complex I inhibitor. A recent study has revealed that rotenone, a famous Parkinsonian toxin, also affects the D1 and D2 receptor in the *striatum* and *substantia nigra* region of the brain (Paul et al., 2010). Thus this provides logical interpretation about the receptors that these mitochondrial complex I inhibitors, which are highly lipophilic act on the dopamingeric neuronal cell population in the mid brain region. We and another group have shown that tebufenpyrad and pyridaben, two mitochondrial complex I inhibitors function functions similar to rotenone in affecting the mitochondria by impairing mitochondrial dynamics in the dopaminergic neuronal cells (Charli et al., 2016; Sherer et al., 2007). But, they vary in their potency levels to affect the mitochondria as discussed in Chapter 1 of this thesis. Combining these two proof of concepts and set of evidences, we here in this review extrapolate this idea, to our mitochondrial inhibiting pesticides and complex I inhibitors, tebufenpyrad and pyridaben (Hypothesis - Figure 1.4).
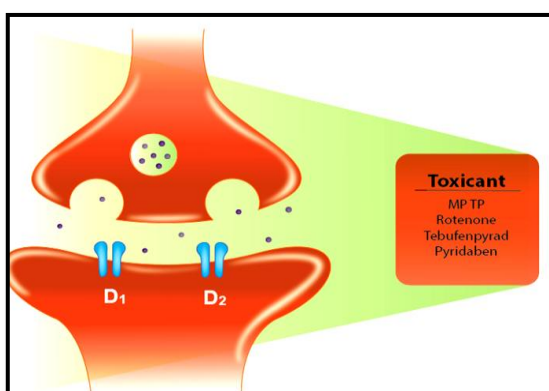
Figure 1.4 Illustrative hypothesis on the action of mitochondrial complex 1 inhibitors on D1 and D2 receptors at the synapse of dopaminergic neurons

There are a set of sixteen PARK genes identified so far that are associated with the pathogenesis and genetics of PD. We have discussed about some of them as mentioned above in this section. The importance pertaining to our line of interest is with regard to their positioning and encasement in the chromosomes. The comparative speculative analysis, understanding the chromosomal location of these PARK genes and the D1 and D2 receptor genes, will enable in surmising and opening clues regarding the susceptibility of dopaminergic neurons to oxidative stress and specific apoptotic cell death. The table below briefly highlights the location of each of those PARK genes and dopamine receptor genes (receptors D1, D2, D3, D4 and D5) in their corresponding chromosomes (Klein and Westenberger, 2012) and (https://www.ncbi.nlm.nih.gov/genome/guide/human/) (Table 1.1).

Table 1.1 PARK genes and dopamine receptor genes in corresponding chromosomes

Chromosome Number	PARK and dopamine receptor genes
1	DJ1, PINK1, ATP13A2
2	G1GYF2, HTRA2
3	D3, EIF4G1
4	D5, SNCA, UCHL
5	D1
6	PARKIN
11	D2, D4, TH
12	LRRK2
16	VPS35
22	PLA2G6, FBX07

As mentioned previously in this review, D1 and D2 receptor specific genes DRD1 and DRD2 are located in chromosomes 5 and 11 respectively. Hence approaching the idea of susceptibility of dopaminergic neurons to oxidative stress mediated by exposure to mitochondrial complex I inhibitors will be the inceptive first step for our novel interpretation (Chromosomes of interest - Figure 1.5).
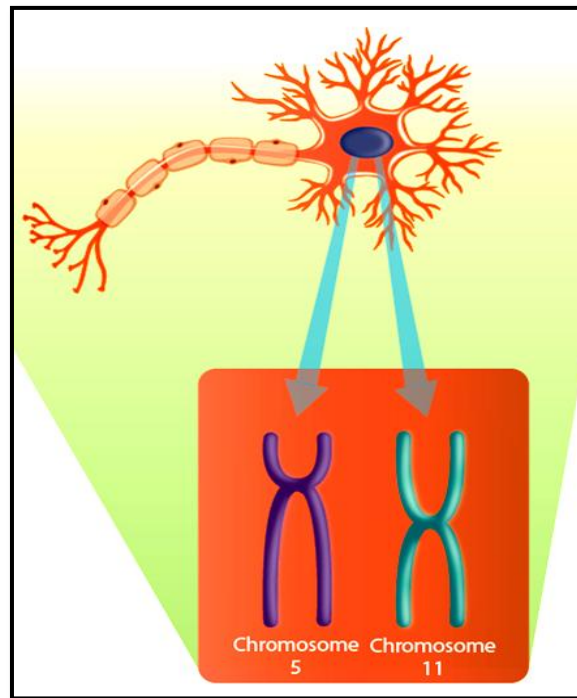
Figure 1.5 Pictorial sketch highlighting chromosomes 5 and 11 of dopaminergic neurons

Chromosome 5 is the fifth largest chromosome of the 23 chromosomal pairs in humans and represents nearly 6% of the total DNA and encodes for approximately 1700 genes (Schmutz et al., 2004). Although D1 receptor gene is encoded in this chromosome, there have been no reported PARK genes encoded in chromosome 5. It has been shown by Dr. Foroud's group after analyzing the combined data from a very large sample of familial PD, that it is unlikely that a PD susceptibility gene is located on chromosome 5 (Foroud et al., 2006). This study consisted of analysis of genomic data from 1238 affected individuals from 569 multiplex PD families,

which were genotyped for a common set of 20 microsatellite markers spanning an 80 cM region on chromosome 5. Even with, such an evidence from this conclusive study performed a decade back, we suspected the role of certain genes in chromosome 5 along with *DRD1,* to be intuitively involved in manipulating dopaminergic neuronal cells susceptible to apoptotic cell death mediated by the mitochondrial dysfunction induced post chronic exposure to complex I inhibitor such as MPTP, rotenone, tebufenpyrad and pyridaben. Below are some genes that really interests us in our investigation on the susceptibility of dopaminergic neurons to oxidative stress mediated through mitochondrial dysfunction.

One such suspected candidate gene short listed on chromosome 5 was *CPLX2.* This encodes for Complexin-2 protein. Complexin-2 is a soluble protein that regulates the activity of SNARE complexes necessary for vesicle fusion. The functional specificity of complexin-2 is dependent on its conformation state (Krishnakumar et al., 2011). It has been shown that complexin-2 knock out in mice results in 60-70% increase in neurotransmitter release (Hu et al., 2002; Reim et al., 2001). A recently in a blood based RNA biomarker study, complexin-1 gene CPLX1, has been associated with the risk of PD in the patients affected by PARK4 mutation (Lahut et al., 2017). It has also been shown recently that protein levels of complexin-1 were elevated in midbrain/brainstem tissue of mice with A53T-SNCA over-expression and of mice with *SNCA*-knockout, thus showing its role in alpha-synuclein pathology (Gispert et al., 2015). These existing results suggests that there might be a potential role for complexin in contributing to the susceptibility of dopaminergic neuronal cell death in terms of interaction and function with respect to alpha-synuclein and regulation of neurotransmitter release.

Another instinctively inferred prospective gene candidate on chromosome 5 is *FASTKD3*. *FASTKD3* encodes for the protein Fas-activated serine/threonine kinase domain 3 (FASTKD3). This protein has recently gained importance as it has been recognised to function as a regulator of mitochondrial gene expression through the function of an unusual RNA-binding domain named RAP (RNA binding domain). Recently it has been shown that in the FASTKD3 knock-out in the human osteosarcoma cells resulted in the increase of mitochondria RNA such as ND2, ND3, COX-2 and CYTB. This study also revealed that the RAP domain of the FASTKD3 is required for the stability of the mitochondrial mRNA and also FASTKD3 is required for efficient COX1 mRNA translation without altering mRNA levels. Thereby suggesting its importance associated with reduced mitochondrial complex IV assembly and activity (Boehm et al., 2016). FASTKD3 consists of a N-terminal mitochondrial targeting domain and the protein's essential responsibility is regulation of cellular respiration (Simarro et al., 2010). Recently, we had verified the presence and abundance of the FASTKD3 gene expression in the control human brains (average recorded from 6 different human brains). This study involves simulation of human brain using the Brain Explorer 2.0 software and we identified prominent expression of FASTKD3 in the *substantia nigra* and *striatum* regions of the human brain (Data not shown). Since this is more of an *insilico*/simulation based analysis, we are working on a more comprehensive study related to PD and expression of *FASTKD3* using human and animal models of PD. These studies and data strongly suggests that FASTKD3 could be one of the most potential target encoded on chromosome 5, that might be susceptible to the mitochondrial inhibiting toxicant

exposure mediated D1 receptor damage, that could make the dopaminergic neurons more susceptible to oxidative stress leading to cell death.

In addition to these genes discussed above, there are several others that might have some relevant role in the susceptibility of dopamingeric neuronal cells to the toxicity and cell death post exposure to mitochondrial complex I inhibiting pesticides. These genes are housed in chromosome 5and have a underlying significant role in protein trafficking, transport, RNA regulation and binding. Their functional roles are summarized as given in the Table 1.2 below.

Table 1.2 Other important genes housed in chromosome 5

Gene	Protein Name	Function
CREBRF	CREB3 regulatory factor	Controller of mTOR and S-Phase cell cycle.
EGR1	Early growth response protein 1	`Transcriptional regulator and neuronal plasticity
FBXL7	F-box/LRR repeat protein 7	Ubiquitin protein ligase complex
EIF4E1B	Eukaryotic translation initiation factor 4E family member 1B	mRNA cap binding
LARP 1	La-related protein 1 or La-ribonucleoprotein 1	Interacts with the 5'mRNA Cap and involved in P-Bodies formation
TBCA	Tubulin Specific Chaperone A	B-Tubulin stability and homeostasis
SNCAIP	Synphilin-1 or α-synuclein interacting protein	Interaction with α-synuclein in the presynaptic region and involved in certain specific neurodegenerative mechanisms

Chromosome 11 is an average size chromosome with the most gene and disease rich density of content found in the human genome. It houses about 2500 genes including the about 1500 protein coding genes and around 800 pseudo genes. The interesting functional responsibility that lights up is that chromosome 11

comprises and houses about 40 % of the total of 856 olfactory receptor genes (Taylor et al., 2006). Despite this chromosome involved in many disease's contribution, it has still not been related or associated to PD or PD-like pathology. One of the noteworthy information in this relevance, is housing of *DRD2* gene on chromosome 11, which is predominantly involved in the dopamine D2 receptor functions. Thus this allows us to suspect the role of *DRD2* and other genes related to it that are housed on chromosome 11, in dopaminergic neuronal cell's precarious susceptibility to mitochondrial complex I inhibitor class of environmental pesticides.

Our heuristically decifered candidate gene of interest on chromosome 11 is, *NRGN. NRGN* is housed on chromosome 11 and it encodes for the protein called Neurogranin. It is a synaptic protein, that belongs to the calmodulin-binding family of proteins. It is expressed primarily in the brain, in particular found in the dendritic spine and majorly participates in the PKC signalling pathway. In the synaptic region functions by regulating the calmodulin availability and orchestrates the binding of calmodulin to Ca^+ and is dynamically involved in neuronal plasticity. In general, PKC mediated phosphorylation lowers the binding ability of neurogranin (Díez-Guerra, 2010). In PD neurogranin has been demonstrated to possess a noteworthy role in terms of synaptic function and cognition. Neurogranin levels were observed to be significantly lowered in the CSF correlating with cognitive impairment in the mild to moderate PD samples compared to the controls (Selnes et al., 2017). In contrary to this finding, an epidemiological study by another group determined the concentration of neurogranin in CSF of PD patients using the enzyme-linked immunosorbent assay. This study consisted of 139 participants (87 controls and 52 Parkinson's disease patients) and they show increased concentrations of neurogranin in the PD

patients in a disease specific manner and was associatively linear to cognitive and motor symptom severity (Bereczki et al., 2017). It was identified by RT-PCR that neurogranin had a direct expressional increase of 2.5 fold upon over-expressing human alpha synuclein in the mouse brain, compared to the control non-transgenic mice. Also, co-immunoprecipitation studies using the superior temporal cortex from humans confirmed interaction between alpha synuclein and neurogranin. Additionally it was noticed that there was decreased interaction between α-synuclein and neurogranin in the brains of patients diagnosed with PD compared to the normal control brains (Koob et al., 2014). Regardless of such available plethora of results and studies, the fundamental role of neurogranin has not been very well characterised with respect to their chromosomal location, gene expression patterns post oxidative stress in the brain during PD, interactive response and link with the PARK genes or other important protein alterations that are observed markedly in the dopaminergic neurons in PD cases. Hence this makes *NRGN* potential component to study the apoptotic pathway simulated and augmented in the dopaminergic neuronal cells mediated to dysfunction D2 receptor dynamics post exposure to mitochondrial complex I specifically targeting compounds/pesticides such as MPTP, rotenone, pyridaben and tebufenpyrad.

The table below summarizes some additional genes and their functional role housed in chromosome 11 (Table 1.3). These genes were spotted and highlighted since, they are involved in a number of protein translational regulation processes, mitochondria function and apoptotic signalling. Hence could be targets of investigation for our future studies.

Table 1.3 Other important genes housed in chromosome 11

Gene	Protein Name	Function
ACAT1	Acetoacetyl-CoA thiolase	Regulator of mitochondrial acetylation
AKIP1	Akinase interacting protein 1	cAMP dependent PK signalling on NF-κB activation cascade
FNBP4	Formin binding protein 4	Formin dependent actin polymerization
VPS26B	Vacuolar protein sorting 26B	Part of the retromer complex along with VPS35 and VPS29
TIMM10	Mitochondrial import inner membrane translocase subunit Tim10	Import and binding of protein within the mitochondrial inner membrane.
TH	Tyrosine Hydroxylase	Conversion of the amino acid L-tyrosine to L-DOPA in the dopaminergic neurons.
SLC17A6	Solute Carrier Family 17	Vesicular glutamate receptor
NFRKB	Nuclear factor related to kappa-B-binding protein	Regulatory component of chromatin remodeling INO80 complex. Modulates the deubiquitinase activity of UCHL5 in the INO80 complex.
MADD	Map kinase activating death domain protein	Marker of apoptotic cell death

Although in this review we have predicted and suspected that there are other genes part from the PARK genes that might be involved in the pathogenesis and progression of PD by targeting the increasing susceptibility of the D2 and D2 receptors to mitochondrial complex I inhibitor class of pesticides or toxicants. This newly moulded concept of an idea needs further data based validation, which is exactly our current work in progress.

The importance and role of chromosomes in PD pathology and symptoms has not been well studied. This may be due to the complexity and the unchartered territory in the dark world of the chromosomes containing numerous functional genes, pseudo genes and other components such as introns, exons and regulators of gene expression.

Thus these unanswered questions made us culminate and incept an idea in terms of D1 and D2 receptor genes DRD1 and DRD2 respectively, for studying the susceptibility of dopaminegric neuronal cells to oxidative stress induced by mitochondrial complex I inhibiting pesticides/toxicants such as MPTP and rotenone.

Further these ideas were extrapolated and predicted for exposures to neurotoxic environmental pesticides suchs such as tebufenpyrad and pyridaben in the dopaminergic neuronal cells. Additionally, our present review further unravels the importance and functional relevance of certain genes (encoding for specific proteins) based on their contributions and role in mitochondrial health dynamics, protein trafficking, protein disposal machinery and synpatic functions. This novel approach enables us to understand the side of the disease from a newer but yet less ventured resaerch and diagnostic perspective.

We are currently working on testing some of the predicted genes on chromosome 5 and 11, as their functions had been discussed above regarding their locations on correspondingly housed chromosomes. Our current undergoing studies might open up new novel pathways with respect to the mitochondrial dysfunction and its earlier detection in PD, hence that will facilitate in the contribution towards discovery of intervening drug targets and biomarker inventions and also early diagnostic tools for the early diagnose of PD.

CHAPTER II : ALTERATIONS IN MITOCHONDRIAL DYNAMICS INDUCED BY TEBUFENPYRAD AND PYRIDABEN IN A DOPAMINERGIC NEURONAL CELL CULTURE MODEL

Adhithiya Charli, Huajun Jin, Vellareddy Anantharam, Arthi Kanthasamy and

Anumantha G. Kanthasamy[*]

Parkinson's Disorder Research Laboratory, Iowa Center for Advanced Neurotoxicology,

Department of Biomedical Sciences, Iowa State University, Ames, IA 50011

*To whom correspondence should be addressed: Dept. of Biomedical Sciences, Iowa State University, 2062 College of Veterinary Medicine Building, Ames, IA 50011. Tel: 515-294-2516; Fax: 515-294-2315; Email: akanthas@iastate.edu

Keywords: Tebufenpyrad, pyridaben, pesticides, neurotoxicity, mitochondrial dysfunction, oxidative stress, Seahorse Bioanalyzer.

The abbreviations used are:

3-(4,5-dimethylthiazol-2-yl)-5-(3-carboxymethoxyphenyl)-2-(4-sulfophenyl)-2H-tetrazolium (MTS) ; reactive oxygen species (ROS), Superoxides (SOX), 5-(and-6)-chloromethyl-2′,7′-dichlorodihydrofluorescein diacetate (CM-H$_2$DCFDA), carbonyl cyanide 4-trifluoromethoxy-phenylhydrazone (FCCP), Adenosine triphosphate (ATP) and oxygen consumption rate (OCR).

Abstract

Tebufenpyrad and pyridaben are two agro-chemically important acaricides that function like the known mitochondrial toxicant rotenone. Although these two compounds have been commonly used to kill populations of mites and ticks in commercial greenhouses, their neurotoxic profiles remain largely unknown. Therefore, we investigated the effects of these two pesticides on mitochondrial structure and function in an *in vitro* cell culture model using the Seahorse bioanalyzer and confocal fluorescence imaging. The effects were compared with rotenone. Exposing rat dopaminergic neuronal cells (N27 cells) to tebufenpyrad and pyridaben for 3 h induced dose-dependent cell death with an EC_{50} of 3.98 μM and 3.77 μM, respectively. Also, tebufenpyrad and pyridaben (3 μM) exposure induced reactive oxygen species (ROS) generation and m-aconitase damage, suggesting that the pesticide toxicity is associated with oxidative damage. Morphometric image analysis with the MitoTracker red fluorescent probe indicated that tebufenpyrad and pyridaben, as well as rotenone, caused abnormalities in mitochondrial morphology, including reduced mitochondrial length and circularity. Functional bioenergetic experiments using the Seahorse XF96 analyzer revealed that tebufenpyrad and pyridaben very rapidly suppressed the basal mitochondrial oxygen consumption rate similar to that of rotenone. Further analysis of bioenergetic curves also revealed dose-dependent decreases in ATP-linked respiration and respiratory capacity. The luminescence-based ATP measurement further confirmed that pesticide-induced mitochondrial inhibition of respiration is accompanied by the loss of cellular ATP. Collectively, our results suggest that exposure to the pesticides tebufenpyrad and pyridaben induces neurotoxicity by rapidly initiating mitochondrial dysfunction and

oxidative damage in dopaminergic neuronal cells. Our findings also reveal that monitoring the kinetics of mitochondrial respiration with Seahorse could be used as an early neurotoxicological high-throughput index for assessing the risk that pesticides pose to the dopaminergic neuronal system.

Introduction

A growing body of evidence suggests that exposure to neurotoxic pesticides in agricultural settings is associated with increased risk for developing Parkinson's disease (PD) (Baltazar et al., 2014; Freire and Koifman, 2012; Parron et al., 2011). Among the pesticides associated with PD, rotenone is a well-characterized inhibitor of mitochondrial complex I that occurs naturally in tropical legumes (Cabeza-Arvelaiz and Schiestl, 2012; Greenamyre et al., 2001). Experimentally, exposure to rotenone was shown to reliably produce Parkinson's-like pathology in various animal models of PD (Betarbet et al., 2000; Greenamyre et al., 2010; Johnson and Bobrovskaya, 2015; Testa et al., 2005). Furthermore, recent epidemiological evidence has linked human rotenone exposure with PD (Spivey, 2011; Tanner et al., 2011).

The pathogenic mechanisms underlying rotenone-induced Parkinsonism are not fully understood, but possibly involve inhibition of mitochondrial respiratory chains and induction of oxidative damage (Johnson and Bobrovskaya, 2015; Sherer et al., 2003). Mitochondria are pivotal to the homeostatic functioning of cells and thus the central nervous system. The primary role of mitochondria is to provide energy to cells *via* oxidative phosphorylation (Chan, 2006; Hoppins et al., 2007; Jin et al., 2014a; Zhang and Chan, 2007). Some of the critical biochemical abnormalities resulting from mitochondrial dysfunction are increased generation of reactive oxygen species (ROS), loss of ATP production during cellular respiration and impaired Ca^{2+}

ion channels (Schapira, 2007; Winklhofer and Haass, 2010). Neurotoxic stress also induces structural damage to mitochondria including mitochondrial fragmentation and mitophagy (Lin et al., 2012; Lin and Beal, 2006).

Tebufenpyrad (IUPAC name: N-[(4-tert-butylphenyl)methyl]-4-chloro-5-ethyl-2-methylpyrazole-3-carboxamide) and pyridaben (IUPAC name: 2-tert-butyl-5-[(4-tert-butylphenyl)methylsulfanyl]-4-chloropyridazin-3-one) are common acaricides used to kill populations of mites and ticks in commercial greenhouses. Tebufenpyrad is chemically classified as a pyrazole carboxyamide, which is registered for use in greenhouses for the protection of ornamental plants (EPA PC Code- 090102). Pyridaben is chemically classified as a pyridazinone, whose major application is in greenhouses and vineyards (EPA PC Code- 129105). Similar to rotenone, tebufenpyrad and pyridaben have been shown to function as mitochondrial complex I inhibitors (classified by the IRAC-Insecticide Resistance Action Committee - http://www.irac-online.org/modes-of-action/). Although their intended mode of action and target toxicity are similar to those of rotenone, both tebufenpyrad and pyridaben have not been studied in detail with respect to their neurotoxicity. Therefore, in this study, we evaluated the neurotoxic effects of tebufenpyrad and pyridaben in rat dopaminergic neuronal cells, with particular emphasis on their effects on mitochondrial dynamics and their roles in dopaminergic neuronal cell death.

Materials and Methods

Chemicals and Reagents. We purchased tebufenpyrad (96% purity) from AK Scientific Inc. (Union City, CA), pyridaben (99.1% purity) from Chem Services (West Chester, PA), and rotenone (95-98% purity) and hydrogen peroxide (30 wt. % in H_2O) from Sigma (St. Louis, MO). DMSO was purchased from Fisher Scientific (Fair

Law, NJ). We purchased RPMI 1640 media, fetal bovine serum (FBS), L-glutamine, penicillin, streptomycin and Sytox green nucleic acid fluorescence stain from Molecular Probes (Eugene, OR), the Muse® Count &Viability Assay Kit (Catalog # MCH100102) from EMD Millipore (Billerica, MA), and the 5-(and-6)-chloromethyl-2′,7′-dichlorodihydrofluorescein diacetate (CM-H_2DCFDA) fluorescent probe and MitoTracker red CMXROS and MitoTracker green dyes from Invitrogen (Carlsbad, CA). The Cell Titer 96® AQueous Non-Radioactive Cell Proliferation assay kit and Cell Titer Glo Luminescent Cell Viability assay kit were bought from Promega (Madison, WI). The Aconitase assay kit was purchased from Abcam (Cambridge, MA). Oligomycin, hydrogen peroxide, carbonyl cyanide 4-trifluoromethoxy-phenylhydrazone (FCCP) and antimycin A were purchased from Sigma Aldrich (St. Louis, MO), and the Seahorse FluxPak calibration solution was bought from Seahorse Biosciences (Billerica, MA).

Cell culture and treatment paradigm. The rat immortalized mesencephalic dopaminergic neuronal cell line ($1RB_3AN_{27}$, also known as N27 cells) was a kind gift from Dr. Kedar N. Prasad (University of Colorado Health Sciences Center, Denver, CO). These N27 cells have the potential to differentiate and produce dopamine in culture when exposed to a suitable cAMP triggering agent, and once the cells are differentiated they possess increased tyrosine hydroxylase (TH) expression and dopamine levels (Adams et al., 1996; Zhang et al., 2007). In this study, undifferentiated cells were grown in RPMI 1640 medium containing 10% FBS, 2 mM L-glutamine, 50 units of penicillin, and 50 µg/ml streptomycin, as described previously (Anantharam et al., 2002; Jin et al., 2011c; Prasad et al., 1998). In general, cells were plated in a tissue culture plate or flask in accordance to the experimental

requirements and was cultured overnight in a humidified atmosphere of 5% CO_2 at 37°C. The cell density plated for each experiment has been provided in the methods section. The cells were treated with the specified concentrations of tebufenpyrad and pyridaben for 0-3 h in serum-free RPMI media. For all experiments with N27 cells, treatments were performed when the cells were 65-70% confluent. The pesticides tebufenpyrad and pyridaben are lipophilic in nature and are hence dissolved in DMSO. In the ROS generation and aconitase activity experiments, cells were treated with 100 μM H_2O_2 for 45 min as a positive control. Similarly, 1 μM rotenone for 3 h was used as a positive control in the SYTOX Green assay, Muse Annexin V/7-AAD assay, ATP production, and the mitochondrial dysfunction and damage studies.

MTS cell viability assays. Cell viability was measured using the Cell Titer 96® AQueous Non-Radioactive Cell Proliferation (MTS assay) kit from Promega as described previously (Jin et al., 2014b). Briefly, N27 cells were plated at 0.8×10^4 cells/well in 96-well plates one day before treatment. The next day cells were treated in serum-free RPMI media with different concentrations of tebufenpyrad or pyridaben (0, 1, 2, 3, 5, 7, 9, 10 and 30 μM) for a time period of 3 h. Following treatment, 10 μl of MTS solution reagent mix was added to each plate well and incubated at 37°C for 45 min. At the end of incubation, the formazan crystals that formed in the live cells were dissolved by adding 25 μl of DMSO to each well. Finally, readings were taken at a wavelength of 490 nm and another reference reading for each well was taken at 670 nm to eliminate background. The data were then plotted as a dose-response curve (depicting the EC_{50}) using Prism 4.0 (GraphPad Software, San Diego, CA).

SYTOX Green cytotoxicity assays. Cell death after exposing the N27 cells to 3 μM of tebufenpyrad or pyridaben was determined using the SYTOX Green cytotoxicity,

as previously described (Jin et al., 2011a; Latchoumycandane et al., 2011a). The SYTOX green dye only permits dead cells to produce green fluorescence. In brief, N27 cells were grown in 24-well cell culture plates (4 x 10^4 cells/well) and treated with 3 μM of tebufenpyrad or pyridaben along with 1 μM SYTOX Green dye for 3 h. Fluorescent images were then taken using fluorescence microscopy (Cytation 3, Biotek, Winooski, VT) that was coupled with a 40X objective and Gen5 imaging software. For further validation, the green fluorescence was quantitatively measured at an excitation wavelength of 485 nm and an emission wavelength of 538 nm with the use of a fluorescence microplate reader (Cytation3, Biotek).

Annexin V/7-AAD apoptosis assay. The cytotoxic effects of tebufenpyrad and pyridaben on N27 cells were also analyzed with the Annexin V/7-AAD assays using the Muse® Annexin V and Dead Cell Assay kit from Millipore (Billerica, MA). Annexin V, which is membrane permeable, labels all cells containing a nucleus. The second component of the kit is 7-AAD, which stains the membrane of the cells that have been compromised and are dying or dead. This synergistic functioning of the two components differentiates between cell populations based on their health (Khan et al., 2012; Marusiak et al., 2014). The assay was performed according to manufacturer's protocol. Briefly, N27 cells were grown in 6-well culture plates (3 x 10^5 cells/well) and treated with 3 μM of tebufenpyrad or pyridaben for 3 h. Following the treatment, cells were pelleted and then resuspended in 100 μl of complete growing media, followed by adding 100 μl of Muse Annexin V and Dead Cell Reagent to each tube. The tubes were mixed thoroughly and then incubated at room temperature for 20 min without light exposure. After incubation, the tubes were read individually using

Muse™ Cell Analyzer (0500-3115, Millipore). Default gate settings were used to distinguish the cells in the live, early-apoptotic, late-apoptotic and dead categories.

ATP production measurement. ATP was measured using the Cell Titer Glo Luminescent Cell Viability assay kit, according to the manufacturer's instructions. N27 cells (0.8 x 10^4 cells/well) were seeded in a black opaque-walled 96-well cell culture plate with transparent top and bottom. Following the treatments with tebufenpyrad (3 μM) and pyridaben (3 μM) for 3 h, the plates were equilibrated for 15 min at room temperature. Once this process was completed, an equal volume of CellTiter-Glo ®Reagent was added to match the volume of media in each well. The plates were uniformly mixed to lyse the cells and were incubated at room temperature for 30 min to stabilize the luminescence signal, which was recorded by setting the integration time to around 0.25-1 sec per well.

Measurement of ROS generation. ROS generation was measured using the CM-H_2DCFDA fluorescent probe as previously described (Ghosh et al., 2007; Gordon et al., 2010) with minor modifications. The N27 cells were grown (0.8 x 10^4 cells/well) in a 96-well culture plate and the treatments were carried out with tebufenpyrad (3 μM) and pyridaben (3 μM) for 3 h. Briefly, CM-H_2DCFDA was added at a final concentration of 10 μM into each treatment well to incubate with the toxicants. By following this procedure, the dye gets completely bound to the generated ROS and loaded into the cell. After the treatment, cells were washed with Hank's Buffered Salt Solution (HBSS) containing calcium and magnesium to remove the toxicants and excess dye. Fluorescence was measured using a fluorescence plate reader (excitation 488 nm and emission 515 nm).

Aconitase activity assay. An aconitase activity assay kit from Abcam was used to measure mitochondrial aconitase (m-aconitase) activity levels. N27 cells were grown (1 x 10^6 cells/flask) in a T25 cell culture flask and were exposed to tebufenpyrad (3 µM) and pyridaben (3 µM) for 3 h. In brief, cells were collected after treatment and resuspended in the supplied assay buffer on ice followed by centrifugation at 2000 x g for 5 min at 4°C. The resulting supernatant was collected and further centrifuged at 20,000 x g for 15 min to collect the mitochondrial fraction. The pellet was thoroughly mixed with 100 µl of ice-cold assay buffer and sonicated for 15 sec at 4°C. The lysate was then used to measure aconitase activity as per the manufacturer's protocol. Measurements were made at a wavelength of 450 nm using a microplate reader. The OD values were normalized to the protein concentration of each sample and the results were expressed as percentage control.

Mitochondrial dysfunction assay. Cells were grown (4 x 10^4 cells/well) in a 24-well culture plate and were treated with tebufenpyrad (3 µM) and pyridaben (3 µM) for 3 h. After treatment, the media was removed and 300 µl of 200 nM MitoTracker green dye diluted in serum-free RPMI media was added into each well and incubated at 37°C for 15 min. Following incubation, a microplate reading was taken at an excitation wavelength of 485 nm and an emission wavelength of 520 nm.

Mitochondria structural depiction assay / Imaging. N27 cells were grown (4 x 10^4 cells/well) in a 24-well culture plate on coverslips pre-coated with poly-D-lysine. Following treatment with tebufenpyrad (3 µM) and pyridaben (3 µM) for 3 h, cells were washed carefully once with PBS. Then 300 µl of 200 nM CMXROS MitoTracker red dye diluted in serum-free RPMI media was added and incubated at 37°C for 12 min. After incubation, wells were gently washed with PBS 3 to 5 times

and then fixed in 4% paraformaldehyde (PFA) for 30 min. The wells were washed with PBS three times and the coverslips were mounted onto glass slides for microscopic imaging using a confocal microscope (model TE2000-U, Nikon) with 60X magnification. Image analysis used in the mitochondria structural depiction assays was performed using ImageJ. Quantification of mitochondrial parameters such as mitochondrial length and degree of circularity was accomplished using a macro text file plug-in for ImageJ (Dagda et al., 2009). For analyzing the images, 6 images per group were quantified and two separate experiments were performed.

Measurement of mitochondrial oxygen consumption by Seahorse XF96 analyzer. Mitochondrial oxygen consumption was measured using a Seahorse XF96 Extracellular Flux analyzer (Seahorse Bioscience, North Billerica, MA) at the Dr. Balaraman Kalyanaraman's laboratory (Medical College of Wisconsin, Milwaukee) as described previously (Dranka et al., 2011; Dranka et al., 2012). The Seahorse XF96 Extracellular Flux analyzer is a sensitive, high-throughput instrument that makes real-time measurements of respiration rates of cells with or without oxidative stress. In our studies, we employed two different strategies to monitor the effects of tebufenpyrad and pyridaben on oxygen consumption rates (OCR) in N27 cells. One was the direct injection strategy to test the instantaneous effect on oxygen consumption rates (OCR) in N27 cells immediately after tebufenpyrad and pyridaben injections, and the other was to analyze the mitochondrial bioenergetics of N27 cells after incubation with tebufenpyrad and pyridaben by measuring the OCR at different stages. N27 cells were seeded at a density of 2×10^4 per well into a V7-PS culture plate and incubated overnight in 5% CO_2 at 37°C. For the direct injection method, the Seahorse Flux Pak cartridge was equilibrated using the equilibration buffer for one hour and then

carefully loaded with different concentrations of tebufenpyrad or pyridaben (0.5, 1, 3 and 6 µM). Following this process, the V7-PS culture plate cover was replaced with the Flux Pak cartridge and the plate was loaded into the Seahorse XF96 analyzer for direct injection. For the mitochondrial bioenergetics method, cells were first treated with different concentrations of tebufenpyrad or pyridaben (0.5, 1, 3, 6 µM) for 3 h in 5% CO_2 at 37°C. During this time, the Seahorse FluxPak cartridge was equilibrated and the corresponding injection ports were loaded with the mito-stressor agents oligomycin (1 µg/ml), FCCP (1 µM) and antimycin A (10 µM). Once the mito-stressors were loaded in their corresponding position in the cartridge, the treated plate was introduced into the Seahorse analyzer covered with the Flux Pak cartridge. The analyzer was then programmed to measure the basal OCR readouts in five specified time intervals before progressing to inject the mito-stressors. These stressors were injected after every three cycles of measuring OCR (Fig. 7A). Further calculations of ATP-linked respiration and respiratory capacity were performed as described (Dranka et al., 2011; Dranka et al., 2012).

Statistical analysis. All statistical data analyses were performed using Prism 4.0 (GraphPad Software, San Diego, CA). The EC50 for each of the two pesticides tebufenpyrad and pyridaben was determined from the dose-response curve generated by Prism 4.0. Data were analyzed using one-way ANOVA with the Tukey-Kramer post-test for comparing all treatment groups with that of the control. Differences with $p < 0.05$ were considered significant.

Results

Tebufenpyrad and pyridaben treatments elicit significant neurotoxic response in the N27 dopaminergic neuronal cells

The effect of the two pesticides tebufenpyrad and pyridaben on the viability of N27 dopaminergic neuronal cells was evaluated by the MTS cell viability assay. An N27 culture comprises a homogenous population of TH-positive dopaminergic neuronal cells derived from the rat's mesencephalic region and are widely used as a versatile model of dopaminergic neurodegeneration (Anantharam et al., 2002; Harischandra et al., 2014a; Levesque et al., 2010). To generate dose-response curves, N27 cells were treated with increasing concentrations of tebufenpyrad or pyridaben (0-30 µM) for time periods of 3 h each. These 3-h treatments with tebufenpyrad or pyridaben resulted in concentration-dependent cytotoxicity in N27 cells (Figs. 1A-B). It is noteworthy that these two pesticides have similar neurotoxic effects on N27 cells with EC_{50} values of 3.98 ± 0.21 µM (95% CI) and 3.77 ± 0.21 µM (95% CI) for tebufenpyrad and pyridaben, respectively.

To further substantiate the cytotoxic effects of the two pesticides on N27 cells, we treated N27 cells with 3 µM of tebufenpyrad or pyridaben for 3 h and measured cell death using the SYTOX Green cytotoxicity and Muse Annexin V/7AAD assays. As a positive control, we treated N27 cells with 1 µM rotenone for 3 h. The SYTOX Green dye is a nuclear-specific probe that is excluded from cells with intact membranes, while it binds the nucleic acids of cells that have damaged membranes (Asaithambi et al., 2014; Roth et al., 1997; Sherer et al., 2003). Similar to rotenone, exposure to tebufenpyrad or pyridaben led to significantly greater toxicity in N27 cells than in control cells (Fig. 1C). Consistent with this, quantification of cell

cytotoxicity using the Muse Annexin V/7AAD assay revealed significant loss of cell viability occurring in the cells treated with tebufenpyrad or pyridaben compared to the control cells (Fig. 1D). A similar toxicity was observed with the rotenone-treated positive control cells. Moreover, the Muse Annexin V/7AAD assay also showed that cells undergo apoptotic cell (Fig. 1D). Collectively, these data clearly indicate that tebufenpyrad and pyridaben induce neurotoxic effects in N27 dopaminergic neuronal cells. Based on these results, we chose a working concentration of 3 μM for both tebufenpyrad and pyridaben treatments in subsequent experiments.

Tebufenpyrad and pyridaben induce oxidative damage

To explore the role of oxidative stress in tebufenpyrad- and pyridaben-induced neurotoxicity, we first examined the effect of tebufenpyrad and pyridaben on intracellular ROS generation. N27 cells were treated with vehicle, tebufenpyrad or pyridaben for 30, 60, and 180 min and the rate of ROS generation was quantified using the CM-H2DCFDA fluorescent probe. Hydrogen peroxide was used as a positive control in the experiment. Both tebufenpyrad and pyridaben, at a concentration of 3 μM, induced a time-dependent increase in ROS production, starting as early as 30 min (Figs. 2A-B). At 180 min, both pesticides induced approximately a 3-fold increase of ROS levels. These results suggest that ROS generation might be an early biochemical change that precedes cell death following tebufenpyrad and pyridaben exposure in dopaminergic neuronal cells. To further characterize the involvement of oxidative stress in tebufenpyrad and pyridaben neurotoxicity, we performed m-aconitase activity assays. Aconitase is a mitochondrial protein that catalyzes the conversion of citrate to isocitrate in the TCA cycle. This enzyme complex has an iron sulfur cluster that is very sensitive to oxidative damage

(Ghosh et al., 2010; Kalyanaraman, 2013). The loss of aconitase enzyme activity is commonly used as a measure of mitochondrial oxidative damage (Cantu et al., 2009). We observed significant reductions of m-aconitase activity in cells treated with tebufenpyrad and pyridaben (Fig. 3). Hydrogen peroxide, as a positive control, produced similar results. Together, these data indicate that tebufenpyrad and pyridaben induce oxidative damage to mitochondria in dopaminergic cells.

Tebufenpyrad and pyridaben significantly induce mitochondrial structural damage and dysfunction in dopaminergic neuronal cells

To gain further insight into the mechanisms underlying tebufenpyrad- and pyridaben-induced dopaminergic cell death, we studied their effects on mitochondrial function. We first monitored mitochondrial function by using the cell-permeable mitochondria-selective dye MitoTracker green, which passively diffuses across the plasma cell membrane and accumulates in active mitochondria. Treatments with tebufenpyrad and pyridaben led to about a 40% loss of MitoTracker green fluorescence when compared to control cells (Fig. 4), strongly suggesting the loss of mitochondrial function.

To visualize the structural abnormalities of mitochondria following tebufenpyrad and pyridaben exposure, we performed a detailed confocal microscopic analysis using MitoTracker red dye in N27 dopaminergic cells. Mitochondria from control cells appeared as long, thread-like structures that were well-linked and randomly distributed throughout the cells. However, in the tebufenpyrad- and pyridaben-treated groups, they appeared as disintegrated circular structures that were not connected or linked to one another (Fig. 5A), indicative of mitochondrial fission. Using ImageJ analysis, we quantified structural features including mitochondrial

length (Fig. 5B) and mitochondrial circularity (Fig. 5C). In contrast to the control group, the mitochondria in tebufenpyrad- and pyridaben-treated cells were significantly shorter and more circular, further indicating a striking loss of mitochondrial structural integrity post-exposure. Collectively, our data suggest that tebufenpyrad and pyridaben exposure induces a profound structural impairment to mitochondria in dopaminergic neuronal cells.

Tebufenpyrad and pyridaben reduce oxygen consumption rates and increase mitochondrial stress levels

After demonstrating that tebufenpyrad and pyridaben induce mitochondrial impairment, we directly measured mitochondrial oxygen consumption rates and stress levels over time following pesticide exposure. We employed the Seahorse mitochondrial analyzer to perform two different sets of experiments. One set involved the direct injection method (Figs. 6A) after the measurement of basal respiration, which helped us to assess the effects of tebufenpyrad and pyridaben on the instantaneous respiration rate of dopaminergic neuronal cells. The second set of experiments, using the Seahorse analyzer post-pesticide treatment, involved measuring key parameters of mitochondrial bioenergetics (Fig. 7A) including basal respiration, ATP-linked respiration and respiration capacity.

To study the dose-response effect on respiration rates immediately after the direct injection process, we injected N27 dopaminergic cells with 0.5, 1, 3 and 6 μM of tebufenpyrad and pyridaben, both of which dose-dependently affected respiration rates (Figs. 6B and C). The lowest concentration of 0.5 μM tebufenpyrad did not affect baseline respiration rates significantly. However, the 1, 3 and 5 μM doses of tebufenpyrad significantly decreased the respiration rate immediately following

exposure to the pesticide. The pyridaben treatment produced a much more detrimental effect on mitochondrial respiration. Even its lowest dose of 0.5 μM induced a steep decrease in baseline respiration, and this effect continued to worsen at higher exposure concentrations (Fig. 6C). Thus, pyridaben has a more potent effect than tebufenpyrad on mitochondrial respiration rate in dopaminergic neuronal cells.

Measuring mitochondrial respiration kinetics with the Seahorse analyzer allowed us to determine the effect of toxic agents on the three critical stages of respiration. The first stage involves the addition of an ATP synthase inhibitor, oligomycin, which suddenly decreases the oxygen consumption rate (OCR). The next stage is the addition of FCCP, which acts as an uncoupler that increases mitochondrial oxygen consumption by disinhibiting the flow of protons across the mitochondrial inner membrane due to uncoupling of the electron transport chain. The final stage is the addition of antimycin A, which is a respiratory chain inhibitor that shuts down mitochondrial activity completely. After exposing N27 cells to different concentrations of tebufenpyrad (0.5, 1, 3 and 6 μM) and running the bioenergetics stages, we calculated ATP-linked respiration and respiratory capacity (Dranka et al., 2010; Jekabsons and Nicholls, 2004). As depicted in the Seahorse bioenergetics map (Fig. 7A), tebufenpyrad-treated cells revealed dramatic changes in all three stages of mitochondrial respiration in contrast to control cells. Quantitative analysis showed a dose-dependent decrease in basal respiration, ATP-linked respiration and respiratory capacity produced by tebufenpyrad. At the higher doses of 3 and 6 μM tebufenpyrad, mitochondrial oxygen consumption did not recover following FCCP treatment, indicating that these dose ranges produce irreversible damage to mitochondrial function (Figs. 7B-E). Similarly, pyridaben exposure (0.5, 1, 3 and 6 μM for 3 h) also

produced a dose-dependent decrease in basal respiration, ATP-linked respiration and respiratory capacity, which were all exceedingly low for all doses of pyridaben (Figs. 7F-I). Comparing the bioenergetics data of tebufenpyrad and pyridaben showed that pyridaben was more potent than tebufenpyrad. Collectively, these results show that both tebufenpyrad and pyridaben profoundly impair mitochondrial respiration in dopaminergic neuronal cells.

Tebufenpyrad and pyridaben deplete intracellular bioenergy levels in dopaminergic neuronal cells

To further confirm that tebufenpyrad- and pyridaben-induced mitochondrial inhibition reduces cellular biogenetics, we employed a highly sensitive luminescence-based assay to assess the cellular ATP content in N27 neuronal cells. The cells were treated with 3 μM tebufenpyrad or pyridaben for 3 h. We used 1 μM rotenone as a positive control under the same experimental conditions, since it is a potent agent for shutting down mitochondria and disrupting the electron transport chain (ETC) (Sherer et al., 2007). Both tebufenpyrad and pyridaben dramatically depleted intracellular ATP in dopaminergic neuronal cells (Fig. 8). The positive control rotenone also reduced cellular ATP content. These results suggest that tebufenpyrad and pyridaben exposure induces severe energy deficits resulting from mitochondrial impairment in dopaminergic neuronal cells.

Discussion

Our study clearly demonstrates that the two greenhouse pesticides tebufenpyrad and pyridaben exert noteworthy neurotoxic effects on dopaminergic neuronal cells. Systematic characterization of the toxicological mechanisms

underlying tebufenpyrad and pyridaben neurotoxicity reveals that these pesticides disrupted mitochondrial dynamics by inducing severe structural, functional, and oxidative damage. Our present study provides strong evidence that tebufenpyrad and pyridaben induce neurotoxicity by targeting mitochondrial structure and function in dopaminergic neuronal cells.

Tebufenpyrad and pyridaben are widely used pesticides in greenhouses and vineyards. Despite their widespread use, the potential neurotoxic effects of these compounds on the dopaminergic neuronal system are not well studied. But a recent study has reported that pyridaben exposure induced a 24% TH neuronal loss in the substantia nigra (SN) of mice. The authors also performed an RNAseq analysis and reported that mice exposed to certain pesticides exhibited gene expression patterns bearing significant correspondence to pathways that were well-known in human PD cases (Gollamudi et al., 2012). The results reported above have important implications about the neurotoxicological effects that tebufenpyrad and pyridaben might have on animal and human dopaminergic neuronal systems. In the present study, we used the MTS viability assay to calculate EC_{50} values of 3.98 and 3.77 µM for tebufenpyrad and pyridaben, respectively (Figs. 1A-B). Further cytotoxicity studies using the SYTOX Green and Muse Annexin V/7-AAD assays revealed that tebufenpyrad and pyridaben at a concentration of 3 µM elicit a similar toxicity to that of rotenone (1 µM) in N27 cells (Figs. 1C-D). An overview study using bovine and rat mitochondria demonstrated the mitochondrial complex I-specific inhibitory actions of tebufenpyrad and pyridaben with respect to their potency as it related to rotenone (Degli Esposti, 1998). Adding on, the cytotoxicity trend in SK-N-MC human neuroblastoma cells has previously been shown to be: pyridaben > rotenone > tebufenpyrad (Sherer et al.,

2007). In our study, exposing N27 dopaminergic neuronal cells to tebufenpyrad or pyridaben showed similar inhibitory effects on mitochondrial respiration, ATP production and oxidative damage. Variation in the toxicity and the effects of mitochondrial dysfunction induced by tebufenpyrad and pyridaben in different studies might be based on cell type, their species of origin, the organ of localization of the cells to which the pesticides are targeted and other factors such as concentrations and duration of treatment. The results from MTS and ATP production assays also showed that these environmental toxicants cause significant dopaminergic neuronal cell death at certain doses and durations of exposure. Clearly, further investigations examining exposure routes and risk levels *in vivo* are needed to better understand the environmental risk posed by these two compounds. Another noteworthy result contributing to the significant dopaminergic toxicity of tebufenpyrad and pyridaben was the rapid, time-dependent generation of reactive oxygen species (Fig. 2). Additionally, tebufenpyrad and pyridaben treatments reduced m-aconitase activity (Fig. 3), which is a clear sign of oxidative damage instigated by the production of superoxides (Gardner, 2002). M-aconitase is a major iron-sulfur enzyme that has been used as a marker of oxidative damage following various neurotoxic chemical exposures including pesticides (Cantu et al., 2009; Drechsel and Patel, 2008). To our knowledge, this is the first report demonstrating the sensitivity of mitochondrial aconitase to the greenhouse pesticides tebufenpyrad and pyridaben.

Both tebufenpyrad and pyridaben are considered to be mitochondrial inhibitors (by IRAC). Our experimental evidence supports this classification by demonstrating the potent effects of the pesticides on mitochondria in dopaminergic neuronal cells. Exposure of N27 cells to tebufenpyrad and pyridaben for 3 h induced a remarkable

loss of mitochondrial function and ATP production (Figs. 4 and 8). Similar studies with other complex-1 inhibitors such as rotenone have been shown to cause PD-like symptoms through neuronal loss and apoptosis (Greenamyre et al., 2001). We microscopically observed a clear structural morphological change in the mitochondria after exposure to tebufenpyrad and pyridaben when compared to the healthy control group (Fig. 5). This provided clear evidence of structural damage occurring apart from the mitochondrial dysfunction induced by the greenhouse toxicants. Thus, tebufenpyrad and pyridaben are both potently able to cause extensive mitochondrial damage leading to dopaminergic neuronal cell death. These results advance our understanding of the detrimental effects of tebufenpyrad and pyridaben as mitochondrial complex-1 inhibitors in inducing selective neuronal damage to the nigrostriatal dopaminergic system similar to rotenone exposure in animal models. Our analysis of mitochondrial respiration kinetics using the high-throughput Seahorse XF96 analyzer provided valuable information regarding the extent of the mitochondrial dysfunctional response to these pesticides. The Seahorse Bioanalyzer facilitates the precise measurement of oxygen consumption rates of intact live cells using a set of highly sensitive and specialized electrodes. This makes it a high-throughput system requiring a minimal number of cells and is also more efficient when compared to the traditional polarographic methods (Dranka et al., 2011; Rogers et al., 2011; Sauerbeck et al., 2011). Direct injection of the pesticides using the Seahorse XF96 analyzer clearly showed an instantaneous reduction in respiration rates after exposing N27 dopaminergic cells to different concentrations of tebufenpyrad and pyridaben (Figs. 6A-C). Further analysis of Seahorse respiration curves revealed that the pesticides induced severe mitochondrial stress characterized

by impaired basal respiration, ATP-linked respiration and respiratory capacity (Fig. 7). Notably, the Seahorse analyzer findings revealed pyridaben to be more potent than tebufenpyrad even at lower doses, suggesting that analysis of mitochondrial function by the high-throughput Seahorse system will be an invaluable tool to determine rank-order potency of pesticides having potential mitochondrial toxicity. Incorporating such analyses in pesticide development will minimize the off-target toxicity to the human nervous system. Overall, our study provides pivotal neurotoxicological data demonstrating that these two neurotoxicants cause significant damage to the dopaminergic neuronal oxygen consumption system, thereby leading to significant mitochondrial dysfunction and oxidative damage.

A very recent report by the Washington State Department of Agriculture (WSDA) stated that there were 20 farm workers working in a cherry orchard who had been poisoned by an off-target exposure to a mixture of pesticides that were being applied in a neighboring pear orchid. Interestingly, one of the components of the pesticide mixture was revealed to be pyridaben. The affected farmers were medically treated for neurological, respiratory, ocular and gastrointestinal symptoms (Calvert et al., 2015). In terms of human exposure studies in greenhouse settings, female workers exposed to an organophosphate exhibited longer reaction times and reduced motor stability when compared to an unexposed group of women. Adding to these symptoms, the affected group also suffered from depression, hypertension and fatigue (Bazylewicz-Walczak et al., 1999). A 2006 study of the school children of greenhouse workers in Ecuador demonstrated a long-term maternal effect from prenatal exposure to greenhouse pesticides causing deficits in their motor coordination and visual memory (Grandjean et al., 2006). The evidence from these

greenhouse epidemiological studies suggests that pesticide exposure in greenhouses might have a significant effect on the human nervous system, thereby instigating a number of neurodegenerative symptoms. Keeping in mind the neurotoxic effects of exposure to pesticides in greenhouses, the results from our experimental studies suggest that persistent exposure to complex 1 inhibitors, such as tebufenpyrad and pyridaben, represents a neurological occupational hazard that could adversely affect greenhouse workers. Since tebufenpyrad and pyridaben have a terrestrial field dissipation half-life of about 50 and 11 days, respectively (TOXNET and NLM - CASRN: 119168-77-3 and CASRN: 96489-71-3), persistent exposure in closed environments such as a greenhouse setting likely poses a risk to humans. Several screening methodologies using cell model systems have been explored recently for rapid identification of adverse effects of environmental pesticide contaminations (Heusinkveld et al., 2014; Meijer et al., 2014).

In summary, we report here an interesting finding that the neurotoxic effects of tebufenpyrad and pyridaben are mainly manifested as damage to both structural and functional aspects of mitochondria in dopaminergic neuronal cells. The extent to which these greenhouse pesticides alter the mitochondrial dynamics could be used as a marker of *in vitro* pesticide neurotoxicity. Considering the enhanced vulnerability of dopaminergic neuronal cells to mitochondrial impairment produced by tebufenpyrad and pyridaben in our study, chronic exposure to these greenhouse pesticides may have implications in environmentally-linked PD. Further studies in animal models and epidemiological studies in greenhouse workers will clarify the potential risk of greenhouse pesticides in the etiology of PD.

References

Adams, F.S., La Rosa, F.G., Kumar, S., Edwards-Prasad, J., Kentroti, S., Vernadakis, A., Freed, C.R., and Prasad, K.N. (1996). Characterization and transplantation of two neuronal cell lines with dopaminergic properties. Neurochem Res 21, 619-627.

Anantharam, V., Kitazawa, M., Wagner, J., Kaul, S., and Kanthasamy, A.G. (2002). Caspase-3-dependent proteolytic cleavage of protein kinase Cdelta is essential for oxidative stress-mediated dopaminergic cell death after exposure to methylcyclopentadienyl manganese tricarbonyl. The Journal of neuroscience : the official journal of the Society for Neuroscience 22, 1738-1751.

Asaithambi, A., Ay, M., Jin, H., Gosh, A., Anantharam, V., Kanthasamy, A., and Kanthasamy, A.G. (2014). Protein kinase D1 (PKD1) phosphorylation promotes dopaminergic neuronal survival during 6-OHDA-induced oxidative stress. PLoS One 9, e96947.

Baltazar, M.T., Dinis-Oliveira, R.J., de Lourdes Bastos, M., Tsatsakis, A.M., Duarte, J.A., and Carvalho, F. (2014). Pesticides exposure as etiological factors of Parkinson's disease and other neurodegenerative diseases--a mechanistic approach. Toxicology letters 230, 85-103.

Bazylewicz-Walczak, B., Majczakowa, W., and Szymczak, M. (1999). Behavioral effects of occupational exposure to organophosphorous pesticides in female greenhouse planting workers. Neurotoxicology 20, 819-826.

Betarbet, R., Sherer, T.B., MacKenzie, G., Garcia-Osuna, M., Panov, A.V., and Greenamyre, J.T. (2000). Chronic systemic pesticide exposure reproduces features of Parkinson's disease. Nat Neurosci 3, 1301-1306.

Cabeza-Arvelaiz, Y., and Schiestl, R.H. (2012). Transcriptome analysis of a rotenone model of parkinsonism reveals complex I-tied and -untied toxicity mechanisms common to neurodegenerative diseases. PLoS One 7, e44700.

Calvert, G.M., Rodriguez, L., Prado, J.B., and (CDC), C.f.D.C.a.P. (2015). Worker illness related to newly marketed pesticides--Douglas County, Washington, 2014. MMWR Morb Mortal Wkly Rep 64, 42-44.

Cantu, D., Schaack, J., and Patel, M. (2009). Oxidative inactivation of mitochondrial aconitase results in iron and H2O2-mediated neurotoxicity in rat primary mesencephalic cultures. PLoS One 4, e7095.

Chan, D.C. (2006). Mitochondria: dynamic organelles in disease, aging, and development. Cell 125, 1241-1252.

Dagda, R.K., Cherra, S.J., Kulich, S.M., Tandon, A., Park, D., and Chu, C.T. (2009). Loss of PINK1 function promotes mitophagy through effects on oxidative stress and mitochondrial fission. J Biol Chem 284, 13843-13855.

Degli Esposti, M. (1998). Inhibitors of NADH-ubiquinone reductase: an overview. Biochim Biophys Acta 1364, 222-235.

Dranka, B.P., Benavides, G.A., Diers, A.R., Giordano, S., Zelickson, B.R., Reily, C., Zou, L., Chatham, J.C., Hill, B.G., Zhang, J., *et al.* (2011). Assessing bioenergetic function in response to oxidative stress by metabolic profiling. Free Radic Biol Med 51, 1621-1635.

Dranka, B.P., Hill, B.G., and Darley-Usmar, V.M. (2010). Mitochondrial reserve capacity in endothelial cells: The impact of nitric oxide and reactive oxygen species. Free Radic Biol Med 48, 905-914.

Dranka, B.P., Zielonka, J., Kanthasamy, A.G., and Kalyanaraman, B. (2012). Alterations in bioenergetic function induced by Parkinson's disease mimetic compounds: lack of correlation with superoxide generation. Journal of neurochemistry 122, 941-951.

Drechsel, D.A., and Patel, M. (2008). Role of reactive oxygen species in the neurotoxicity of environmental agents implicated in Parkinson's disease. Free Radic Biol Med 44, 1873-1886.

Freire, C., and Koifman, S. (2012). Pesticide exposure and Parkinson's disease: epidemiological evidence of association. Neurotoxicology 33, 947-971.

Gardner, P.R. (2002). Aconitase: sensitive target and measure of superoxide. Methods Enzymol 349, 9-23.

Ghosh, A., Chandran, K., Kalivendi, S.V., Joseph, J., Antholine, W.E., Hillard, C.J., Kanthasamy, A., and Kalyanaraman, B. (2010). Neuroprotection by a mitochondria-targeted drug in a Parkinson's disease model. Free Radic Biol Med 49, 1674-1684.

Ghosh, S., Patel, N., Rahn, D., McAllister, J., Sadeghi, S., Horwitz, G., Berry, D., Wang, K.X., and Swerdlow, R.H. (2007). The thiazolidinedione pioglitazone alters mitochondrial function in human neuron-like cells. Mol Pharmacol 71, 1695-1702.

Gollamudi, S., Johri, A., Calingasan, N.Y., Yang, L., Elemento, O., and Beal, M.F. (2012). Concordant signaling pathways produced by pesticide exposure in mice correspond to pathways identified in human Parkinson's disease. PLoS One 7, e36191.

Gordon, R., Hogan, C.E., Neal, M.L., Anantharam, V., Kanthasamy, A.G., and Kanthasamy, A. (2010). A simple magnetic separation method for high-yield isolation of pure primary microglia. J Neurosci Methods 194, 287-296.

Grandjean, P., Harari, R., Barr, D.B., and Debes, F. (2006). Pesticide exposure and stunting as independent predictors of neurobehavioral deficits in Ecuadorian school children. Pediatrics 117, e546-556.

Greenamyre, J.T., Cannon, J.R., Drolet, R., and Mastroberardino, P.G. (2010). Lessons from the rotenone model of Parkinson's disease. Trends in pharmacological sciences 31, 141-142; author reply 142-143.

Greenamyre, J.T., Sherer, T.B., Betarbet, R., and Panov, A.V. (2001). Complex I and Parkinson's disease. IUBMB Life 52, 135-141.

Harischandra, D.S., Jin, H., Anantharam, V., Kanthasamy, A., and Kanthasamy, A.G. (2014). α-Synuclein Protects against Manganese Neurotoxic Insult during the Early Stages of Exposure in a Dopaminergic Cell Model of Parkinson's Disease. Toxicol Sci.

Heusinkveld, H.J., van den Berg, M., and Westerink, R.H. (2014). In vitro dopaminergic neurotoxicity of pesticides: a link with neurodegeneration? Vet Q 34, 120-131.

Hoppins, S., Lackner, L., and Nunnari, J. (2007). The machines that divide and fuse mitochondria. Annu Rev Biochem 76, 751-780.

Jekabsons, M.B., and Nicholls, D.G. (2004). In situ respiration and bioenergetic status of mitochondria in primary cerebellar granule neuronal cultures exposed continuously to glutamate. J Biol Chem 279, 32989-33000.

Jin, H., Kanthasamy, A., Anantharam, V., Rana, A., and Kanthasamy, A.G. (2011a). Transcriptional regulation of pro-apoptotic protein kinase Cdelta: implications for oxidative stress-induced neuronal cell death. J Biol Chem 286, 19840-19859.

Jin, H., Kanthasamy, A., Ghosh, A., Anantharam, V., Kalyanaraman, B., and Kanthasamy, A.G. (2014a). Mitochondria-targeted antioxidants for treatment of Parkinson's disease: preclinical and clinical outcomes. Biochimica et biophysica acta 1842, 1282-1294.

Jin, H., Kanthasamy, A., Ghosh, A., Yang, Y., Anantharam, V., and Kanthasamy, A.G. (2011b). α-Synuclein negatively regulates protein kinase Cδ expression to suppress apoptosis in dopaminergic neurons by reducing p300 histone acetyltransferase activity. J Neurosci 31, 2035-2051.

Jin, H., Kanthasamy, A., Harischandra, D.S., Kondru, N., Ghosh, A., Panicker, N., Anantharam, V., Rana, A., and Kanthasamy, A.G. (2014b). Histone Hyperacetylation Upregulates PKCdelta in Dopaminergic Neurons to Induce Cell Death: Relevance to Epigenetic Mechanisms of Neurodegeneration in Parkinson's Disease. The Journal of biological chemistry.

Johnson, M.E., and Bobrovskaya, L. (2015). An update on the rotenone models of Parkinson's disease: their ability to reproduce the features of clinical disease and model gene-environment interactions. Neurotoxicology 46, 101-116.

Kalyanaraman, B. (2013). Teaching the basics of redox biology to medical and graduate students: Oxidants, antioxidants and disease mechanisms. Redox Biol 1, 244-257.

Khan, A., Gillis, K., Clor, J., and Tyagarajan, K. (2012). Simplified evaluation of apoptosis using the Muse cell analyzer. Postepy Biochem 58, 492-496.

Latchoumycandane, C., Anantharam, V., Jin, H., and Kanthasamy, A. (2011). Dopaminergic neurotoxicant 6-OHDA induces oxidative damage through proteolytic activation of PKCδ in cell culture and animal models of Parkinson's disease. Toxicol Appl Pharmacol 256, 314-323.

Levesque, S., Wilson, B., Gregoria, V., Thorpe, L.B., Dallas, S., Polikov, V.S., Hong, J.S., and Block, M.L. (2010). Reactive microgliosis: extracellular micro-calpain and microglia-mediated dopaminergic neurotoxicity. Brain 133, 808-821.

Lin, M., Chandramani-Shivalingappa, P., Jin, H., Ghosh, A., Anantharam, V., Ali, S., Kanthasamy, A.G., and Kanthasamy, A. (2012). Methamphetamine-induced neurotoxicity linked to ubiquitin-proteasome system dysfunction and autophagy-related changes that can be modulated by protein kinase C delta in dopaminergic neuronal cells. Neuroscience 210, 308-332.

Lin, M.T., and Beal, M.F. (2006). Mitochondrial dysfunction and oxidative stress in neurodegenerative diseases. Nature 443, 787-795.

Marusiak, A.A., Edwards, Z.C., Hugo, W., Trotter, E.W., Girotti, M.R., Stephenson, N.L., Kong, X., Gartside, M.G., Fawdar, S., Hudson, A., *et al.* (2014). Mixed lineage kinases activate MEK independently of RAF to mediate resistance to RAF inhibitors. Nat Commun 5, 3901.

Meijer, M., Hendriks, H.S., Heusinkveld, H.J., Langeveld, W.T., and Westerink, R.H. (2014). Comparison of plate reader-based methods with fluorescence microscopy for measurements of intracellular calcium levels for the assessment of in vitro neurotoxicity. Neurotoxicology 45, 31-37.

Parron, T., Requena, M., Hernandez, A.F., and Alarcon, R. (2011). Association between environmental exposure to pesticides and neurodegenerative diseases. Toxicology and applied pharmacology 256, 379-385.

Prasad, K.N., Clarkson, E.D., La Rosa, F.G., Edwards-Prasad, J., and Freed, C.R. (1998). Efficacy of grafted immortalized dopamine neurons in an animal model of parkinsonism: a review. Mol Genet Metab 65, 1-9.

Rogers, G.W., Brand, M.D., Petrosyan, S., Ashok, D., Elorza, A.A., Ferrick, D.A., and Murphy, A.N. (2011). High throughput microplate respiratory

measurements using minimal quantities of isolated mitochondria. PLoS One 6, e21746.

Roth, B.L., Poot, M., Yue, S.T., and Millard, P.J. (1997). Bacterial viability and antibiotic susceptibility testing with SYTOX green nucleic acid stain. Appl Environ Microbiol 63, 2421-2431.

Sauerbeck, A., Pandya, J., Singh, I., Bittman, K., Readnower, R., Bing, G., and Sullivan, P. (2011). Analysis of regional brain mitochondrial bioenergetics and susceptibility to mitochondrial inhibition utilizing a microplate based system. J Neurosci Methods 198, 36-43.

Schapira, A.H. (2007). Mitochondrial dysfunction in Parkinson's disease. Cell Death Differ 14, 1261-1266.

Sherer, T.B., Betarbet, R., Testa, C.M., Seo, B.B., Richardson, J.R., Kim, J.H., Miller, G.W., Yagi, T., Matsuno-Yagi, A., and Greenamyre, J.T. (2003). Mechanism of toxicity in rotenone models of Parkinson's disease. The Journal of neuroscience : the official journal of the Society for Neuroscience 23, 10756-10764.

Sherer, T.B., Richardson, J.R., Testa, C.M., Seo, B.B., Panov, A.V., Yagi, T., Matsuno-Yagi, A., Miller, G.W., and Greenamyre, J.T. (2007). Mechanism of toxicity of pesticides acting at complex I: relevance to environmental etiologies of Parkinson's disease. J Neurochem 100, 1469-1479.

Spivey, A. (2011). Rotenone and paraquat linked to Parkinson's disease: human exposure study supports years of animal studies. Environmental health perspectives 119, A259.

Tanner, C.M., Kamel, F., Ross, G.W., Hoppin, J.A., Goldman, S.M., Korell, M., Marras, C., Bhudhikanok, G.S., Kasten, M., Chade, A.R., *et al.* (2011). Rotenone, paraquat, and Parkinson's disease. Environmental health perspectives 119, 866-872.

Testa, C.M., Sherer, T.B., and Greenamyre, J.T. (2005). Rotenone induces oxidative stress and dopaminergic neuron damage in organotypic substantia nigra cultures. Brain Res Mol Brain Res 134, 109-118.

Winklhofer, K.F., and Haass, C. (2010). Mitochondrial dysfunction in Parkinson's disease. Biochim Biophys Acta 1802, 29-44.

Zhang, D., Kanthasamy, A., Yang, Y., Anantharam, V., and Kanthasamy, A. (2007). Protein kinase C delta negatively regulates tyrosine hydroxylase activity and dopamine synthesis by enhancing protein phosphatase-2A activity in dopaminergic neurons. The Journal of neuroscience : the official journal of the Society for Neuroscience 27, 5349-5362.

Zhang, Y., and Chan, D.C. (2007). New insights into mitochondrial fusion. FEBS Lett 581, 2168-2173.
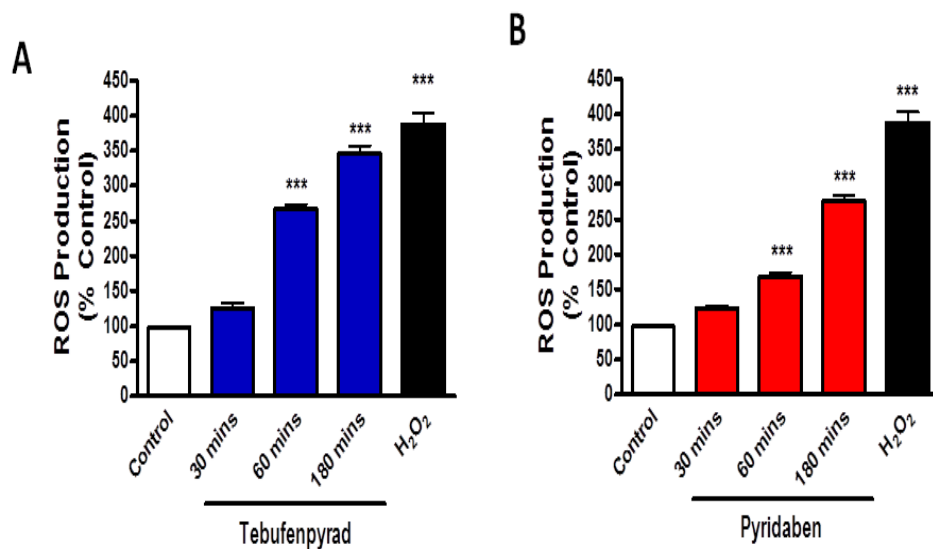
Figures

Table 1: Comprehensive evaluation comparing tebufenpyrad and pyridaben. Both tebufenpyrd and pyridaben functions based on similar modes of action and they target similar system, but they slightly differ in their functional aspects, area of usage and molecular weights.

Name of pesticides/ Toxicant	Molecular weight	Example of trade names	Class of pesticide	Targeted system/process	Mode of action	Use
Tebufenpyrad	333.8	Masai, Pyranica	Pyrazole	Metabolic processes / Energy production	Mitochondrial complex 1 inhibitor	Green house acaricide
Pyridaben	364.9	Nexter, Pyramite, Sanmite	Pyridazinone	Metabolic processes / Energy production	Mitochondrial complex 1 inhibitor	Green house / vineyard acaricide
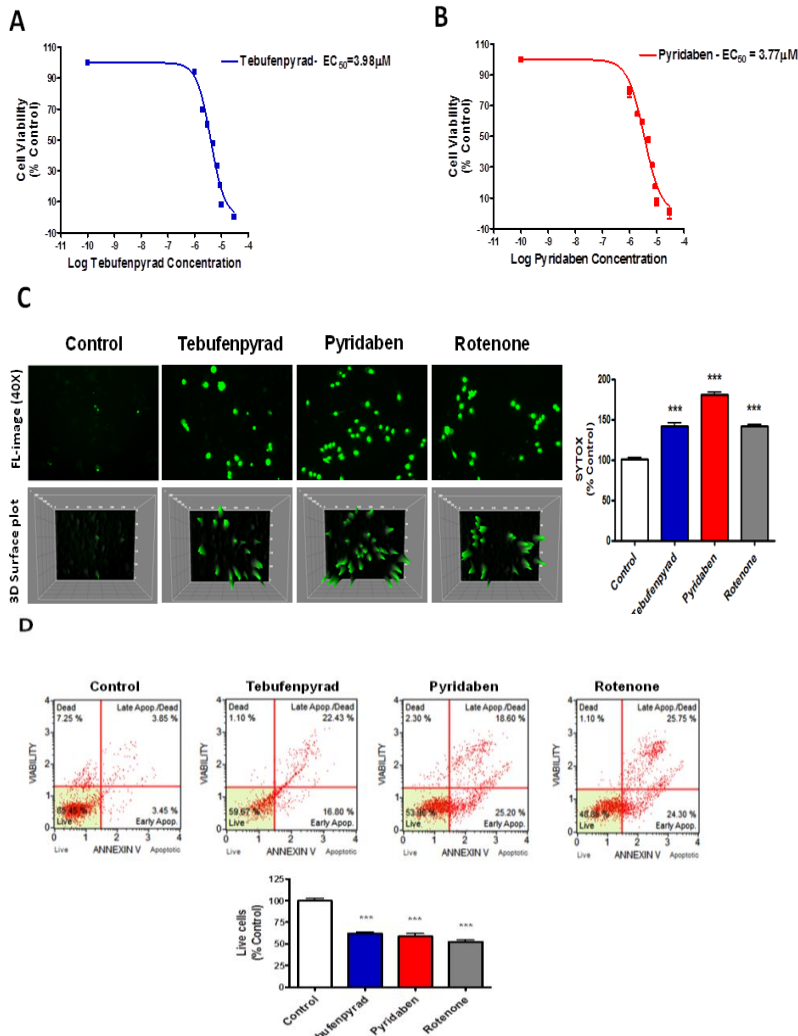
Figure 1: Dose-dependent cytotoxic effect on N27 dopaminergic neuronal cells post-exposure to tebufenpyrad and pyridaben

N27 cells were treated with varying concentrations (0, 1, 2, 3, 5, 7, 9, 10 and 30 μM) of tebufenpyrad (A) and pyridaben (B) for 3 h and then assayed for MTS cell viability, expressed as a percentage of controls. The results represent two individual experiments performed in octuplicate. (C) The N27 cells were treated with tebufenpyrad (3 μM) and pyridaben (3 μM) for 3 h, and the cytotoxic effect was measured using SYTOX Green assays. Representative SYTOX Green staining images are shown. The top view of the SYTOX Green images is also shown as a 3D surface plot in the left bottom panel. Asterisks ***$p < 0.001$ for control versus pesticide-treated groups. The results represent the mean ± S.E. of two individual experiments performed in quadruplicate. (D) Muse Annexin V/7-AAD assays were additionally performed to measure the cytotoxicity of tebufenpyrad (3 μM) and pyridaben (3 μM) for 3 h on N27 cells. Asterisks ***$p < 0.001$ for control versus pesticide-treated groups. The results represent the mean ± S.E. of two separate experiments performed in quadruplicate.

Figure 2: Tebufenpyrad and Pyridaben increased ROS generation in a time-dependent manner

N27 cells were exposed to 3 µM of tebufenpyrad (A) and pyridaben (B) for 30, 60 and 180 min. Cells were then assayed for intracellular ROS production using H_2-DCFDA dye. Hydrogen peroxide (100 µM for 45 min) was used as a positive control. Asterisks ***$p < 0.001$ for control vs treated groups, represented as the mean $\pm$ S.E. of three separate experiments performed in hexaplicate.
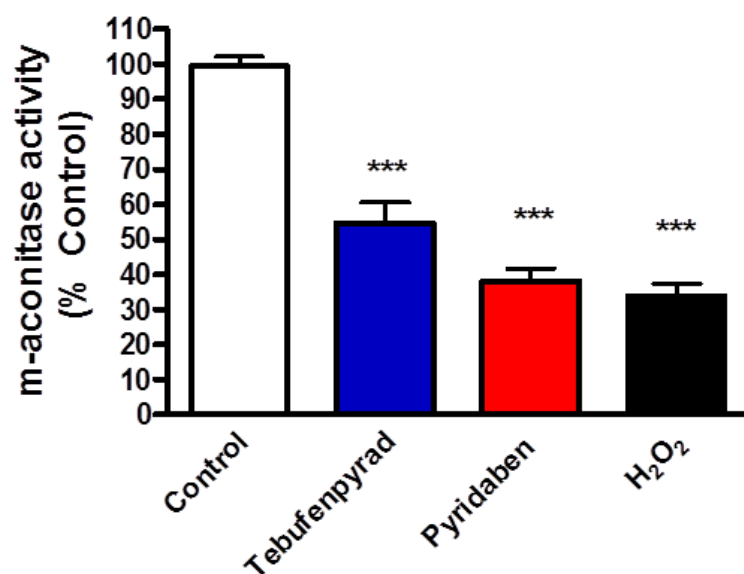
Figure 3: Effect of tebufenpyrad and pyridaben on mitochondrial aconitase enzyme activity in N27 dopaminergic cells

N27 cells were treated with 3 μM of tebufenpyrad and pyridaben for 3 h in serum-free RPMI media. Aconitase activity was measured post-exposure using an aconitase activity kit. Hydrogen peroxide (100 μM) treatment for 45 min was used as a positive control. Aconitase activity is expressed as a percentage of controls. Asterisks ***p < 0.001 for control vs treated groups, represented as the mean ± S.E. of three separate experiments performed in hexaplicate.
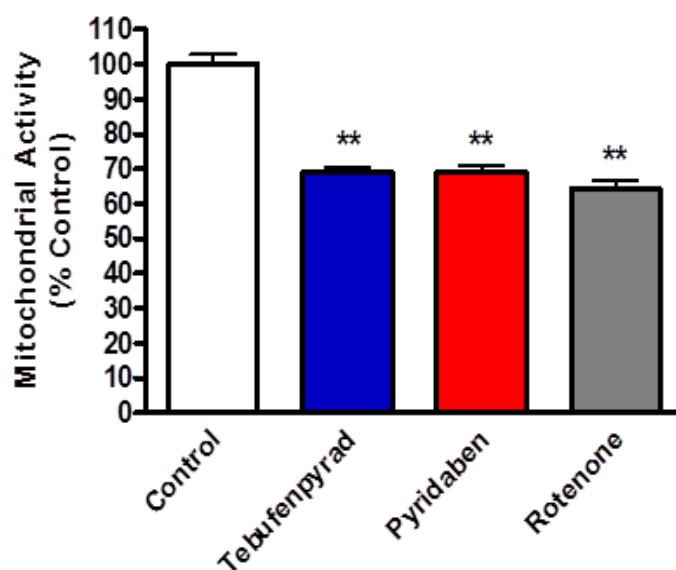
Figure 4: Effect of tebufenpyrad and pyridaben on mitochondrial function in N27 dopaminergic cells

N27 cells were treated with 3 µM of tebufenpyrad and pyridaben for 3 h and assayed for mitochondrial function using the MitoTracker green dye assay. Rotenone (1 µM for 3 h) was used as a positive control. After treatment and incubation with the MitoTracker green dye, readings were taken using a plate reader at an excitation wavelength of 485 nm and an emission wavelength of 520 nm. Values are expressed as relative mitochondrial activity. Asterisks $**p < 0.01$ for control versus treated groups, represented as the mean ± S.E. of three separate experiments performed in hexaplicate.
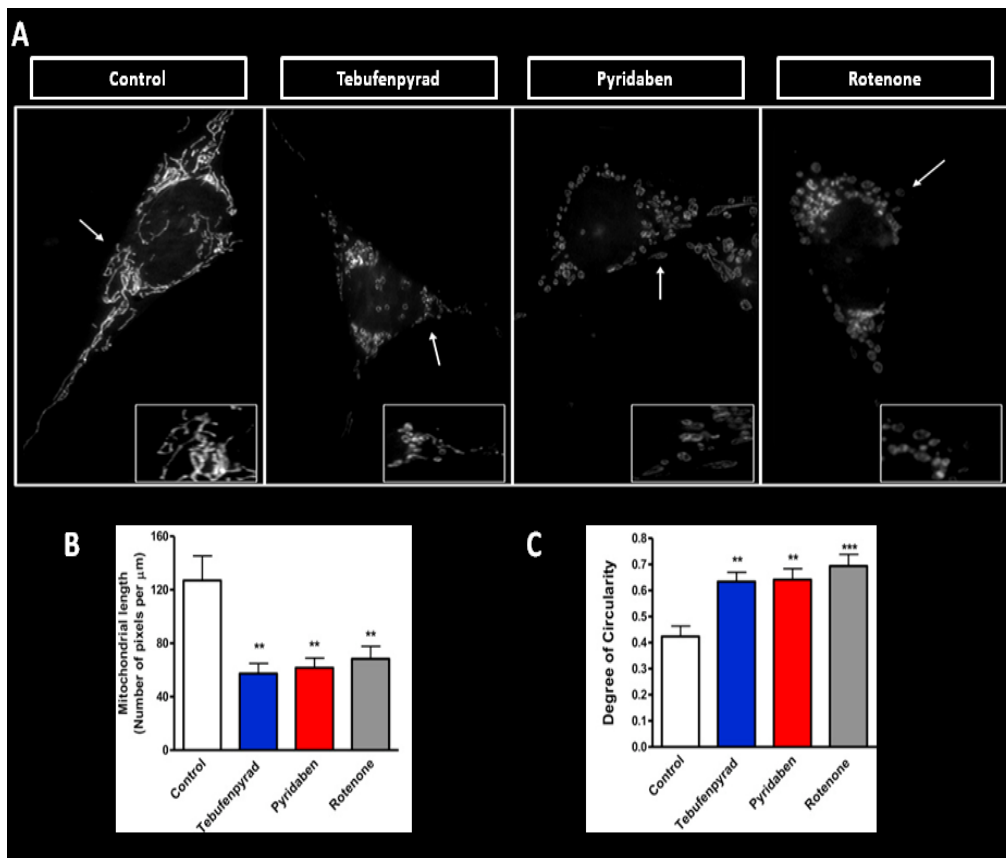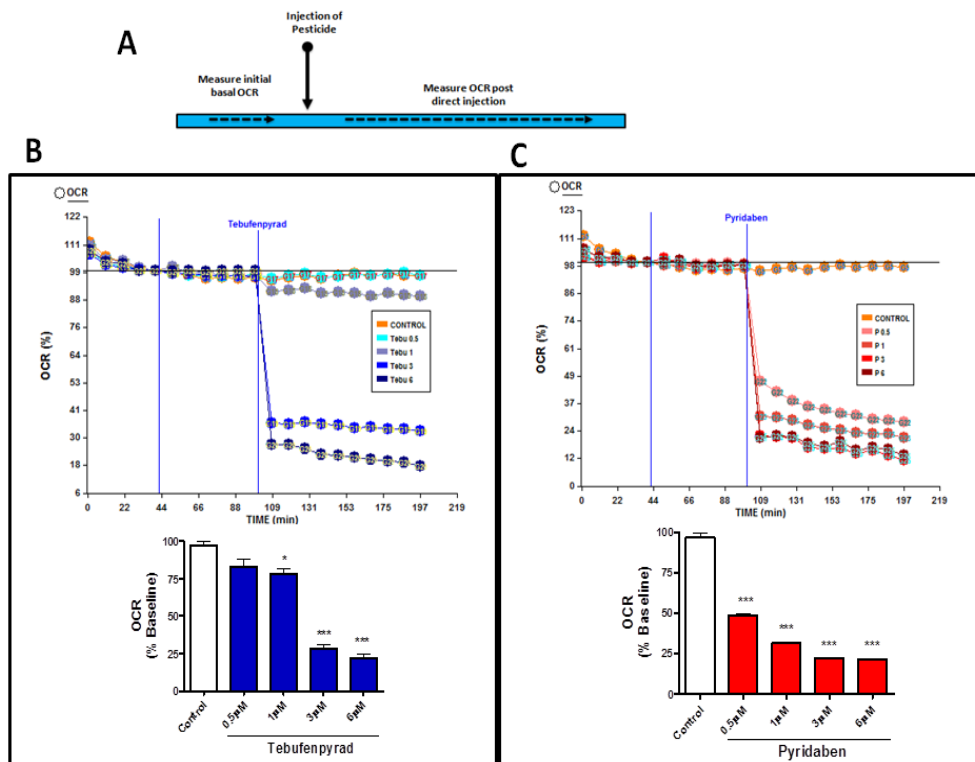
Figure 5: Tebufenpyrad and pyridaben induced significant structural damage to the mitochondria of N27 cells

(A) N27 cells were exposed to 3 µM tebufenpyrad and pyridaben for 3 h. Rotenone (1 µM for 3 h) was used as a positive control. Structural changes to mitochondria were then stained by MitoTracker red dye. Images were obtained using a confocal microscope (60 X magnification). Mitochondrial length (B) and degree of circularity (C) were quantified using ImageJ. Asterisks **p < 0.01 and ***p < 0.001 for control versus pesticide-treated groups, represented as the mean ± S.E. of two separate experiments performed in hexaplicate.

Figure 6: Direct injection of tebufenpyrad and pyridaben to N27 cells leads to plummeting oxygen consumption rates (OCR)

(A) Schematic representation of direct injection method was employed to analyze instantaneous effects on N27 dopaminergic cells after injecting different concentrations of tebufenpyrad and pyridaben. N27 cells grown in a V7-PS culture plate one day prior to the treatment were injected with different concentrations of tebufenpyrad and pyridaben (0.5, 1, 3 and 6 μM) under serum-free conditions. Immediately post-injection, the OCR value was measured using the Seahorse XF96 analyzer. (B and C) Quantification of the output OCR post-injection. Asterisks $*p < 0.05$ and $***p < 0.001$ for control versus treatment groups, represented as the mean ± S.E. of two separate experiments performed in quadruplicate.
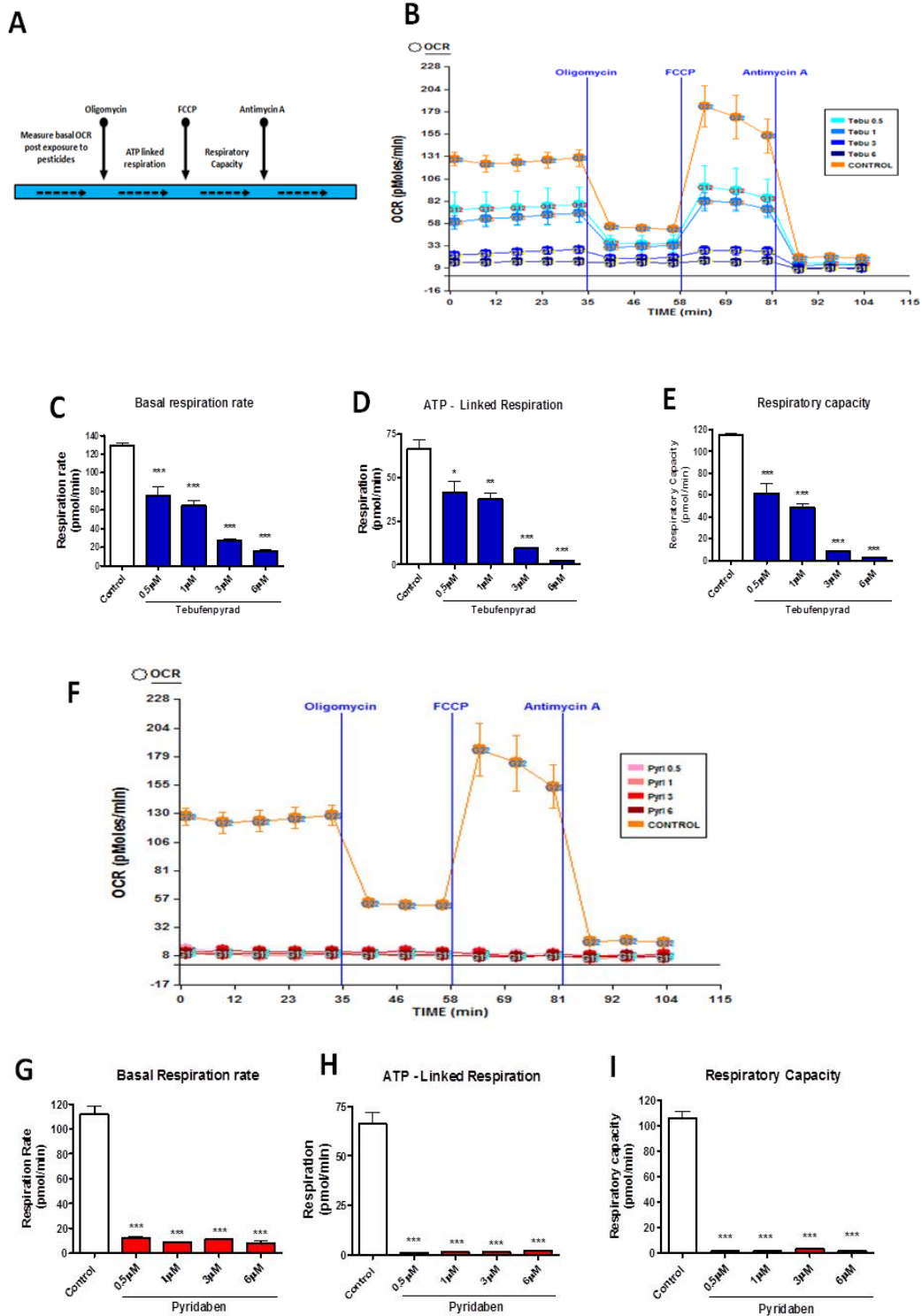
Figure 7: Effect of tebufenpyrad and pyridaben on mitochondrial stress level in N27 dopaminergic cells

(A) Schematic representation of the bioenergetics study to measure and analyze the dose-related effects of tebufenpyrad and pyridaben on mitochondrial dynamics in N27 cells. The dopaminergic neuronal cells were incubated with different concentrations

of tebufenpyrad or pyridaben (0.5, 1, 3 and 6 μM) in serum-free RPMI for 3 h and then the plate was de-gassed and made ready for the OCR measurement using the Seahorse XF96 analyzer. Mitochondrial dynamics were measured using three-stage injection of mito-stressors. Stage 1 injected 1 μg/ml oligomycin, Stage 2 injected 1 μM FCCP and Stage 3 injected 10 μM antimycin A (see Figs. 7B and F). Throughout these stages the analyzer continuously measures OCR. (C-E) Different parameters like basal respiration, ATP-linked respiration and respiratory capacity were estimated from the output OCR values after completion. (G-I) Experiments were repeated under the same conditions with pyridaben. Asterisks ***$p < 0.001$ for control versus treatment groups, represented as the mean ± S.E. of two separate experiments performed in quadruplicate.
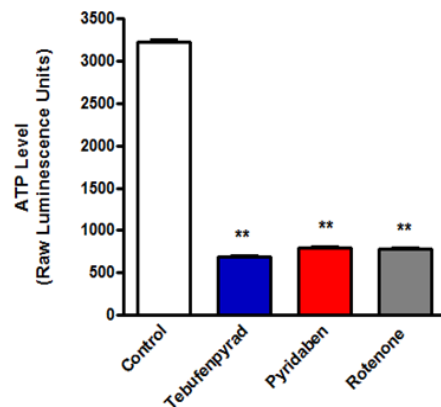
Figure 8: Tebufenpyrad and pyridaben treatment significantly reduced cellular ATP production in N27 dopaminergic cells
N27 cells were exposed to 3 µM of tebufenpyrad or pyridaben for 3 h in serum-free RPMI media. Cell viability was measured with respect to the amount of cellular ATP produced using the Luminescent Cell Viability assay kit and was represented as raw luminescence units (RLU). Rotenone (1 µM for 3 h) was used as a positive control. Asterisks ***p < 0.001 for control versus treated groups, represented as the mean ± S.E. of three separate experiments performed in hexaplicate.
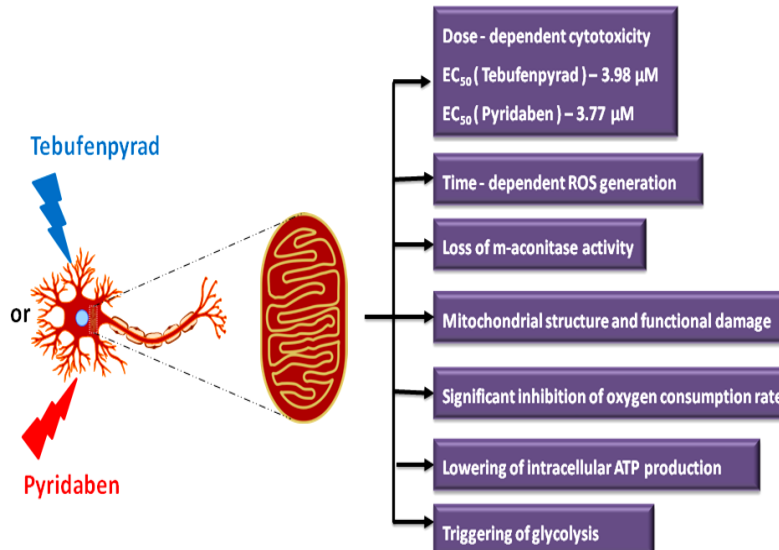
Figure 9: A schematic comparison between Control and Pyridaben or Tebufenpyrad treated N27 cells illustrating the significant effect of tebufenpyrad and pyridaben on mitochondrial function, structure and bioenergetic dynamics. Drawing was created by A.Charli using biomedical PowerPoint toolkit from Motifolio.

CHAPTER III: MITOCHONDRIA-IMPAIRING PESTICIDE TEBUFENPYRAD PROMOTES PKCδ ACTIVATION THAT FUNCTIONS AS A LAMINB1 KINASE TO INDUCE NUCLEAR MEMBRANE DAMAGE IN DOPAMINERGIC NEURONAL MODELS OF PARKINSON'S DISEASE

Adhithiya Charli; Jie Luo; Bharathi Palanisamy; Emir Malovic; Huajun Jin;

Vellareddy Anantharam; Arthi Kanthasamy; Anumantha Kanthasamy*

Parkinson's Disorder Research Laboratory, Iowa Center for Advanced Neurotoxicology,

Department of Biomedical Sciences, Iowa State University, Ames, IA 50011

*To whom correspondence should be addressed: Dept. of Biomedical Sciences, Iowa State University, 2062 College of Veterinary Medicine Building, Ames, IA 50011. Tel: 515-294-2516; Fax: 515-294-2315; Email: akanthas@iastate.edu

The abbreviations used are:

Dimethyl Sulphoxide (DMSO), Protein kinase Cδ (PKCδ), Cleavage-Resistant Mutant (CRM), Clustered Regularly Interspaced Short Palindromic Repeats (CRISPR), Site-directed mutageneis (SDM), Tebufenpyrad (Tebu), fetal bovine serum (FBS), *substantia nigra* (SN).

Abstract

Chronic exposure to neurotoxic pesticides is implicated in the etiopathogenesis of Parkinson's disease (PD). Dopaminergic neurons are highly vulnerable to the neurotoxic effects of mitochondrial complex-1-inhibiting pesticides, however, the cellular and molecular mechanisms are not well understood. Previously, we demonstrated novel PKC isoform PKCδ is highly expressed in dopaminergic neurons and plays a key role in their pesticide-induced apoptosis via caspase-3-mediated proteolytic activation. Herein, we further characterized the downstream molecular events of PKCδ signaling that govern dopaminergic neuronal cell death induced by the mitochondria-impairing pesticide Tebufenpyrad (Tebu). Tebu (0.01-10μM) induced dose- and time-dependent neurotoxicity in the N27 dopaminergic neuronal cells; rotenone was used as a positive control. Tebu-induced cell death was accompanied by PKCδ phosphorylation of T505 activation loop phosphorylation and caspase-3-dependent proteolytic activation of the kinase. *In silico* analyses identified that the threonine site on laminB1 (T575) is likely to be phosphorylated by PKCδ, suggesting that laminB1 serves as a key downstream target of the kinase. High resolution 3D confocal microscopic analysis revealed co-localization of activated PKCδ and laminB1 as well as structural defects in the nuclear membrane in Tebu-exposed N27 cells. Interestingly, Tebu did not induce any PKCδ activation, and thus no laminB1 phosphorylation, in N27 cells stably expressing the PKCδ cleavage resistant mutant. Furthermore, CRISPR/Cas9-based stable knockdown of PKCδ significantly attenuated Tebu-induced laminB1 phosphorylation when compared to control CRISPR/Cas9 N27 cells. Also, upon replacing threonine with glycine using site-directed mutagenesis on LaminB1, the phosphorylation of LaminB1 by the

activated PKCδ post teubufenpyrad exposure in the N27 cells was blocked. Another interesting evidence was obtained using the organotypic slice of midbrain from PKCδ-/- pups, which demonstrated absence of LaminB1 damage and phosphorylation of LaminB1 (T575) post tebufenpyrad exposure when compared to the PKCδ+/+ pups. We observed PKCδ activation, LaminB1 phosphorylation and LaminB1 loss in nigral dopaminergic neurons from PD brains, but not control brains, thus providing translational relevance. Collectively, our data reveal that PKCδ functions as laminB1 kinase to disassemble the nuclear membrane during the dopaminergic neuronal cell death process triggered by exposure to mitochondrial complex-1-inhibiting pesticides. This mechanistic insight may have important implications for the etiology of environmentally-linked PD.

Introduction

Parkinson's disease is a chronic progressive neurodegenerative disorder and is expressed by serious movement difficulties, affecting about 1% of adults older than 60 years. The disease is attributed to selective loss of neurons in the substantia nigra, which results in drastic depletion of dopamine in the striatum region and its cause is unclear in most individuals (Samii et al., 2004). The main clinical features of PD include akinesia, tremors, rigidity, bradykinesia, walking difficulties and postural instability. The etiology of PD is not well understood, but it is a multi-factorial contribution from various environmental, genetic, epigenetic and inflammatory factors. (Levy et al., 2009). Of all these factors, environmental influence triggering PD is being well studied in recent years, to minimize the risk of using certain pesticides and also to prevent any off target reactions which might lead to detrimental end points. It is well known that the mitochondria plays a pivotal role in the

homeostatic functioning of a cell by providing energy via oxidative phosphorylation (Jin et al., 2014a; Zhang and Chan, 2007). Hence aberrant mitochondrial dysfunction and changes in its dynamics due to persistent pesticides exposure would lead to impairment of cell functions and resulting in apoptosis (Charli et al., 2016; Lin et al., 2012; Schapira, 2007). Chronic pesticides exposure have also been shown to cause a number of protein modifications and outcomes in overwhelming epidemiological cases of PD (Corrigan et al., 2000; Fleming et al., 1994; Priyadarshi et al., 2000; Spivey, 2011; Tanner et al., 2011). We in this chapter primarily will be focusing on the activation of the Protein kinase Cδ (PKCδ) mediated through the oxidative stress induced by the exposure of mitochondrial complex 1 inhibiting pesticide on the dopaminergic neuronal cells.

We have extensively studied about PKCδ and its role in apoptotic signaling leading to PD in the past two decades. PKCδ, a member of the novel PKC family, is a well known and characterized redox-sensitive kinase and it is present in various cell types. Oxidative stress activates the PKCδ kinase by translocation, tyrosine phosphorylation, or proteolysis. During proteolysis, caspase-3 cleaves the native PKCd (72–74 KDa) into 41-kDa catalytically active and 38-kDa regulatory fragments marking the activation of the kinase. The proteolytic activation of PKCδ also plays a key role in promoting apoptotic cell death in various cell types, including neuronal cells. PKCδ is also said to amplify apoptotic signalling via positive feedback activation of the caspase cascade. Thus, the dual role of PKCδ as a mediator and amplifier of apoptosis may be important in the pathogenesis of major neurodegenerative disorders, such as Parkinson's disease, Alzheimer's disease and Huntington disease (Kanthasamy et al., 2003a). The Caspase dependent activation of

PKCδ is one of the most well studied activation mechanisms. It has been shown that MPP$^+$, an oxidized product of the reaction between MPTP (mitochondrial complex I inhibitor) and monoamine oxidase B in the brain has got the ability to potentiate caspase-3 dependent proteolytic activation of PKCδ in dopaminergic neuronal cells (Kaul et al., 2003; Wiemerslage et al., 2013). We have also reported previously that dieldrin, an organochloride form of a pesticide could promote PKCδ mediated dopaminergic neuronal apoptosis (Saminathan et al., 2011). Interestingly, we have demonstrated previously that PKCδ proteolytic cleavage by a caspase-3 cleavage-resistant mutant (PKCδ-CRM) N27 cells were resistant to manganese, MG-132 and 6-OHDA mediated apoptosis (Latchoumycandane et al., 2011a; Latchoumycandane et al., 2005; Sun et al., 2008). Thus showing PKCδ activation plays a critical role oxidative stress in apoptosis. Previously it is reported that, activation of PKCδ in the HL60 post ara-C was observed in a caspase-3 dependent mechanism with concomitant lamin B phosphorylation and proteolysis. This same study also also noted that the inhibition of PKCδ delayed lamin proteolysis (Cross et al., 2000). Despite such evidences, role of PKCδ functioning as a potential laminB1 kinase has not been well understood during the environmental linked neurotoxicant exposure mediated oxidative stress and mitochondrial dysfunction leading to neurodegeneration.

We have previously demonstrated the activation mechanisms of PKCδ and its downstream targets leading to pro-apoptotic signaling in various neurotoxicants cell culture and animal models of PD (Kanthasamy et al., 2003b; Kaul et al., 2005; Kaul et al., 2003; Saminathan et al., 2011; Sun et al., 2008). The present study aimed to investigate the activation of PKCδ post exposure to mitochondrial complex 1 inhibiting pesticide tebufenpyrad in dopamingeric neurons. Here we also show that

activation of PKCδ prior to tebufenpyrad exposure and its potential to cause lamin damage by phosphorylation of laminB1 at T575.

Materials and Methods

Chemicals and Reagents. We purchased tebufenpyrad (96% purity) from AK Scientific Inc. (Union City, CA), DMSO and GeneArt™ Site-Directed Mutagenesis System Kit (A13282) was purchased from Fisher Scientific (Fair Law, NJ). We purchased RPMI 1640 media, fetal bovine serum (FBS), L-glutamine, penicillin, and streptomycin from Molecular Probes (Eugene, OR), Mission Lentiviral Packaging Mix (SHP001; Sigma-Aldrich), Lenti-X p24 Rapid Titer Kit (632200; Clontech, Mountain View, CA), puromycin (Sigma-Aldrich), PKCδ, phospho-PKCδ (T505), laminB1 from Santa Cruz Biotechnology, Inc. (Santa Cruz, CA), phospho-laminB1 (T575) Cell Signaling Technology (Danvers, MA), Caspase-3 substrate, Ac-DEVD-AMC, was purchased from Bachem Biosciences, Inc. (King of Prussia, PA).

Cell culture and treatment paradigm. The rat immortalized mesencephalic dopaminergic neuronal cell line (1RB$_3$AN$_{27}$, also known as N27 cells) was a kind gift from Dr. Kedar N. Prasad (University of Colorado Health Sciences Center, Denver, CO). These N27 cells have the potential to differentiate and produce dopamine in culture when exposed to a suitable cAMP triggering agent, and once the cells are differentiated they possess increased tyrosine hydroxylase (TH) expression and dopamine levels (Adams et al., 1996; Zhang et al., 2007). In this study, undifferentiated cells were grown in RPMI 1640 medium containing 10% FBS, 2 mM L-glutamine, 50 units of penicillin, and 50 μg/ml streptomycin, as described previously (Anantharam et al., 2002; Jin et al., 2011c; Prasad et al., 1998). In general, cells were plated in a tissue culture plate or flask in accordance to the experimental

requirements and was cultured overnight in a humidified atmosphere of 5% CO_2 at 37°C. The cell density plated for each experiment has been provided in the methods section. The cells were treated with the specified concentration 3 µM of tebufenpyrad for 0-3 h in serum-free RPMI media. For all experiments with N27 cells, treatments were performed when the cells were 65-70% confluent. The pesticides tebufenpyrad is lipophilic in nature and are hence dissolved in DMSO.

Cleavage Resistant Mutant - Protein Kinase Cδ (CRM- PKCδ). The CRM- PKCδ stable N27 cell line was created as previously explained in detail and published by (Sun et al., 2008).

CRISPR/Cas9-based knockout of PKCδ in N27 cells. The lentivirus-based CRISPR/Cas9 KO plasmid, pLVU6gRNA-Ef1aPuroCas9GFP-PKCδ, with the PKCδ gRNA target sequence GCGTCGTCCTCCGCCTGCAGGG), was purchased from Sigma-Aldrich. To make lentivirus, the lenti-CRISPR/Cas9 PKCδ KO plasmid and control plasmid were transfected into 293FT cells using the Mission Lentiviral Packaging Mix (SHP001; Sigma-Aldrich) according to the manufacturer's instructions. The lentivirus was harvested 48 h post-transfection and titers were measured using the Lenti-X p24 Rapid Titer Kit (632200; Clontech, Mountain View, CA). For stable KD of PKCδ in N27 cells, six-well plates containing 0.1×10^6 /well had lentivirus added the following morning to the media at an MOI of 100. After 24 h, fresh media supplemented with puromycin (50 µg/ml) was added to the cells for stable cell selection.

Caspase-3 activity assay. Caspase-3 activity were determined as previously described (Anantharam et al., 2002; Kanthasamy et al., 2008). N27 cells in a density of 1×10^6 cells per T25 cell culture flask were seeded the previous day, and briefly the

following day after exposure to tebufenpyrad, the cells were washed once with PBS and re-suspended in lysis buffer containing 50 mM Tris/HCl (pH 7.4), 1 mM EDTA, 10 mM EGTA, and 10 μM digitonin. Cells were then incubated at 37°C for 20–30 min to allow complete lysis. Lysates were quickly centrifuged and cell-free supernatants were incubated with 50 μM Ac-DEVD-AMC (caspase-3 substrate) at 37°C for 1 hr. Caspase activity was then measured using a microplate reader (Molecular Devices Corp., Sunnyvale, CA) with excitation at 380 nm and emission at 460 nm. Caspase activity was calculated as fluorescence unit (FU) per mg protein per hr and was presented as percentage of control.

Site - Directed Mutagenesis. The site directed mutagenesis was performed on the N27 cells for replacing the threonine with glycine at 575 in LaminB1. mCherry-LaminB1-10 was a gift from Michael Davidson (Addgene plasmid # 55069) and was used as template. GeneArt™ Site-Directed Mutagenesis System Kit (A13282) purchased from Fisher Scientific and was used in accordance to the manufacturer's protocol and instructions to mutate threonine, at position 575, into glycine. The synthesis primers used were as follows: GAGGAAGAACTTTTCCACCAGCAGGGAGGCCCAAGAGCATCCAATAGAA GCTG (Forward primer) and CACAGCTTCTATTGGATGCTCTTGGGCCTCCCTGCTGGTGGAAAAGTTCTT CCTC (Reverse primer). The resulting PCR product was purified using PCR Purification Kit (Qiagene) and transformed into DH5alpha E. coli. (Invitrogen). Five positive colonies were randomly picked and expanded to harvest DNA plasmid. The plasmids from each colony were sequenced by Sanger sequencing to confirm mutation at position 575 and the correct plasmids were transfected into 293FT cells.

The highest-expressing plasmid, judged by brightness of mCHERRY (Excitation = 587; Emission = 610) was chosen for transfection into N27 cells for making the mutant.

Phospho-Site identification and Analysis. The Phosphosite analysis was performed on LaminB1, firstly to identify the presence of susceptible site on LaminB1 which are prone to undergoing phosphorylation mediated through an activated kinase. NetPhos 2.0 server (online tool) was used for the identification of phosphorylation sites on LaminB1. Further analysis was performed using PhosphoPICK Site analysis (online tool) to identify the kinase that drove the phosphorylation of the specific site on LaminB1. The procedure for running the PhosphoPICK online service tool was followed as previously performed by (Patrick et al., 2017; Patrick et al., 2015). Protein sequence data for LaminB1 and PKCδ were obtained from the repository of Protein Data Bank (PDB).

NetPhos 2.0 server - http://www.cbs.dtu.dk/services/NetPhos-2.0/

PhosphoPICK Site analysis - http://bioinf.scmb.uq.edu.au/phosphopick/snpanalysis

Organotypic slice culture. All the experiments involving animals followed protocols approved by Iowa State University's Institutional Animal Care and Use Committee (IACUC). Organotypic slice culture was prepared as previously described (Falsig and Aguzzi, 2008; Harischandra et al., 2014b; Kondru et al., 2017). In brief, brain slices were prepared from 9- to 12-day-old mouse pups from PKCδ+/+ and PKCδ-/- colony using a microtome (Compresstome™ VF-300, Precisionary Instruments). After dissecting out the whole brain, the brain was oriented in the coronal plane in the Compresstome's specimen tube, which had been prefilled with 2% low-melting-point agarose. The agar was quickly solidified

by clasping the specimen tube with a chilling block, and then the specimen tube was inserted into the slicing reservoir filled with freshly prepared, ice-cold Gey's balanced salt solution supplemented with the excitotoxic antagonist, kynurenic acid (GBSSK). To prepare GBSS, we added the following in solution in the following order from 10x stocks to obtain the final concentrations per liter: 8 g NaCl, 0.37 g KCl, 0.12 g Na_2HPO_4, 0.22 g $CaCl_2 \cdot 2H_2O$, 0.09 g KH_2PO_4, 0.07 g $MgSO_4 \cdot 7H_2O$, 0.210 g $MgCl_2 \cdot 6H_2O$, 0.227 g $NaHCO_3$. The compression lip located in the cutting chamber helps stabilize the brain specimen while obtaining 300-μm thick slices with the blade set at a medium vibration speed. Slices were collected at the specimen tube's outlet and transferred to another plate with fresh prefilled GBSSK. The slices were washed twice in 6 ml ice-cold GBSSK, transferred to Millicell 6-well plate inserts (3-5 slices per insert) and were incubated in a humidified atmosphere of 5% CO_2 at 37 °C. Culture media was exchanged every other day for 10-14 days with fresh media. Slice cultures were harvested post treatments with tebufenpyrad (20 nM for 24 hrs) by washing twice in 2 ml of ice-cold PBS. The whole cell lysates was performed as mentioned in the below method section on western blot analysis. Finally the Western blot and Immuhisto-chemical analysis for these slices were performed as described below.

Human Post-mortem PD brain samples. We obtained frozen *substantia nigra* tissue samples and cryostat sections from the brains of confirmed post-mortem human PD patients and age-matched neurologically normal individuals from the brain banks at the Miller School of Medicine, University of Miami, FL and the Banner Sun Health Research Institute, AZ. For western blot experiments, the whole cell lysates were prepared as mentioned below in the method section on western blot analysis.

Substantia nigra tissue sections were fixed with 4% paraformaldehyde (PFA) solution (in 0.1 M phosphate-buffered saline, pH 7.4). Cryostat sections were used for immuno-histochemistry experiments as described below. All human post-mortem samples were procured, stored and distributed according to the applicable regulations and guidelines involving consent, protection of human subjects and donor anonymity. Since the post-mortem human brain tissues were obtained from approved national brain banks, Institutional Review Board (IRB) approval from Iowa State University was not required.

Western blot Analysis. N27 dopaminergic neuronal cells were seeded (5×10^{6} cells per T175 cell culture flask). Post treatment of N27 cells with tebufenpyrad (3 μM- 3 h) in a T175 flasks, cell lysates for western blotting analysis were prepared using modified RIPA buffer, as previously described (Kanthasamy et al., 2006b; Latchoumycandane et al., 2011b). Equal amounts of protein (30-35 μg) were loaded for each sample and separated on using 12% SDS-PAGE gels. Proteins were then transferred to a nitrocellulose membrane (BioRad) for immunoblotting and blocked using a blocking buffer specifically formulated for fluorescent Western blotting (Rockland Immunochemicals). The nitrocellulose membrane was subjected to primary antibodies overnight incubation, followed by secondary IR dye-800 conjugated anti-rabbit dye or Alexa Flour 680 conjugated anti-mouse IgG for 1 h at room temperature. Primary antibodies against PKCδ, phospho-PKCδ (T505), laminB1 or phospho-LaminB1 (T575) in blocking buffer solution were then added to the membranes and incubated overnight at 4°C. After another four to five washes, an infrared dye-tagged secondary antibody was added for 1 h. β-Actin was used as a loading control. Western blot images were captured with Odyssey IR Imaging system (LICOR) and data were

analyzed using Odyssey 3.0 software. Similar methodology as mentioned above for western blot analysis and tebufenpyrad treatment was followed and performed on the Control CRISPR/Cas9, PKCδ CRISPR/Cas9 knockdown N27 cells and PKCδ-CRM N27 cells.

Immuno-cytochemistry analysis. Immunofluorescence studies in N27 dopaminergic neuronal cells were performed according to previously published protocols with some modifications (Gordon et al., 2011; Gordon et al., 2016). Briefly, 4 x 10^4 N27 cells were grown on poly-D-lysine-coated coverslips and treated the following day. At the end of treatment with tebufenpyrad, cells were fixed with 4% PFA, washed in PBS and incubated in blocking buffer (PBS containing 2% BSA, 0.5% Triton X-100 and 0.05% Tween 20) for 1 h at room temperature. The coverslips were then incubated overnight at 4°C with respective primary antibodies diluted in PBS containing 2% BSA. Samples were then washed several times in PBS and incubated with Alexa 488 and 555 dye-conjugated secondary antibodies. The nuclei were labeled with Hoechst stain (10 μg/mL) and coverslips were mounted with Fluoromount medium (Sigma Aldrich) on glass slides for visualization.

Immuno-histochemistry analysis. Immunohisto-chemistry (IHC) studies were performed on sections from the *substantia nigra* midbrain region of human post mortem brains as described previously (Ghosh et al., 2013; Gordon et al., 2016; Jin et al., 2011b; Sarkar et al., 2017). Briefly, the fixed brain sections were subjected to antigen retrieval using citrate buffer (10 mM sodium citrate, pH 8.5) for 30 min at 90°C. Sections were then washed several times in PBS and blocked with PBS containing 2% BSA, 0.2% Triton X-100 and 0.05% Tween 20 for 1 h at room temperature. Sections were then incubated with primary antibodies overnight at 4°C

and washed 7 times in PBS on a Belly Dancer Shaker (SPI supplies). The sections were incubated with Alexa 488 and 555 dye-conjugated secondary antibodies for 60-75 min at room temperature and their cell nuclei were stained with Hoechst dye. Sections were mounted on slides using Prolong antifade gold mounting medium (Invitrogen) or using with Fluoromount medium (Sigma Aldrich) according to the manufacturers's instructions. Samples were visualized finally visualized and analyzed using Leica DMIRE2 confocal microscope. For the slice culture samples similar staining strategic method was employed, but with mild modifications in the methodology and experimental conditions as previously described in detail and illustrated by (Aguzzi and Falsig, 2012; Harischandra et al., 2014b; Kondru et al., 2017; Sonati et al., 2013).

Confocal imaging and Z stack image capturing and 3D reconstruction. Confocal imaging was performed at the Iowa State University Microscopy Facility, using a Leica DMIRE2 confocal microscope with the 63X oil objectives and Leica Confocal Software. For the cells, one optical series of Z-stack covered 5-7 optical slices of 0.5 μm thickness each. For slices culture tissue sections and human sections of midbrain region we had employed 12-15 optical slices of 0.5 μm thickness each. The IMARIS software 10.0 was used to analyze the Z stack images. The surface reconstruction wizard in the IMARIS software version 10.0 was used to make 3-D reconstructed images for seeing architectural changes and picture definition. Further details to the images marking topographic alterations were reconstructed using modules in IMARIS such as Normal Shading and 3D surface developer.

Statistical data analysis. All *in vitro* data were determined from at least 2-3 biologically independent experiments, each done with a minimum of three biological

replicates. Data analysis was performed using Prism 4.0 software (GraphPad Software, San Diego, CA). Data were analyzed using one-way ANOVA with the Tukey-Kramer post-test for comparing all treatment groups with that of the control. Differences with $p < 0.05$ were considered statistically significant.

Results

Tebufenpyrad triggers PKCδ activation and increase in caspase-3 activity in the dopaminergic neuronal cell culture model of PD

In our previous years of research, we have shown that MPP^+ and dieldrin induced PKCδ activation in dopaminergic neuronal cells. This activation is depicted by the cleavage of PKCδ into two fragments, one is regulatory and the other is catalytic fragment. Also, phosphorylation of PKCδ at threonine residue position 505, further confirms the activated form of PKCδ (Kaul et al., 2003; Saminathan et al., 2011). Since tebufenpyrad is also a neurotoxic toxicant we wanted to investigate its role in acting as a caspase-3 dependent and PKCδ activation initiator. N27 cells were treated with tebufenpyrad (3 µM) for 1-3 hr and the whole cell lysates were made for performing western blots as shown in our previous studies (Asaithambi et al., 2014; Ay et al., 2015; Carvour et al., 2008; Kitazawa et al., 2001). To show the activation of PKCδ, we have checked for the hallmark signs of cleavage of activated PKCδ and also phosphorylation of PKCδ at T505 using the western blot analysis. These two evidences clearly demonstrated the significant activation of PKCδ triggered by tebufenpyrad exposure in the N27 cells (Figure 1A). Also, to prove the role of caspase-3 in activating PKCδ, we had performed the caspase-3 activity assay on the N27 cells treated with tebufenpyrad (Figure 1B). The caspase-3 assay was carried out as mentioned in our previous studies (Afeseh Ngwa et al., 2009; Carvour et al., 2008;

Gordon et al., 2012; Kanthasamy et al., 2008; Sun et al., 2008). Cumulatively, our results suggested that tebufenpyrad exposure mediated the PKCδ activation in the N27 cells in an caspase-3 dependent manner.

Activated PKCδ phosphorylates laminB1 and modulates lamin damage

PKCδ is a well studied kinase that is known to phosphorylate other proteins (Kanthasamy et al., 2003a; Weng et al., 2015; Xue et al., 2015). So, keeping that in mind we wanted unravel some sites on laminB1 that could be phosphorylated by activate PKCδ. LaminB1 was our target protein of interests primarily because it was known and shown almost two decades ago that PKCδ functioned as a potential apoptotic Lamin Kinase (Cross et al., 2000). We studied this idea of activated PKCδ being a prospective kinase that phosphorylates LaminB1 in the N27 cell model system using two online *insilico* tools that will enable the identification and analysis of phosphorylation sites on LaminB. Firstly, NetPhos 2.0 server was used to identify the sites on LaminB1 that were predicted to be susceptible to kinase action and phosphorylation. The results from NetPhos 2.0 server analysis vividly projected a picture on site Threonine 575 (T575) of LaminB1. The predicted hit for T575 was marked to a scale of 0.975 (Fig. 2A). Furthermore, the analysis using the PhosphoPICK Site analyzer online, it was identified that PKCδ exclusively had promising effect of functioning as a valid and potential kinase for LaminB1. In other words, it was determined that activated PKCδ functioned as a very dependable kinase to phosphorylate LaminB1 (predicted p-value = 0.000392) (Fig. 2A). Additional validation and verification of this prediction was confirmed using the *invitro* model of PD. The western blot analysis showed that post exposure of N27 cells to tebufenpyrad (3 μM) for 1-3 h, there was prominent upregulation of phospho-LaminB1 (T575).

This phosphorylation of LaminB1 further marked the damage of the nuclear membrane by expressing a decrease in LaminB1 levels (Fig.2B). Adding on, further visual investigation was carried out using the immuno-cytochemistry analysis and confocal microscopy. These analysis demonstrated loss of LaminB1 architecture and integrity and activation of PKCδ marked by phosphorylation of PKCδ (T505) (Fig. 3A and B). Also, an interesting observation using the confocal microscopy was that the activated PKCδ localised on with the damaged/damaging nuclear membrane marked using LaminB1 (Fig. 3A) on the N27 dopaminergic neuronal cells.

This study lead to the identification of site T575 on LaminB1 as one of the high targets of activated PKCδ. We treated the N27 cells with and observed by western blot analysis the significant increase in phospho-laminB1 (T575) and also loss of laminB1. Thus showing that PKCδ might be involved in phosphorylating laminB1 at T575 and acting as a lamin kinase thereby inducing laminb1 loss.

PKCδ cleavage resistant mutant N27 cells (PKCδ- CRM) and Stable PKCδ CRISPR/Cas9 Knockdown N27 cells were resistant against tebufenpyrad induced PKCδ activation and laminB1 phosphorylation

Cleavage of PKCδ is one the hallmarks demonstrating its activity. Hence blocking its caspase-3 dependent cleavage inhibits its activation during oxidative stress (Latchoumycandane et al., 2011a; Sun et al., 2008). In order to study the role of PKCδ in acting as a lamin kinase and causing laminB1 damage we exposed the PKCδ-CRM N27 cells with tebufenpyrad (3 µM) for 3 hr. Following the treatment the cells were collected and the whole cell lysates were made as described above. We first checked for the caspase-3 dependent PKCδ cleavage and phospho-PKCδ (T505) for activation. We found that there was no change in either of these two proteins, thereby

showing tebufenpyrad exposure onto the PKCδ-CRM N27 cells did not activate PKCδ (Fig 4D). Adding on, we were further interested in checking for laminB1 and phospho-laminB1(T575). Doing so, we found that there no laminB1 loss or phosphorylation of laminB1 (Fig 4E). Furthermore, we had tested a similar strategy using the CRISPR/Cas9 based PKCδ knockdown N27 stable cell system to validate the importance and role of activated PKCδ in phosphorylating LaminB1.

Control CRISPR/Cas9 and PKCδ CRISPR/Cas9 Knockdown N27 cells were treated tebufenpyrad (3 µM) for 3 hr. Following the treatment the cells were collected and the whole cell lysates were made as described above and previously. The PKCδ CRISPR/Cas9 Knockdown N27 cells possessed a 90% message level knockout of PKCδ compared to the Control CRISPR/Cas9. This stable knockdown was developed using the CRISPR/Cas9 methodology as described in the methods section. It was observed that the PKCδ CRISPR/Cas9 Knockdown N27 cells post tebufenpyrad treatment did not have any observable phosphorylation of PKCδ at T505 and as a consequence no activation of PKCδ (Fig 4C). Adding on, the inhibition in the activation of PKCδ also lead to restricted LaminB1 damage and phosphorylation of LaminB1 at T575 in the PKCδ CRISPR/Cas9 Knockdown compared to the Control CRISPR/Cas9 N27 cells post treatment with tebufenpyrad (Fig 4A and B). The immuno-cytochemistry analysis performed using fluorescent labeled antibodies and confocal microscopy, also revealed concordantly that the PKCδ CRISPR/Cas9 Knockdown compared to the control CRISPR/Cas9 N27 cells, did not show any activation of PKCδ and LaminB1 loss (nuclear membrane damage) (Fig. 4F). This results also states that there was no clear phosphorylation of LaminB1 at T575, which is mark for nuclear membrane damage.

Cumulatively, it is very comprehendible that PKCδ activation is essential in functioning as a lamin kinase and also in causing lamin damage. Hence the inhibition of PKCδ activation might play a very crucial role in mediating the prevention of lamin damage.

Site-directed mutagenesis of T575 on LaminB1 prevented its phosphorylation based activation and damage post tebufenpyrad induced oxidative stress in the N27 dopaminergic neuronal cells

An efficient molecular strategy of site-directed mutageneis was employed for lucidly describing the role of threonine 575 site specific phosphorylation of LaminB1 by activated PKCδ upon tebufenpyrad exposure in the dopaminergic neuronal cells. Here in this techniques (as previous mentioned in the methods section), the threonone site at 575 was replaced by glycine, a smaller amino acid which keeps the protein in its stable conformation. Now we have a LaminB1 which possess glycine at 575 instead of threonine in the N27 cell line system. Post treatment of these N27 cells which have prior undergone site-directed mutageneis with tebufenpyrad (3 μM) for 3 hr, there was no phosphorylation of LaminB1 at site 575 and also no LaminB1 loss was observed (Fig. 5 A and B). This clearly demonstrates the important role of site 575 on LaminB1, which contributes for the destruction of nuclear membrane upon phosphorylation at 575. Therefore, amalgamation of this result suggests the important role of site 575 on LaminB1 as a specific site of phosphorylation triggered by the activated PKCδ post exposure of the dopaminergic neuronal N27 cells to the mitochondrial inhibiting toxicant tebufenpyrad.

Organotypic slice culture of PKCδ-/- pups demonstrates protection against LaminB1 loss and LaminB1 phosphorylation (T575)

Organotypic slice culture has been developing as a promising technique in recent years in brain related research. Although it has been in existence for several decades, its translational importance and usage as an *exvivo* method for validating , proving hypotheses and toxicity studies, has made it a potential and implacable tool (Harischandra et al., 2014c; Humpel, 2015; Kondru et al., 2017; Testa et al., 2005; Ullrich and Humpel, 2009). We have employed the organotypic slice culture methodology to understand the LaminB1 phosphorylation mechanism and the role of PKCδ function as a LaminB1 kinase in the midbrain post exposure to mitochondrial inhibiting pesticides tebufenpyrad, translating the model system from *invitro* to *exvivo*. In our present study, we had prepared the organotypic slices (350 μm thickness) from the midbrain of 9-12 day old PKCδ+/+ and PKCδ-/- pups as described in detail in the methods section above. These slices were treated with teubfenpyrad at a dose of 20 nM for 24 hrs. The western blot analysis and immunofluorescence suing confocal microscopy post tebufenpyrad treatment reveal that the PKCδ-/- pups demonstrate protection against LaminB1 loss and also phsophorylation of LaminB1 at T575. Whereas the PKCδ+/+ post tebufenpyrad exposure, shows susceptibility to LaminnB1 damage or loss and also visual noteworthy LaminB1 phosphorylation (T575) was observed (Fig. 6 A and B). This data suggests a specific role of PKCδ as a LaminB1 kinase, mediating the damage of LaminB1 and nuclear membrane in a exvivo model system post exposure to the mitochondrial toxicant such as tebufenpyrad. Thus marking a functional target of PKCδ kinase activity.

LaminB1 phosphorylation and PKCδ activation in substantia nigra of postmortem Parkinson's disease brains

The above results from data it is suggested that PKCδ upon activation by oxidative stress induced by tebufenpyrad exposure, functions as a LaminB1 kinase, phosphorylating LaminB1 at threonine 575. It has been shown previously through many epidemiological studies and animal models of PD that oxidative stress is one of the critical factors associated with the loss of dopaminergic neurons by apoptosis (Banerjee et al., 2009; Bose and Beal, 2016; Dauer and Przedborski, 2003; Kanthasamy et al., 2010; Przedborski and Ischiropoulos, 2005). Hence we in this study developed a translational evidence subtitling the function of activated PKCδ as a LaminB1 kinase. In this study we had employed 11 control and 11 PD post mortem *substantia nigra* tissues for our analysis. The western blot analysis revealed a significant augmentation of phospho- PKCδ (T505) compared to the control brains. This upregulation of phospho- PKCδ (T505), marked the activated state of PKCδ (Fig 7A) (Afeseh Ngwa et al., 2009; Kanthasamy et al., 2006b; Kanthasamy et al., 2003b). Further analysis demonstrated, the loss of LaminB1 and upregulation of phospho-LaminB1 (T575) in the PD post mortem *substantia nigra* compared to the control brain samples (Fig 7A). Adding on, the immuno-histochemical staining study on human midbrain sections, demonstrated a loss in LaminB1 expression and also structural impaired or damage nuclear membrane damage in the PD samples compared to the controls (Fig 7B). Cumulatively, this data observed by the analysis of PD and control *substantia nigra* tissues and sections, depicts and shows similar trend of mechanism of PKCδ functions as a LaminB1 kinase, from our above shown *invitro* and *exvivo* studies. Thus suggesting and highlighting the importance of functional of

role of activated PKCδ as a LaminB1 kinase, post oxidative stress induced in dopaminergic neuronal cells.

Discussion

In our present study, we have attempted to elucidate the role of activated protein kinase cδ (PKCδ), in functioning as a LaminB1 kinase and henceforth initiating the process of nuclear membrane damage prior to exposure to tebufenpyrad in the N27 neuronal cells. Although, a similar idea had been demonstrated couple decades ago in an oncological setting, the exact mechanism and the cause for PKCδ functioning as a lamin kinase still remained unexplained and in the dark. Our study, demonstrated the accentuated ability of tebufenpyrad mediated oxidative stress, causing a caspase-3 dependent PKCδ activation. Furthermore, the activated PKCδ also lead to the phosphorylation of LaminB1 at T575, thereby leading to LaminB1 loss and nuclear membrane damage.

It has been very well studied in the past decades, the effect of mitochondrial dysfunction post pesticides exposure causes changes in oxidative phosphorylation, alterations in mitochondrial DNA replication, functional dynamics and respiration. These have all been noted prominently as critical contributing factors for the pathogenesis of Parkinson's disease (PD)(Greenamyre et al., 2001; Lin and Beal, 2006; Sherer et al., 2007) (Afeseh Ngwa et al., 2011; Kitazawa et al., 2004; Kitazawa et al., 2001). Our toxicant of interest here is tebufenpyrad, a greenhouse pesticide in the United States of America and many other parts of the world (EPA PC Code-090102). It is primarily used for the protection of ornamental plants against the action of mites and spiders. Tebufenpyrad has been classified as a mitochondrial complex 1 inhibitor by the Insecticide Resistance Action Committee (IRAC). We have recently

shown significant alterations in mitochondrial functional dynamics and structure, post exposure to tebufenpyrad in the N27 dopmaniergic neuronal cells, thereby underlining tebufenpyrad's potent neurotoxic effects (Charli et al., 2016).

In this chapter we have extended our studies, in searching for answers regarding the ability of tebufenpyrad exposure to initiate PKCδ activation, LaminB1 loss and nuclear membrane damage in the dopaminergic neurons. Our lab in several of our previous studies have shown that exposure of dopaminergic neuronal cells to dieldrin and MPP^{+}, lead to caspase-3 dependent exacerbated activation of PKCδ, thereby triggering a cascade pro-apoptotic signaling (Kaul et al., 2003; Saminathan et al., 2011; Wiemerslage et al., 2013). In this present study, we had treated the N27 dopaminergic neuronal cells with tebufenpyrad (3 μM) for 3 hr and observed the activation of PKCδ. The activation of PKCδ was confirmed by the hallmark proteolytic cleavage and phosphorylation of PKCδ at T505 (Fig. 1A). Additionally we had observed the significant increase in caspase-3 activity post tebufenpyrad treatment, hence making the PKCδ activation a caspase-3 dependent mechanism (Fig. 1B). Following these studies, the novel idea of identifying the specific target for activated PKCδ to function as an activated kinase was systematically unraveled using online phosphosite analysis tools such as NetPhos Server 2.0 and PhosphoPICK site analysis. These tools unopened an interesting target of LaminB1. It was predicted being one of the most susceptible target for PKCδ upon its activation by oxidative stress conditions induced by tebufenpyrad exposure. The NetPhos Server2.0, predicted the site on LaminB1 that was most prone to phosphorylation modeification (predicted value - 0.975) and the PhosphoPICK Site analysis enabled to determine predicted effect of activated PKCδ on the LaminB1. After meticulous analysis and

prediction it was identified that T575 on LaminB1 was the most susceptible site for phosphorylation induced by the activated PKCδ (Fig. 2A). Further study using the western blot analysis method, we had demonstrated LaminB1 down-regulation and increase in phospho-LaminB1 (T575) post tebufenpyrad exposure in the N27 cells (Fig. 2B). Adding on, similar study using immuno-cytochemistry staining and confocal microscopy was performed in order to obtain a visual perspective detail. It was observed using confocal microscopy that the activated PKCδ localized on the nuclear membrane stained with LaminB1 in the form of a crown like structure and also the activation of PKCδ was confirmed by the phosphorylation of PKCδ at T505 (Fig. 3A and B). Further carefully inspection provided us the evidence of loss LaminB1, thereby visually depicting the nuclear membrane damage in the N27 cells post tebufenpyrad exposure. Thus confirming the tebufenpyrad induced activation of PKCδ and LaminB1 loss.

In our study, PKCδ' s activation plays a vital part in functioning as a lamin kinase post the exposure of N27 cells with tebufenpyrad. In order to further strength this hypothesis, we had generated the PKCδ-CRM N27 cells and PKCδ CRISPR/Cas9 knockdown stable N27 cell lines. Previously, it has been shown that PKCδ functions as an apoptotic lamin kinase in the HL-60 cells (Cross et al., 2000). Hence, proving the kinase function of activated PKCδ targeted to the phosphorylation of LaminB1 in the dopaminergic neuronal cells is an crucial factor. We have shown previously using the PKCδ-CRM N27 cells that the important step of PKCδ proteolytic cleavage marks its activation and kinase functional role (Sun et al., 2008). In this present study, the first cell culture model system we had employed was the PKCδ-CRM N27 cells treated with tebufenpyrad as mentioned above. It was vividly observed that the PKCδ-

CRM N27 cells post tebufenpyrad treatment did not demonstrate PKCδ activation, further analysis also revealed that PKCδ-CRM N27 cells also did not demonstrate any LaminB1 loss or phosphorylation of LaminB1 at T575. Thus this result suggested that PKCδ is indeed a critical component in functioning as a LaminB1 kinase and nuclear membrane damage (Fig. 4D and E). The second *invitro* model system that we had employed was the PKCδ CRISPR/Cas9 knockdown stable N27 cells. As mentioned above, the control PKCδ CRISPR/Cas9 and PKCδ CRISPR/Cas9 knockdown stable N27 cells were treated with tebufenpyrad and was then compared to the corresponding untreated groups. Upon treatment with tebufenpyrad the PKCδ CRISPR/Cas9 knockdown stable N27 cells did not express any noteworthy upregulation of phospho- PKCδ (T505) compared to the corresponding control CRISPR/Cas9 N27 cells that were exposed to tebufenpyrad. This meant that there was no observed activation of PKCδ in the PKCδ CRISPR/Cas9 knockdown stable N27 cells. As a result, there was also no observed LaminB1 loss and phosphorylation of LaminB1 (T575) (Fig. 4 A, B, C and F).

Using the site-directed mutageneis approach we highlighted the site specific phosphorylation of LaminB1 triggered by PKCδ activation. The method was driven by replacing the threonine site at 575 on LaminB1 with glycine. Thus manipulating the LaminB1, with destructing its protein level integrity. This study was carried post the mutation by treating the wildtype N27 cells and mutant N27 cells with tebufenpyrad and it was compared with their corresponding controls. It was observed that the mutant did not exhibit any loss of LaminB1 or phosphorylation of LaminB1 at site 575 post tebufenpyrad exposure compared to its control. Whereas, the wildtype corroboratively showed LaminB1 loss and phosphorylation at site 575, prior to

tebufenpyrad treatment. Thus iterating that post tebufenpyrad exposure in the N27 cells, the activated PKCδ further functions as a LaminB1 kinase, phosphorylating LaminB1 at T575 and thereby leading to LaminB1 loss and nuclear membrane damage. Also, adding on, evidences from the organotypic slice culture studies of PKCδ+/+ and PKCδ-/- pup midbrains and from the control and PD post mortem *substantia nigra* tissues analyzes, demonstrated the function of activated PKCδ as a LaminB1 kinase (Fig 6A, 6B, 7A and 7B).

Cumulatively, our data demonstrate that the mitochondrial complex 1 inhibiting greenhouse pesticide tebufenpyrad is able to induce a caspase-3 dependent PKCδ activation. The activated PKCδ further functions as a kinase phosphorylating LaminB1 at T575, resulting in the loss of LaminB1 and hence destructing the structural integrity of nuclear membrane resulting in the apoptotic cell death of the N27 dopaminergic neuronal cells. The highlight and critical take from this study is, LaminB1at T575 serves as a susceptible target for activated PKCδ and leads apoptotic neuronal cell death post exposure of mitochondria inhibiting pesticide tebufenpyrad. Thus untangling this novel mechanism would enable to build a bridge to further explore some innovative drug targets and prospective small molecules that could be used against the dopaminergic neuronal degeneration involved in PD.

References

Adams, F.S., La Rosa, F.G., Kumar, S., Edwards-Prasad, J., Kentroti, S., Vernadakis, A., Freed, C.R., and Prasad, K.N. (1996). Characterization and transplantation of two neuronal cell lines with dopaminergic properties. Neurochem Res 21, 619-627.

Afeseh Ngwa, H., Kanthasamy, A., Anantharam, V., Song, C., Witte, T., Houk, R., and Kanthasamy, A.G. (2009). Vanadium induces dopaminergic neurotoxicity via protein kinase Cdelta dependent oxidative signaling mechanisms: relevance to etiopathogenesis of Parkinson's disease. Toxicol Appl Pharmacol 240, 273-285.

Afeseh Ngwa, H., Kanthasamy, A., Gu, Y., Fang, N., Anantharam, V., and Kanthasamy, A.G. (2011). Manganese nanoparticle activates mitochondrial dependent apoptotic signaling and autophagy in dopaminergic neuronal cells. Toxicol Appl Pharmacol 256, 227-240.

Aguzzi, A., and Falsig, J. (2012). Prion propagation, toxicity and degradation. Nat Neurosci 15, 936-939.

Anantharam, V., Kitazawa, M., Wagner, J., Kaul, S., and Kanthasamy, A.G. (2002). Caspase-3-dependent proteolytic cleavage of protein kinase Cdelta is essential for oxidative stress-mediated dopaminergic cell death after exposure to methylcyclopentadienyl manganese tricarbonyl. J Neurosci 22, 1738-1751.

Asaithambi, A., Ay, M., Jin, H., Gosh, A., Anantharam, V., Kanthasamy, A., and Kanthasamy, A.G. (2014). Protein kinase D1 (PKD1) phosphorylation promotes dopaminergic neuronal survival during 6-OHDA-induced oxidative stress. PLoS One 9, e96947.

Ay, M., Jin, H., Harischandra, D.S., Asaithambi, A., Kanthasamy, A., Anantharam, V., and Kanthasamy, A.G. (2015). Molecular cloning, epigenetic regulation, and functional characterization of Prkd1 gene promoter in dopaminergic cell culture models of Parkinson's disease. J Neurochem 135, 402-415.

Banerjee, R., Starkov, A.A., Beal, M.F., and Thomas, B. (2009). Mitochondrial dysfunction in the limelight of Parkinson's disease pathogenesis. Biochim Biophys Acta 1792, 651-663.

Bose, A., and Beal, M.F. (2016). Mitochondrial dysfunction in Parkinson's disease. J Neurochem 139 Suppl 1, 216-231.

Carvour, M., Song, C., Kaul, S., Anantharam, V., and Kanthasamy, A. (2008). Chronic low-dose oxidative stress induces caspase-3-dependent PKCdelta proteolytic activation and apoptosis in a cell culture model of dopaminergic neurodegeneration. Ann N Y Acad Sci 1139, 197-205.

Charli, A., Jin, H., Anantharam, V., Kanthasamy, A., and Kanthasamy, A.G. (2016). Alterations in mitochondrial dynamics induced by tebufenpyrad and pyridaben in a dopaminergic neuronal cell culture model. Neurotoxicology 53, 302-313.

Corrigan, F.M., Wienburg, C.L., Shore, R.F., Daniel, S.E., and Mann, D. (2000). Organochlorine insecticides in substantia nigra in Parkinson's disease. J Toxicol Environ Health A 59, 229-234.

Cross, T., Griffiths, G., Deacon, E., Sallis, R., Gough, M., Watters, D., and Lord, J.M. (2000). PKC-delta is an apoptotic lamin kinase. Oncogene 19, 2331-2337.

Dauer, W., and Przedborski, S. (2003). Parkinson's disease: mechanisms and models. Neuron 39, 889-909.

Falsig, J., and Aguzzi, A. (2008). The prion organotypic slice culture assay--POSCA. Nat Protoc 3, 555-562.

Fleming, L., Mann, J.B., Bean, J., Briggle, T., and Sanchez-Ramos, J.R. (1994). Parkinson's disease and brain levels of organochlorine pesticides. Ann Neurol 36, 100-103.

Ghosh, A., Saminathan, H., Kanthasamy, A., Anantharam, V., Jin, H., Sondarva, G., Harischandra, D.S., Qian, Z., Rana, A., and Kanthasamy, A.G. (2013). The peptidyl-prolyl isomerase Pin1 up-regulation and proapoptotic function in dopaminergic neurons: relevance to the pathogenesis of Parkinson disease. The Journal of biological chemistry 288, 21955-21971.

Gordon, R., Anantharam, V., Kanthasamy, A.G., and Kanthasamy, A. (2012). Proteolytic activation of proapoptotic kinase protein kinase Cδ by tumor necrosis factor α death receptor signaling in dopaminergic neurons during neuroinflammation. J Neuroinflammation 9, 82.

Gordon, R., Hogan, C.E., Neal, M.L., Anantharam, V., Kanthasamy, A.G., and Kanthasamy, A. (2011). A simple magnetic separation method for high-yield isolation of pure primary microglia. Journal of neuroscience methods 194, 287-296.

Gordon, R., Neal, M.L., Luo, J., Langley, M.R., Harischandra, D.S., Panicker, N., Charli, A., Jin, H., Anantharam, V., Woodruff, T.M., *et al.* (2016). Prokineticin-2 upregulation during neuronal injury mediates a compensatory protective response against dopaminergic neuronal degeneration. Nat Commun 7, 12932.

Greenamyre, J.T., Sherer, T.B., Betarbet, R., and Panov, A.V. (2001). Complex I and Parkinson's disease. IUBMB Life 52, 135-141.

Harischandra, D.S., Kondru, N., Martin, D.P., Kanthasamy, A., Jin, H., Anantharam, V., and Kanthasamy, A.G. (2014a). Role of proteolytic activation of protein kinase Cdelta in the pathogenesis of prion disease. Prion 8, 143-153.

Harischandra, D.S., Kondru, N., Martin, D.P., Kanthasamy, A., Jin, H., Anantharam, V., and Kanthasamy, A.G. (2014b). Role of proteolytic activation of protein kinase Cδ in the pathogenesis of prion disease. Prion 8, 143-153.

Humpel, C. (2015). Organotypic brain slice cultures: A review. Neuroscience 305, 86-98.

Jin, H., Kanthasamy, A., Ghosh, A., Anantharam, V., Kalyanaraman, B., and Kanthasamy, A.G. (2014). Mitochondria-targeted antioxidants for treatment of Parkinson's disease: preclinical and clinical outcomes. Biochim Biophys Acta 1842, 1282-1294.

Jin, H., Kanthasamy, A., Ghosh, A., Yang, Y., Anantharam, V., and Kanthasamy, A.G. (2011a). alpha-Synuclein negatively regulates protein kinase Cdelta expression to suppress apoptosis in dopaminergic neurons by reducing p300 histone acetyltransferase activity. The Journal of neuroscience : the official journal of the Society for Neuroscience 31, 2035-2051.

Jin, H., Kanthasamy, A., Ghosh, A., Yang, Y., Anantharam, V., and Kanthasamy, A.G. (2011b). α-Synuclein negatively regulates protein kinase Cδ expression to suppress apoptosis in dopaminergic neurons by reducing p300 histone acetyltransferase activity. J Neurosci 31, 2035-2051.

Kanthasamy, A., Jin, H., Mehrotra, S., Mishra, R., Kanthasamy, A., and Rana, A. (2010). Novel cell death signaling pathways in neurotoxicity models of dopaminergic degeneration: relevance to oxidative stress and neuroinflammation in Parkinson's disease. Neurotoxicology 31, 555-561.

Kanthasamy, A.G., Anantharam, V., Zhang, D., Latchoumycandane, C., Jin, H., Kaul, S., and Kanthasamy, A. (2006). A novel peptide inhibitor targeted to caspase-3 cleavage site of a proapoptotic kinase protein kinase C delta (PKCdelta) protects against dopaminergic neuronal degeneration in Parkinson's disease models. Free Radic Biol Med 41, 1578-1589.

Kanthasamy, A.G., Kitazawa, M., Kanthasamy, A., and Anantharam, V. (2003a). Role of proteolytic activation of protein kinase Cdelta in oxidative stress-induced apoptosis. Antioxid Redox Signal 5, 609-620.

Kanthasamy, A.G., Kitazawa, M., Kaul, S., Yang, Y., Lahiri, D.K., Anantharam, V., and Kanthasamy, A. (2003b). Proteolytic activation of proapoptotic kinase PKCdelta is regulated by overexpression of Bcl-2: implications for oxidative stress and environmental factors in Parkinson's disease. Ann N Y Acad Sci 1010, 683-686.

Kanthasamy, A.G., Kitazawa, M., Yang, Y., Anantharam, V., and Kanthasamy, A. (2008). Environmental neurotoxin dieldrin induces apoptosis via caspase-3-dependent proteolytic activation of protein kinase C delta (PKCdelta): Implications for neurodegeneration in Parkinson's disease. Mol Brain 1, 12.

Kaul, S., Kanthasamy, A., Kitazawa, M., Anantharam, V., and Kanthasamy, A.G. (2003). Caspase-3 dependent proteolytic activation of protein kinase C delta mediates and regulates 1-methyl-4-phenylpyridinium (MPP+)-induced apoptotic cell death in dopaminergic cells: relevance to oxidative stress in dopaminergic degeneration. Eur J Neurosci 18, 1387-1401.

Kitazawa, M., Anantharam, V., Kanthasamy, A., and Kanthasamy, A.G. (2004). Dieldrin promotes proteolytic cleavage of poly(ADP-ribose) polymerase and apoptosis in dopaminergic cells: protective effect of mitochondrial anti-apoptotic protein Bcl-2. Neurotoxicology 25, 589-598.

Kitazawa, M., Anantharam, V., and Kanthasamy, A.G. (2001). Dieldrin-induced oxidative stress and neurochemical changes contribute to apoptopic cell death in dopaminergic cells. Free Radic Biol Med 31, 1473-1485.

Kondru, N., Manne, S., Greenlee, J., West Greenlee, H., Anantharam, V., Halbur, P., and Kanthasamy, A. (2017). Integrated Organotypic Slice Cultures and RT-QuIC (OSCAR) Assay: Implications for Translational Discovery in Protein Misfolding Diseases. Sci Rep 7, 43155.

Latchoumycandane, C., Anantharam, V., Jin, H., and Kanthasamy, A. (2011a). Dopaminergic neurotoxicant 6-OHDA induces oxidative damage through proteolytic activation of PKCδ in cell culture and animal models of Parkinson's disease. Toxicol Appl Pharmacol 256, 314-323.

Latchoumycandane, C., Anantharam, V., Jin, H., Kanthasamy, A., and Kanthasamy, A. (2011b). Dopaminergic neurotoxicant 6-OHDA induces oxidative damage through proteolytic activation of PKCdelta in cell culture and animal models of Parkinson's disease. Toxicol Appl Pharmacol 256, 314-323.

Latchoumycandane, C., Anantharam, V., Kitazawa, M., Yang, Y., Kanthasamy, A., and Kanthasamy, A.G. (2005). Protein kinase Cdelta is a key downstream mediator of manganese-induced apoptosis in dopaminergic neuronal cells. J Pharmacol Exp Ther 313, 46-55.

Levy, O.A., Malagelada, C., and Greene, L.A. (2009). Cell death pathways in Parkinson's disease: proximal triggers, distal effectors, and final steps. Apoptosis 14, 478-500.

Lin, M., Chandramani-Shivalingappa, P., Jin, H., Ghosh, A., Anantharam, V., Ali, S., Kanthasamy, A.G., and Kanthasamy, A. (2012). Methamphetamine-induced neurotoxicity linked to ubiquitin-proteasome system dysfunction and autophagy-related changes that can be modulated by protein kinase C delta in dopaminergic neuronal cells. Neuroscience 210, 308-332.

Lin, M.T., and Beal, M.F. (2006). Mitochondrial dysfunction and oxidative stress in neurodegenerative diseases. Nature 443, 787-795.

Patrick, R., Kobe, B., Lê Cao, K.A., and Bodén, M. (2017). PhosphoPICK-SNP: quantifying the effect of amino acid variants on protein phosphorylation. Bioinformatics 33, 1773-1781.

Patrick, R., Lê Cao, K.A., Kobe, B., and Bodén, M. (2015). PhosphoPICK: modelling cellular context to map kinase-substrate phosphorylation events. Bioinformatics 31, 382-389.

Prasad, K.N., Clarkson, E.D., La Rosa, F.G., Edwards-Prasad, J., and Freed, C.R. (1998). Efficacy of grafted immortalized dopamine neurons in an animal model of parkinsonism: a review. Mol Genet Metab 65, 1-9.

Priyadarshi, A., Khuder, S.A., Schaub, E.A., and Shrivastava, S. (2000). A meta-analysis of Parkinson's disease and exposure to pesticides. Neurotoxicology 21, 435-440.

Przedborski, S., and Ischiropoulos, H. (2005). Reactive oxygen and nitrogen species: weapons of neuronal destruction in models of Parkinson's disease. Antioxid Redox Signal 7, 685-693.

Samii, A., Nutt, J.G., and Ransom, B.R. (2004). Parkinson's disease. Lancet 363, 1783-1793.

Saminathan, H., Asaithambi, A., Anantharam, V., Kanthasamy, A.G., and Kanthasamy, A. (2011). Environmental neurotoxic pesticide dieldrin activates a non receptor tyrosine kinase to promote PKCδ-mediated dopaminergic apoptosis in a dopaminergic neuronal cell model. Neurotoxicology 32, 567-577.

Sarkar, S., Malovic, E., Harishchandra, D.S., Ghaisas, S., Panicker, N., Charli, A., Palanisamy, B.N., Rokad, D., Jin, H., Anantharam, V., *et al.* (2017). Mitochondrial impairment in microglia amplifies NLRP3 inflammasome proinflammatory signaling in cell culture and animal models of Parkinson's disease. NPJ Parkinsons Dis 3, 30.

Schapira, A.H. (2007). Mitochondrial dysfunction in Parkinson's disease. Cell Death Differ 14, 1261-1266.

Sherer, T.B., Richardson, J.R., Testa, C.M., Seo, B.B., Panov, A.V., Yagi, T., Matsuno-Yagi, A., Miller, G.W., and Greenamyre, J.T. (2007). Mechanism of toxicity of pesticides acting at complex I: relevance to environmental etiologies of Parkinson's disease. J Neurochem 100, 1469-1479.

Sonati, T., Reimann, R.R., Falsig, J., Baral, P.K., O'Connor, T., Hornemann, S., Yaganoglu, S., Li, B., Herrmann, U.S., Wieland, B., *et al.* (2013). The

toxicity of antiprion antibodies is mediated by the flexible tail of the prion protein. Nature 501, 102-106.

Spivey, A. (2011). Rotenone and paraquat linked to Parkinson's disease: human exposure study supports years of animal studies. Environ Health Perspect 119, A259.

Sun, F., Kanthasamy, A., Song, C., Yang, Y., Anantharam, V., and Kanthasamy, A.G. (2008). Proteasome inhibitor-induced apoptosis is mediated by positive feedback amplification of PKCdelta proteolytic activation and mitochondrial translocation. J Cell Mol Med 12, 2467-2481.

Tanner, C.M., Kamel, F., Ross, G.W., Hoppin, J.A., Goldman, S.M., Korell, M., Marras, C., Bhudhikanok, G.S., Kasten, M., Chade, A.R., *et al.* (2011). Rotenone, paraquat, and Parkinson's disease. Environ Health Perspect 119, 866-872.

Testa, C.M., Sherer, T.B., and Greenamyre, J.T. (2005). Rotenone induces oxidative stress and dopaminergic neuron damage in organotypic substantia nigra cultures. Brain Res Mol Brain Res 134, 109-118.

Ullrich, C., and Humpel, C. (2009). Rotenone induces cell death of cholinergic neurons in an organotypic co-culture brain slice model. Neurochem Res 34, 2147-2153.

Weng, Y.C., Wang, G., Messing, R.O., and Chou, W.H. (2015). Identification of lipocalin-2 as a PKCδ phosphorylation substrate in neutrophils. J Biomed Sci 22, 21.

Wiemerslage, L., Schultz, B.J., Ganguly, A., and Lee, D. (2013). Selective degeneration of dopaminergic neurons by MPP(+) and its rescue by D2 autoreceptors in Drosophila primary culture. J Neurochem 126, 529-540.

Xue, J., Chen, Y., Wu, Y., Wang, Z., Zhou, A., Zhang, S., Lin, K., Aldape, K., Majumder, S., Lu, Z., and Huang, S. (2015). Tumour suppressor TRIM33 targets nuclear β-catenin degradation. Nat Commun 6, 6156.

Zhang, D., Kanthasamy, A., Yang, Y., Anantharam, V., and Kanthasamy, A. (2007). Protein kinase C delta negatively regulates tyrosine hydroxylase activity and dopamine synthesis by enhancing protein phosphatase-2A activity in dopaminergic neurons. The Journal of neuroscience : the official journal of the Society for Neuroscience 27, 5349-5362.

Zhang, Y., and Chan, D.C. (2007). New insights into mitochondrial fusion. FEBS Lett 581, 2168-2173.

Figures

A)

B)
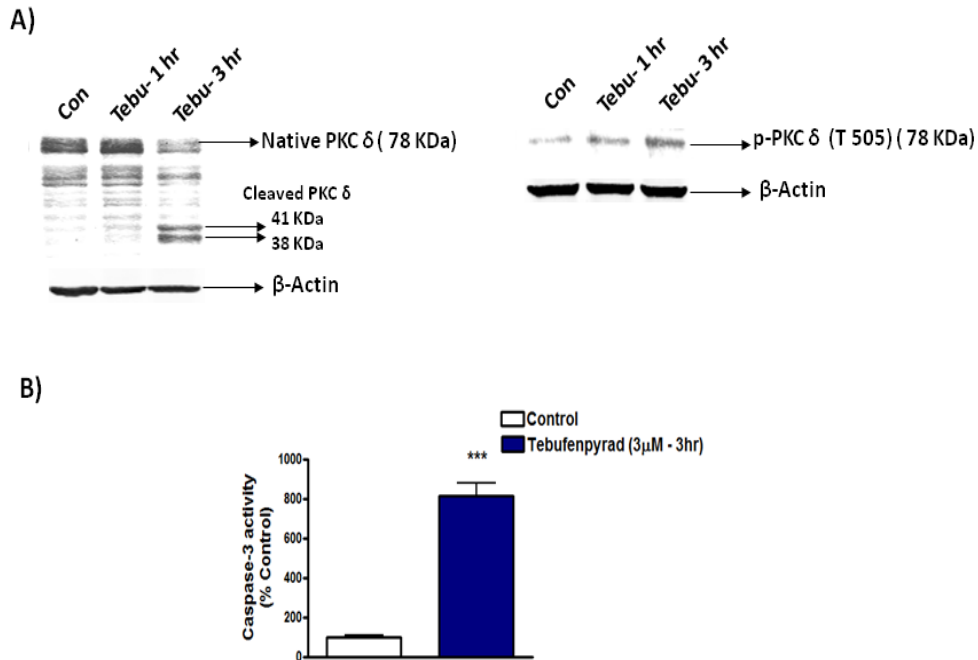
Figure 1: PKCδ activation triggered by oxidative stress induced by tebufenpyrad in N27 cells

(A) Proteolytic cleavage dependent activation of PKCδ and phosphorylation of PKCδ at T505 induced by tebufenpyrad **-** N27 cells were treated with tebufenpyrad (3 μM) for 3 hr and cell lysates were prepared and subjected to Western blot analysis. Representative immunoblots of PKCδ and phospho- PKCδ (T505) as shown above in section A. (B) Tebufenpyrad induced significant caspase-3 activity in the N27 cells **-** The cells were then exposed to tebufenpyrad (3 μM) for 3 hr. Cells were collected and assayed for caspase-3 activity using the Ac-DEVD-AMC caspase-3 substrate. Data shown represent mean ± SEM from two independent experiments performed in quadruplicate (***$p<0.001$).

A)
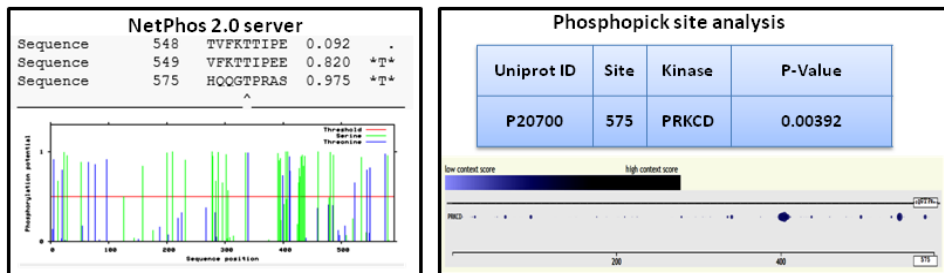
B)

Figure 2: Activated PKCδ functions as a lamin kinase, initiating laminB1 phosphorylation and orchestrates lamin damage

(A) In-silico and phospho site matching analyses shows PKCδ site targets on laminB1- Online analysis tools NetPhos Server 2.0 and PhsphoPICK Site analysis tool was used for the above study. (B) PKCδ phosphorylates laminB1 at T575 and induces lamin damage - N27 cells were treated with tebufenpyrad (3 µM) for 3 hr and cell lysates were prepared and subjected to Western blot analysis. Representative immunoblots of LaminB1 and phospho- LaminB1 (T575).
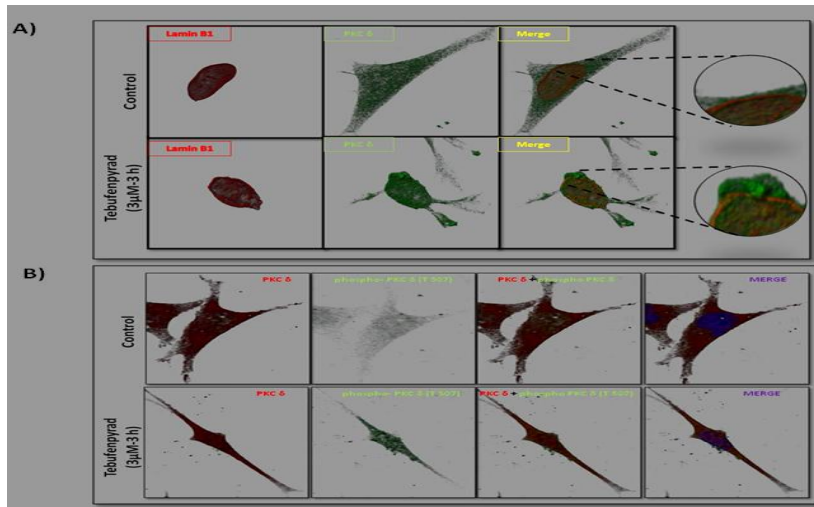
Figure 3: Immuno-cytochemistry shows localisation of activated PKCδ and lamin B1

(A) Localisation of PKCδ onto laminB1 on the nuclear membrane post tebufenpyrad exposure on N27 dopaminergic neuronal cells - N27 cells were treated with tebufenpyrad (3 μM) for 3 hr (B) and were fluorescently stained for PKCδ (green) and LaminB1 (red). phosphorylates laminB1 at T575 and induces lamin damage - N27 cells were treated with tebufenpyrad (3 μM) for 3 hr (B) and were fluorescently stained for PKCδ (red) and phospho- PKCδ (T505) (green). The z-stack images were captured on using a 63X oil immersion lens of the Leica Confocal Microscopy system and the processing of images were performed using IMARIS 10.0 software.
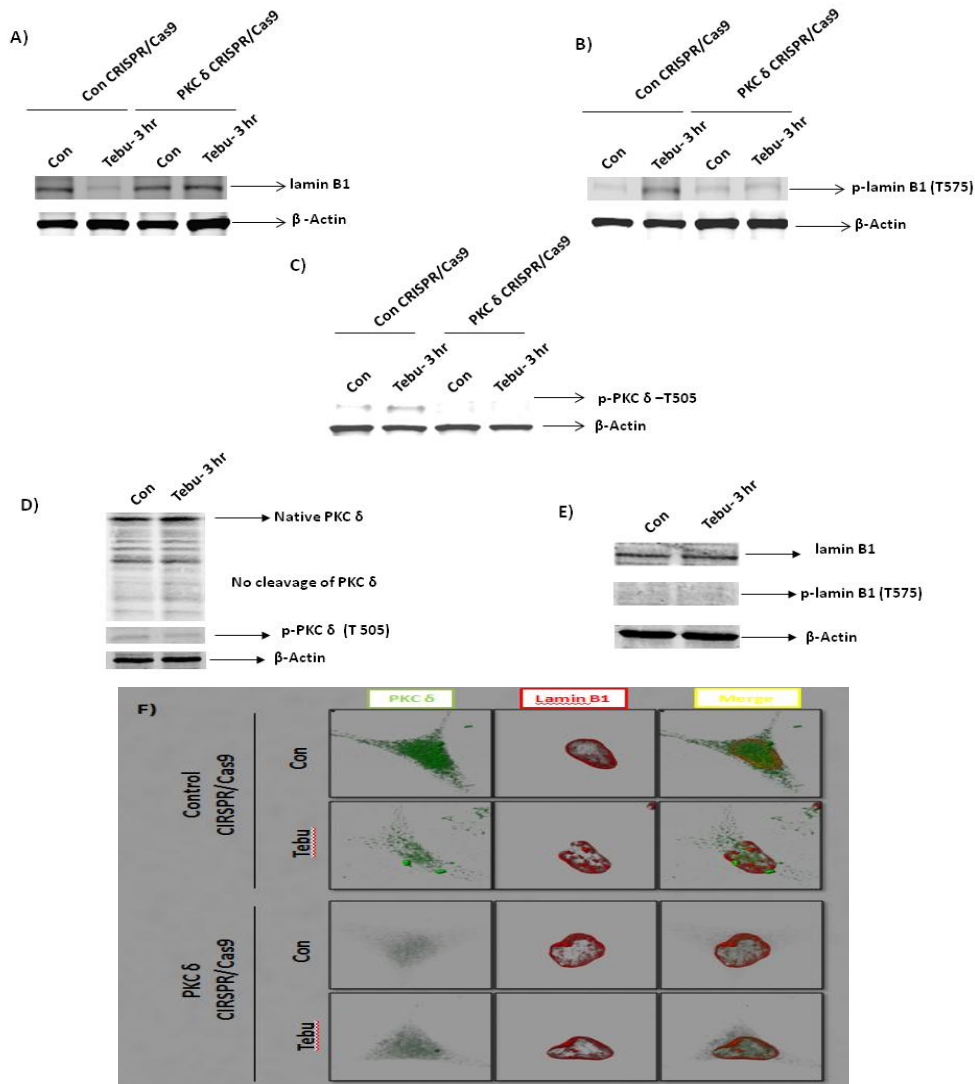
Figure 4: Stable PKCδ CRISPR/Cas9 Knockdown N27 cells and the PKCδ cleavage resistant mutant N27 cells (PKCδ- CRM) were resistant against tebufenpyrad induced PKCδ activation and laminB1 phosphorylation

The cells were treated with tebufenpyrad (3 µM) for 3 hr and cell lysates were prepared and subjected to Western blot analysis. Representative immunoblots of phospho- PKCδ (T505), LaminB1 and phospho- LaminB1 (T575), and β-Actin was used as a loading control for all the western blot analysis. (A-C) Depicted the resistance of PKCδ CRISPR/Cas9 Knockdown N27 cells to tebufenpyrad induced PKCδ activation and laminB1 phosphorylation. (D and E) Depicted the resistance of PKCδ-CRM N27 cells to tebufenpyrad induced PKCδ cleavage and activation and also LaminB1 phosphorylation and LaminB1 loss. (F) Immunocyto-chemistry analysis using confocal microscopy showed resistance of PKCδ CRISPR/Cas9 Knockdown N27 cells to tebufenpyrad induced PKCδ activation and laminB1 phosphorylation compared to the resistance of control CRISPR/Cas9 N27 cells post tebufenpyrad exposure.

Figure 5: Site-directed mutagenesis of T575 on LaminB1 prevented its phosphorylation based activation and damage post tebufenpyrad induced oxidative stress in the N27 dopaminergic neuronal cells
Wildtype and mutant N27 cells were treated with tebufenpyrad (3 µM) for 3 hr and cell lysates were prepared and subjected to Western blot analysis. Repre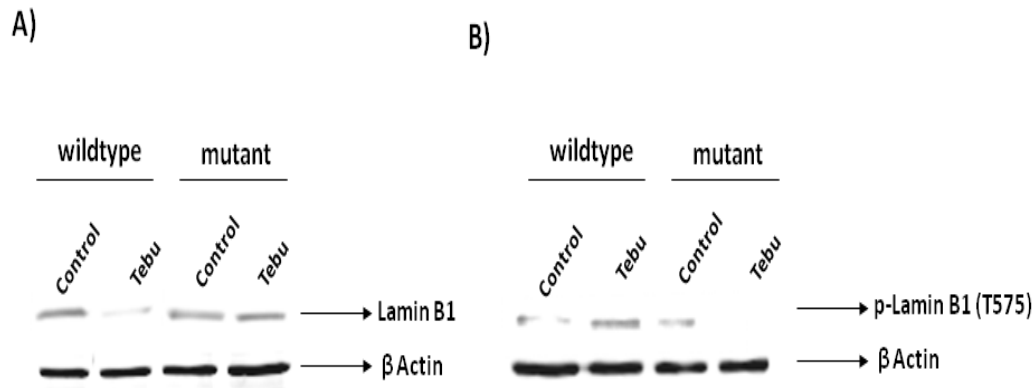sentative immunoblots of LaminB1 and phospho- LaminB1 (T575), and β-Actin was used as a loading control for all the western blot analysis.
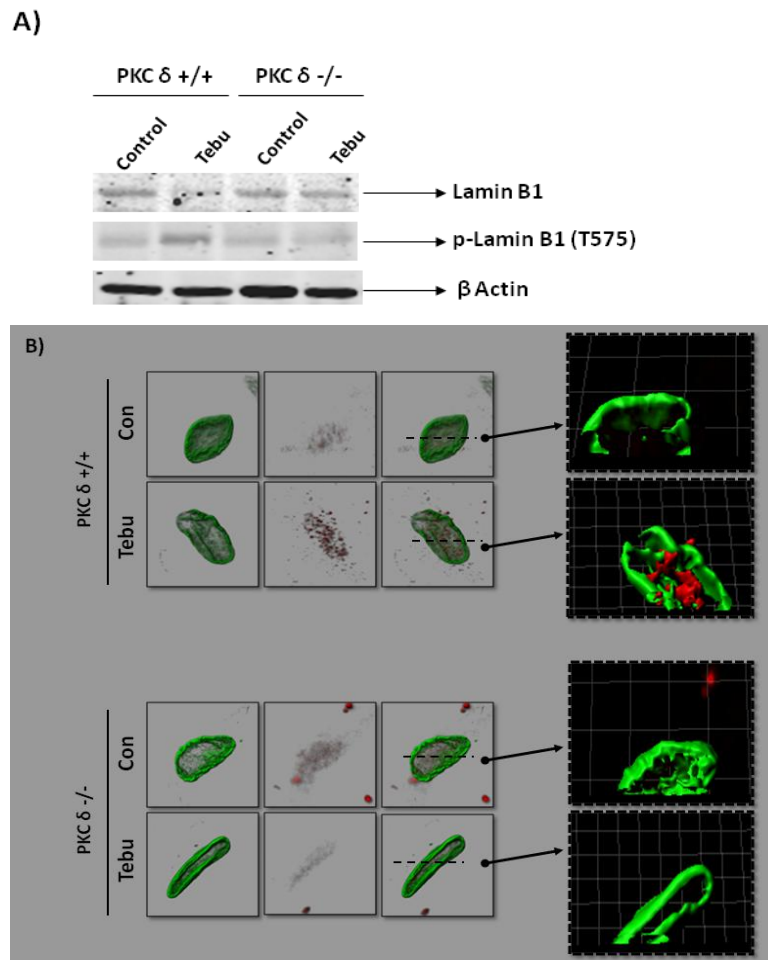
Figure 6 : Absence of PKCδ protects against LaminB1 loss and phosphorylation of LaminB1 (T575) in the organotypic slice culture. The organotypic slices of PKCδ+/+ and PKCδ-/- pups were sectioned (350 μm thickness) and were maintained for 10-14 days and were treated with tebufenpyrad (20 nM for 24 hr). (A) Whole cell lysates were prepared and subjected to Western blot analysis. Representative immunoblots of LaminB1 and p-LaminB1(T575) as shown in section A. β-Actin was used as a loading control. Post treatments the slices were fixed and processed for immuno-histochemistry analysis and microscopy. (B) LaminB1 fluorescently stained (green), p-LaminB1(T575) (red) and Hoechst (blue). The z-stack images were captured on using a 63X oil immersion lens of the Leica Confocal Microscopy system and the processing of images were performed using IMARIS 10.0 software.
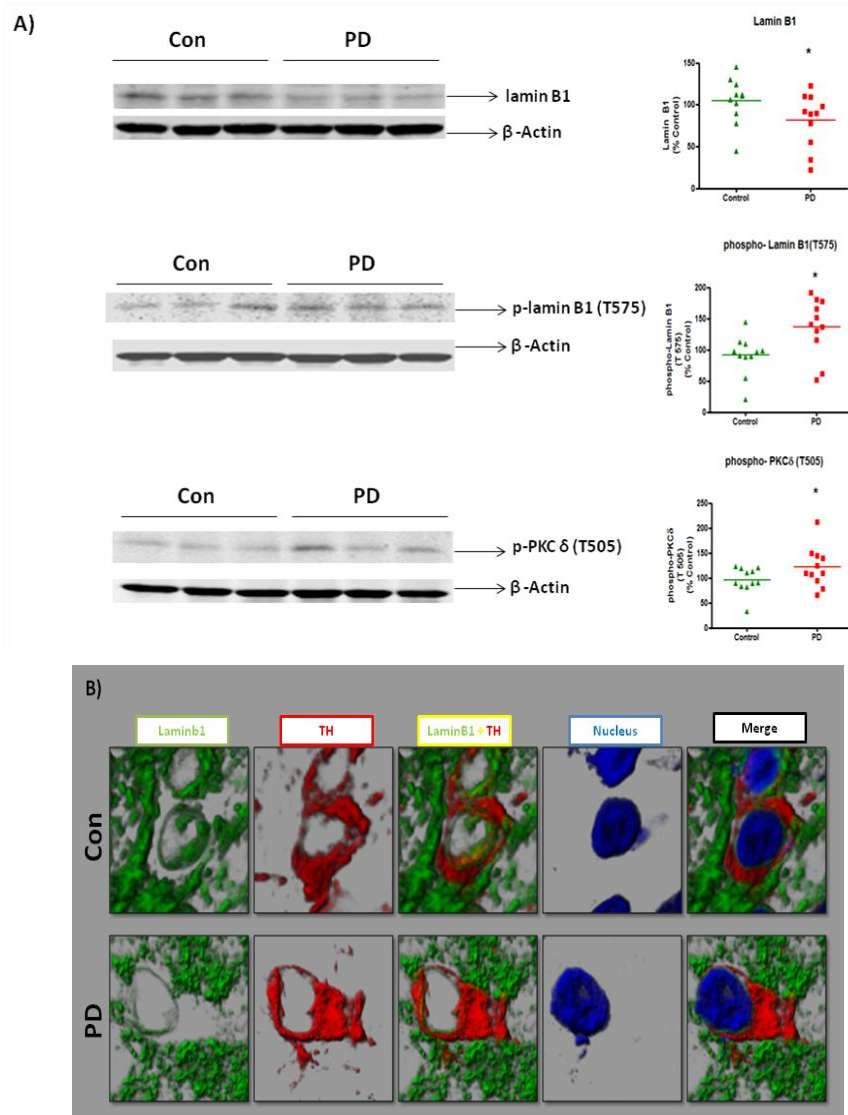
Figure 7 : Absence of PKCδ activation, LaminB1 loss and phosphorylation of LaminB1 (T575) in the *substantia nigra* of postmortem PD brains. (A) *Substantia nigra* of postmortem control and PD brain tissues, were obtained from the brain bank at Miller School of Medicine, University of Miami, FL. Whole cell lysates were prepared and subjected to Western blot analysis. Representative immunoblots of LaminB1, p-LaminB1(T575) and p- PKCδ (T505) as shown. β-Actin was used as a loading control. (B) Sections of *Substantia nigra* from postmortem control and PD brains were obtained from the brain bank at Banner Sun Health Research Institute, AZ. The fluorescent staining was performed for LaminB1 (green) and anti-TH (red). The z-stack images were captured on using a 63X oil immersion lens of the Leica Confocal Microscopy system and the processing of images were performed using IMARIS 10.0 software (Images depicted in normal shading formats one below the other respectively). Data for western blot analysis shown represent mean ± SEM from 11 control and 11 PD individual humans post mortem in total for each group (*$p<0.05$).
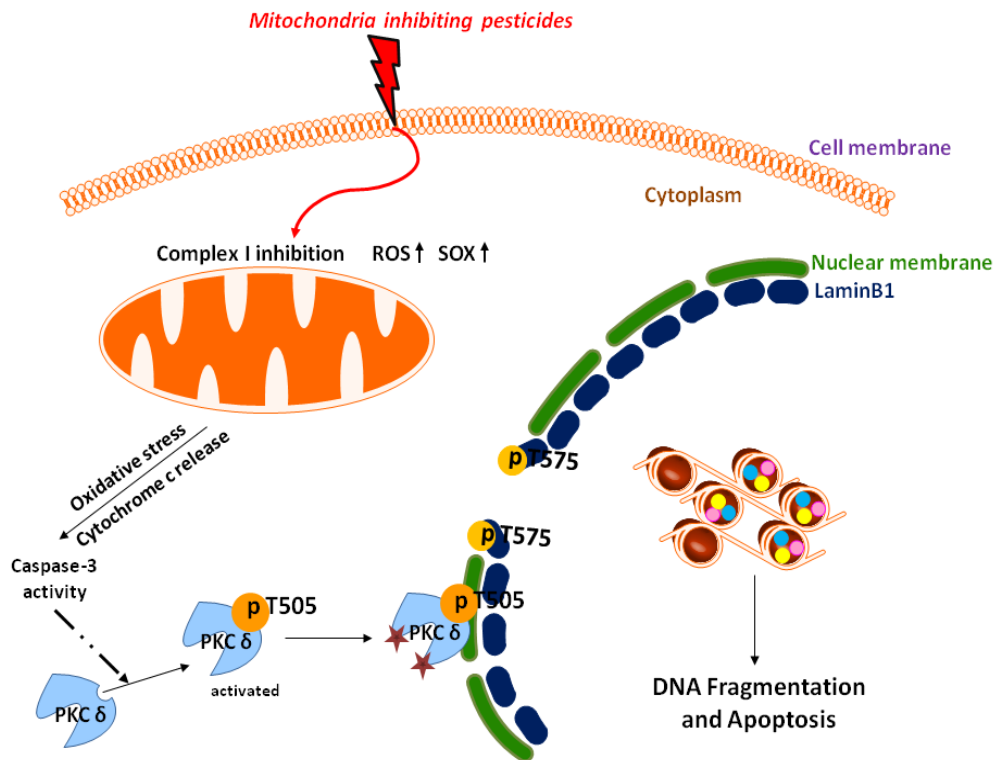
Figure 8 : A schematic illustrating the caspase-3 dependent activation of PKCδ mediating phosphorylation of LaminB1 at T575 and nuclear membrane damage and destruction, in the N27 cells post treatment with mitochindrial inhibiting pesticide tebufenpyrad. Drawing was created by A.Charli using biomedical PowerPoint toolkit from Motifolio.

CHAPTER IV : MITOCHONDRIAL NEUROTOXIC PESTICIDES PROMOTE EPIGENETIC DYSREGULATION BY HISTONE H3 AND H4 HYPERACETYLATION IN DOPAMINERGIC NEURONAL MODELS OF PARKINSON'S DISEASE

Adhithiya Charli, Jie Luo, Monica Langely, Naveen Kondru, Muhammet Ay,

Huajun Jin, Vellareddy Anantharam, Arthi Kanthasamy and

Anumantha G. Kanthasamy[*]

Parkinson's Disorder Research Laboratory, Iowa Center for Advanced Neurotoxicology,

Department of Biomedical Sciences, Iowa State University, Ames, IA 50011

*To whom correspondence should be addressed: Dept. of Biomedical Sciences, Iowa State University, 2062 College of Veterinary Medicine Building, Ames, IA 50011. Tel: 515-294-2516; Fax: 515-294-2315; Email: akanthas@iastate.edu

The abbreviations used are: Dopaminergic (DAergic), substantia nigra pars compacta (SNpc), sodium chloride (NaCl), proteinase K (PK), Dithiothreitol (DTT), ethylenediaminetetraacetic acid (EDTA), mitochondrial transcription factor A (TFAM), Clustered Regularly Interspaced Short Palindromic Repeats (CRISPR), Maximum intensity projection (MIP), Gey's balanced salt solution supplemented with the excitotoxic antagonist, kynurenic acid (GBSSK), Horseradish peroxidase (HRP), Parkinson's disease (PD), Heterochromatin protein-1α (HP-1α), acetylation (Ac), Immunohisto-chemistry (IHC), paraformaldehyde (PFA), oxygen consumption rate (OCR), extracellular acidification rate (ECAR).

Abstract

Growing evidence implicates continual exposure to environmental pesticides in the etiopathogenesis of Parkinson's disease (PD). Previously, we demonstrated that dysregulation of histone acetylation homeostasis induced by environmental pesticides exposure increases the susceptibility of dopaminergic neurons to degenerative processes. Using confocal microscopy and Seahorse bioanalyzer, we recently showed that exposing N27 dopaminergic neuronal cells to the greenhouse pesticide pyridaben induced significant neurotoxicity by affecting mitochondrial structure and function. These observations promoted us to examine whether pyridaben-induced mitochondrial dysfunction influences epigenetic histone acetylation. Western blot analysis revealed that exposure of N27 cells to pyridaben (3 μM) drastically increased histone (specifically H3 and H4) acetylation. The classic mitochondrial complex-1 inhibitor rotenone also induced histone H3/H4 acetylation. Immunocytochemical analysis revealed that pyridaben and rotenone exposure preferentially acetylate lysine sites K23 and K5 on H3 and H4, respectively. 3D-reconstruction of confocal microscopy images performed using IMARIS demonstrated vivid architectural changes in nuclear morphology. Further analysis by means of mitochondria-defective N27 dopaminergic stable cells obtained by CRISPR/Cas9-based knockdown of TFAM protein also revealed hyperacetylation of histone H3/H4 compared to the control CRISPR/Cas9 N27 cells. Similar results of histone H3/H4 hyperacetylation and also, site-specific acetylation of H3 (K23) and H4 (K5) were observed in the transgenic MitoPark mouse model of PD, that is deficient of mitochondrial function and also an age-progressive disease model. Importantly, western blotting and immunohistochemical analysis unraveled hyperacetylation of histone H3/H4 in the

nigral dopaminergic neurons from PD brains. Collectively, our data reveal a novel interplay between mitochondrial dysfunction and epigenetic dysregulation of core histone acetylation, which together may play a critical role in the etiology of environmentally-linked PD.

Introduction

Sporadic Parkinson's disease (PD) is a major environmentally-linked neurodegenerative disease, affecting more than one million people from the United States and imposing an enormous economic burden on patients, their families and society. This chronic and progressive disease is characterized mainly by the loss of dopaminergic (DAergic) neurons in the ventral mesencephalic substantia nigra pars compacta (SNpc), leading to a striatal dopamine deficit, and formation of Lewy body aggregates. PD is characterized as a multi-factorial disease, wherein the components that contribute are more than one to identify. Despite extensive research, the cause of PD remains elusive largely due to a poor mechanistic understanding of the increased susceptibility of nigral DAergic neurons to the degenerative process, but exposure to environmental pesticides, metals, and other chemicals has been implicated in PD's etiology (Benedetto et al., 2009; Goldman, 2014; Kieburtz and Wunderle, 2013; Obeso et al., 2010). Several gene mutations have been identified whose defects account for <10% of total PD cases. The vast majority of PD cases might be associated with environmental chemical exposures (Bonifati, 2014; Lubbe and Morris, 2014; Trinh and Farrer, 2013), with the agrochemical pesticide rotenone being of particular concern, based on epidemiological and experimental studies (Betarbet et al., 2000; Cannon et al., 2009; Dhillon et al., 2008; Drolet et al., 2009; Greenamyre et al.,

2003; Johnson and Bobrovskaya, 2015; Panov et al., 2005; Spivey, 2011; Tanner et al., 2011).

Rotenone was widely applied as a garden insecticide and has a long history of use in the US as a major pesticide to eradicate invasive species of fish. Recent Epidemiological studies have suggested rotenone exposures significantly increases the risk of incurring PD (Dhillon et al., 2008) (Spivey, 2011; Tanner et al., 2011). In the laboratory, chronic administration of rotenone in rats causes selective dopaminergic neuronal death and cytoplasmic α-synuclein (αSyn)-positive Lewy body-like inclusions in surviving dopaminergic neurons, as well as many of the motor features of PD (Betarbet et al., 2000; Cannon et al., 2009; Drolet et al., 2009; Greenamyre et al., 2003; Greenamyre et al., 2010; Inden et al., 2011; Inden et al., 2007; Johnson and Bobrovskaya, 2015; Pan-Montojo et al., 2010; Panov et al., 2005; Sherer et al., 2003). Despite its ban in the U.S since 2007, rotenone is still widely used worldwide in large quantities. Mechanistically, inside the cell rotenone acts as a high-affinity and specific inhibitor of mitochondrial complex I causing bioenergetic deficits (Charli et al., 2015; Drolet et al., 2009; Greenamyre et al., 2010; Greenamyre et al., 2001; Johnson and Bobrovskaya, 2015; Tanner et al., 2011). Both experimental and human evidence has suggested a prominent role for mitochondrial complex I impairment in the pathogenesis of PD (Greenamyre et al., 2001; Johri and Beal, 2012; Lin and Beal, 2006; Mullin and Schapira, 2015).

The pyridaben functioning as an acaricide is used to control populations of mites and ticks in commercial greenhouses, is also classified as a mitochondrial complex I inhibitor. Like rotenone, pyridaben is highly lipophilic and can thus easily cross the blood-brain barrier (BBB). Considering the link between complex I

dysfunction and PD, pyridaben likely poses a disease risk, but the epidemiological evidence is lacking. We and others have demonstrated that exposure to micromolar concentrations of pyridaben induces significant neurotoxicity in cultured neuronal cells and midbrain organotypic slices (Charli et al., 2015; Sherer et al., 2007). Another study of pyridaben-treated C57BL mice found a strong correlations between pyridaben exposure and both DAergic neuron loss and increased αSyn immunoreactivity (Gollamudi et al., 2012). A recent interesting case report was reported in ' The Washington State Department of Agriculture' and this report had documented the occurrence of neurological, ocular and gastrointestinal symptoms in farmworkers poisoned by an off-target exposure to pyridaben (Calvert et al., 2015).

Recent studies have identified various epigenetic changes, particularly histone modifications, as important cellular and molecular correlates of a variety of brain disorders involving significant neuronal loss and dysfunction, especially in stroke, fragile X-associated tremor/ataxia syndrome, and Huntington's and Alzheimer's diseases (Habibi et al., 2011; Kwok, 2010; Marques et al., 2011). Epigentic alterations , in particular histone modifications, including methylation, phosphorylation, acetylation, and ubiquitination, has been linked to many human diseases in recent years (Somech et al., 2004). The acetylation modification in specifically has been associated to be triggered because of the imbalance of histone acetyltransferase HATs and HDACs in the system. This in recent years seems to approached as a critical component in the that suggestively contributes to neurodegenerative diseases (Rouaux et al., 2003; Saha and Pahan, 2006). We have previously demonstrated that exposure to dieldrin or paraquat in the dopamingeric neuronal invitro or invivo models, triggers hyperacetylation of histones H3 and H4 , which further results in

DNA fragmentation and apoptotic cell death of dopamingeric neuronal cells (Song et al., 2010; Song et al., 2011).

However, histone acetylation has not yet been explored as a potential mechanism linking mitochondria-inhibiting pesticides exposure to PD pathogenesis. Therefore, in this present study, we demonstrate novel effects of the mitochondria-inhibiting pesticides rotenone and pyridaben on core histones acetylation modifications in various models of PD. Our results improves the understanding of the effect of mitochondrial impairment on neurodegenerative processes in PD. Also, we show a mechanistic insight into the structural alterations of the chromatin structure and nuclear architecture changes exhibited by the site specific histones H3 and H4 acetylation post pestcicides exposure.

Materials and Methods

Chemicals and Reagents. We purchased pyridaben (99.1% purity) from Chem Services (West Chester, PA), and rotenone (95-98% purity). DMSO and Pierce NE-PER extraction kit was purchased from Fisher Scientific (Fair Law, NJ). We purchased RPMI 1640 media, fetal bovine serum (FBS), L-glutamine, penicillin, streptomycin and Sytox green nucleic acid fluorescence stain from Molecular Probes (Eugene, OR). Histone Acetyltransferase (HAT) Assay kit, anti-acetyl lysine antibody, Anti-histone3 (H3) antibody and Millicell 6-well plate inserts (Biopore filter CM, PTFE inserts 30-mm diameter and 0.4-um pore size, Cat No. PICM03050), from Millipore (Billerica, MA), and the Acetylated H3(K23) and Acetylated H4 (K5) antibodies from Santa Cruz Biotechnology Inc.(Santa Cruz, CA). Anti- HP-1α antibody was bought from Abcam (Cambridge, MA). Caspase-3 substrate, Ac-DEVD-AMC, was purchased from Bachem Biosciences, Inc. (King of

Prussia, PA). BCA protein estimation Kit, Protease and Phosphatase Inhibitor Cocktail, Hoechst nuclear stain from Life Technologies (Gaithersburg, MD). Dieldrin, Dithiothreitol (DTT), ethylenediaminetetraacetic acid (EDTA), 45% glucose, kynurenic acid, proteinase K (PK), sodium chloride (NaCl), Tris-HCl and Triton X-100, Cell Death Detection ELISA Plus Assay Kit, Oligomycin, glucose and Anacardic acid were purchased from Sigma Aldrich (St. Louis, MO), and the Seahorse FluxPak calibration solution was bought from Agilent Technologies (Santa Clara, CA).

Cell culture and treatment paradigm. The rat immortalized mesencephalic dopaminergic neuronal cell line (1RB$_3$AN$_{27}$, also known as N27 cells) was a kind gift from Dr. Kedar N. Prasad (University of Colorado Health Sciences Center, Denver, CO). These N27 cells have the potential to differentiate and produce dopamine in culture when exposed to a suitable cAMP triggering agent, and once the cells are differentiated they possess increased tyrosine hydroxylase (TH) expression and dopamine levels (Adams et al., 1996; Zhang et al., 2007). In this study, undifferentiated cells were grown in RPMI 1640 medium containing 10% FBS, 2 mM L-glutamine, 50 units of penicillin, and 50 μg/ml streptomycin, as described previously (Anantharam et al., 2002; Jin et al., 2011c; Prasad et al., 1998). In general, cells were plated in a tissue culture plate or flask in accordance to the experimental requirements and was cultured overnight in a humidified atmosphere of 5% CO$_2$ at 37°C. The cell density plated for each experiment has been provided in the methods section. The cells were treated with the specified concentrations of pyridaben and rotenone for 0-3 h in serum-free RPMI media. For all experiments with N27 cells, treatments were performed when the cells were 65-70% confluent. The pesticides

pyridaben and rotenone are lipophilic in nature and are hence dissolved in DMSO. In the histones H3 and H4 site specific immuno-staining microscopy analysis and in the pyridaben dose study western blot analysis, N27 cells were treated with 100 μM Dieldrin for 25 min as a positive control. For cytotoxicity studies using the SYTOX, Caspase-3 activity and DNA fragmentation assays the cells were treated with pyridaben (3 μM for 3 hr) or rotenone (1 μM for 3 hr) or pre-treated and co-treated with anacardic acid (8.5 μM for 1 hr) along with each of the pesticides pyridaben or rotenone.

CRISPR/Cas9-based knockdown of TFAM in N27 cells. The CRISPR/Cas9-based knockdown experiments were performed as described previously (Langley et al., 2017). The lentivirus-based CRISPR/Cas9 TFAM knockdown (KD) plasmid, pLVU6gRNA-Ef1aPuroCas9GFP-TFAM, with the TFAM gRNA target sequence directed against the exon 1 sequence (CPR555e5e4099bf84.98), was purchased from Sigma-Aldrich. To make lentivirus, the lenti-CRISPR/Cas9 TFAM KD plasmid and control lentiviral vector were transfected into 293FT cells using the Mission Lentiviral Packaging Mix (SHP001; Sigma-Aldrich) according to the manufacturer's instructions. The lentivirus was harvested 48 h post-transfection and titers were measured using the Lenti-X™ p24 Rapid Titer kit (Cat# 632200; Clontech, Mountain View, CA). For stable knockdown of TFAM in N27 cells, cells were plated at 0.1 x 10^6 cells/well in 6-well plates one day before transduction and then incubated with the TFAM KD lentivirus at an MOI of 100. After 24 h, fresh media supplemented with puromycin (50 μg/ml) was added to the cells for stable cell selection. Our qRT-PCR analysis confirmed that transduction of N27 cells with CRISPR/Cas9-based TFAM

knockdown lentivirus resulted in >80% loss in TFAM mRNA levels relative to control cells.

SYTOX Green cytotoxicity assay. Cell death after exposing the N27 cells to 3 μM of pyridaben or 1 μM of rotenone or along with 8.5 μM pre-treatment and co-treatment with anacardic acid was determined using the SYTOX Green dye, as previously described (Jin et al., 2011a; Latchoumycandane et al., 2011a). The SYTOX green dye only permits dead cells to produce green fluorescence. In brief, N27 cells were grown in 24-well cell culture plates (4 x 10^4 cells/well) and treated with pesticides alone or along with pre-treatment and co-treatment with anacardic acid (8.5 μM for 1 hr) and the pesticides. Fluorescent images were then taken using fluorescence microscopy (Cytation 3, Biotek, Winooski, VT) that was coupled with a 40X objective and Gen5 imaging software. For further validation, the green fluorescence was quantitatively measured at an excitation wavelength of 485 nm and an emission wavelength of 538 nm with the use of a fluorescence microplate reader (Cytation3, Biotek). The results were finally presented as a percentage of control.

Caspase-3 activity assay. Caspase-3 activity were determined as previously described by (Anantharam et al., 2002; Kanthasamy et al., 2008). N27 cells in a density of 1 x 10^6 cells per T25 cell culture flask were seeded the previous day, and briefly the following day after exposure to pyridaben or rotenone or with the anacardic acid pre-treatment, the cells were washed once with PBS and re-suspended in lysis buffer containing 50 mM Tris/HCl (pH 7.4), 1 mM EDTA, 10 mM EGTA, and 10 μM digitonin. Cells were then incubated at 37°C for 20–30 min to allow complete lysis. Lysates were quickly centrifuged and cell-free supernatants were

incubated with 50 μM Ac-DEVD-AMC (caspase-3 substrate) at 37°C for 1 hr. Caspase activity was then measured using a microplate reader (Molecular Devices Corp., Sunnyvale, CA) with excitation at 380 nm and emission at 460 nm. Caspase activity was calculated as fluorescence unit (FU) per mg protein per hr and was presented as percentage of control.

DNA fragmentation. Cell Death Detection ELISA Plus Assay Kit was used to measure the levels of DNA fragmentation, as described previously (Anantharam et al., 2002; Kanthasamy et al., 2006a; Kitazawa et al., 2002; Reyland et al., 1999). Briefly, N27 cells (30,000 cells) were subcultured in 24-well culture plates the previous day. The following day cells were exposed to pyridaben or rotenone or along with the anacardic acid pre-treatment. At the end of 3 hr, cells were processed to determine the extent of DNA fragmentation. Quantitative determination of the amount of fragmented DNA retained by anti-DNA-HRP in the immunocomplex was determined spectrophotometrically with ABTS as an HRP substrate (supplied with the kit). Colorimetric measurements were made at 405 and 490 nm using a SpectroMax 190 spectrophotomer (molecular Devices; molecular Probes; Sunnyvale, CA). The magnitude of DNA fragmentation in the cell lysate was quantified by measuring the difference in absorbance between OD_{405} and OD_{490} nm. The results were finally presented as a percentage of control and compared.

Organotypic slice culture technique. All the experiments involving animals followed protocols approved by Iowa State University's Institutional Animal Care and Use Committee (IACUC). Organotypic slice culture was prepared as previously described (Falsig and Aguzzi, 2008; Harischandra et al., 2014b; Kondru et al., 2017). In brief, brain slices were prepared from 9- to 12-day-old mouse pups

from wild-type (WT, C57BL/6) using a microtome (Compresstome™ VF-300, Precisionary Instruments). After dissecting out the whole brain, the brain was oriented in the coronal plane in the Compresstome's specimen tube, which had been prefilled with 2% low-melting-point agarose. The agar was quickly solidified by clasping the specimen tube with a chilling block, and then the specimen tube was inserted into the slicing reservoir filled with freshly prepared, ice-cold Gey's balanced salt solution supplemented with the excitotoxic antagonist, kynurenic acid (GBSSK). To prepare GBSS, we added the following in solution in the following order from 10x stocks to obtain the final concentrations per liter: 8 g NaCl, 0.37 g KCl, 0.12 g Na_2HPO_4, 0.22 g $CaCl_2 \cdot 2H_2O$, 0.09 g KH_2PO_4, 0.07 g $MgSO_4 \cdot 7H_2O$, 0.210 g $MgCl_2 \cdot 6H_2O$, 0.227 g $NaHCO_3$. The compression lip located in the cutting chamber helps stabilize the brain specimen while obtaining 300-μm thick slices with the blade set at a medium vibration speed. Slices were collected at the specimen tube's outlet and transferred to another plate with fresh prefilled GBSSK. The slices were washed twice in 6 ml ice-cold GBSSK, transferred to Millicell 6-well plate inserts (3-5 slices per insert) and were incubated in a humidified atmosphere of 5% CO_2 at 37 °C. Culture media was exchanged every other day for 10-14 days with fresh media. Slice cultures were harvested post treatments with pyridaben or rotenone (20 nM for 24 hrs) by washing twice in 2 ml of ice-cold PBS. The histone extraction was performed as mentioned in the below method section on Histone Extraction. Finally the histones extracts were analyzed for histones acetylation levels expression using Western blot analysis.

Mitopark Animals. 24-weeks-old MitoPark and corresponding littermate age match control (C57BL/6) mice were housed under standard conditions: constant temperature

(22±1 °C), humidity (relative, 30%), and a 12 h light/dark cycle. Mice were given free access to food and water. Animal care and protocol procedures were approved and supervised by the Institutional Animal Care and Use Committee (IACUC) at Iowa State University (Ames, IA). At the age of 24 weeks old, the mice were sacrificed and the *substantia nigra* brain tissue was collected for further biochemical experiments verifying histone acetylation expression analysis and one set of animals were sacrificed by perfusion method for immuno-histochemistry staining study. The mitopark and littermate control animals were handled and maintained as previously described by (Ay et al., 2017; Ekstrand et al., 2007; Gordon et al., 2016; Langley et al., 2017).

Human Post-mortem PD brain samples. We obtained frozen *substantia nigra* tissue samples and cryostat sections from the brains of confirmed post-mortem human PD patients and age-matched neurologically normal individuals from the brain banks at the Miller School of Medicine, University of Miami, FL and the Banner Sun Health Research Institute, AZ. For western blot experiments, the total histones extracts were prepared as mentioned below in the method section of histone extraction. S*ubstantia nigra* tissue sections were fixed with 4% paraformaldehyde (PFA) solution (in 0.1 M phosphate-buffered saline, pH 7.4). Cryostat sections were used for immuno-histochemistry experiments as described below. All human post-mortem samples were procured, stored and distributed according to the applicable regulations and guidelines involving consent, protection of human subjects and donor anonymity. Since the post-mortem human brain tissues were obtained from approved national brain banks, Institutional Review Board (IRB) approval from Iowa State University was not required.

Histone Extraction. The total histones were extracted as previously described by (Song et al., 2011). After treatment, cells were collected by scraping and were washed thrice with ice-cold PBS. Whole histones were extracted with the PIERCE "NE-PER" kit and eventually dissolved into 0.2N HCl. Briefly, cell pellets were incubated with CERI buffer (supplied by NE-PER kit) plus 0.5% Triton X-100 for 10 min. Nuclei were collected by centrifugation at 2000 $\times g$ for 5 min. Then the pellet was resuspended in 0.2 N HCl and incubated on a rotator for 3 h at 4°C. After centrifuging for 10 min at maximum speed in a microfuge, supernatant was collected for further analysis and the histones protein concentrations was determined using the BCA method of estimation following the manufacturer's instructions. Exactly similar method of histones extraction was carried for the mid-brain organotypic slice culture samples, animal *substantia nigra* tissues from the mitopark and human post-mortem control and parkinson's disease *substantia nigra* tissues.

Western blot Analysis. N27 dopaminergic neuronal cells were seeded (5 x 10^6 cells per T175 cell culture flask). Post treatment of N27 cells with pyridaben or rotenone (1 - 10 μM) for 3 hr in a T175 flasks, the whole cell lysates for western blotting analysis were prepared using modified RIPA buffer, as previously described (Kanthasamy et al., 2006b; Latchoumycandane et al., 2011b). The total global histones extracts lysates were prepared as mentioned above. Equal amounts of protein (35 μg) in the whole cell lysates or histones proteins (20 μg) fractions were loaded for each sample and separated on using 10-15% SDS-PAGE gels. Proteins were then transferred to a nitrocellulose membrane (BioRad) for immunoblotting and blocked using a blocking buffer specifically formulated for fluorescent Western blotting (Rockland Immunochemicals). The nitrocellulose membrane was subjected to primary antibodies

overnight incubation, followed by secondary IR dye-800 conjugated anti-rabbit dye or Alexa Flour 680 conjugated anti-mouse IgG for 1 h at room temperature. Primary antibodies against anti-acetyl lysine, anti AcH3(K23) and anti AcH4 (K5) and HP-1α diluted in blocking buffer solution were then added to the membranes and incubated overnight at 4°C. After another four to five washes, an infrared dye-tagged secondary antibody was added for 1 h. β-Actin (for whole cell lysate) or Anti-H3 (for histones fractions) was used as corresponding loading control. Western blot images were captured with Odyssey IR Imaging system (LICOR) and data were analyzed using Odyssey 3.0 software.

Immunocyto-chemistry analysis. Immunofluorescence studies in N27 dopaminergic neuronal cells were performed according to previously published protocols with some modifications (Gordon et al., 2011; Gordon et al., 2016). Briefly, 4×10^4 N27 cells were grown on poly-D-lysine-coated coverslips and treated the following day. At the end of treatment with pyridaben or rotenone or dieldrin, cells were fixed with 4% PFA, washed in PBS and incubated in blocking buffer (PBS containing 2% BSA, 0.5% Triton X-100 and 0.05% Tween 20) for 1 h at room temperature. The coverslips were then incubated overnight at 4°C with primary antibodies against AcH3(K24) and AcH4(K5), diluted in PBS containing 2% BSA. Samples were then washed several times in PBS and incubated with corresponding Alexa 488 and 555 dye-conjugated secondary antibodies. The nuclei were labeled with Hoechst 44432 stain (10 μg/mL) and coverslips were mounted with Fluoromount medium (Sigma Aldrich) on glass slides for visualization using the Leica DMIRE2 confocal microscope.

Immuno-histochemistry analysis. Immunohisto-chemistry (IHC) studies were performed on sections from the *substantia nigra* midbrain region as described

previously (Ghosh et al., 2013; Gordon et al., 2016; Jin et al., 2011b; Sarkar et al., 2017). Briefly, mice were anesthetized with a mixture of 100 mg/kg ketamine and 10 mg/kg xylazine and then perfused transcardially with freshly prepared 4% paraformaldehyde (PFA) and PBS solution. Extracted brains were post-fixed in 4% PFA for 48 h and 30-µm sections were cut using a freezing microtome (Leica Microsystems). Antigen retrieval was performed in citrate buffer (10 mM sodium citrate, pH 8.5) for 30 min at 90°C. Sections were then washed several times in PBS and blocked with PBS containing 2% BSA, 0.2% Triton X-100 and 0.05% Tween 20 for 1 h at room temperature. Sections were then incubated with primary antibodies overnight at 4°C and washed 7 times in PBS on a Belly Dancer Shaker (SPI supplies). The sections were incubated with Alexa 488 and 555 dye-conjugated secondary antibodies for 60-75 min at room temperature and their cell nuclei were stained with Hoechst dye. Sections were mounted on slides using Prolong antifade gold mounting medium (Invitrogen) or using with Fluoromount medium (Sigma Aldrich) according to the manufacturers's instructions. Samples were visualized finally visualized and analyzed using Leica DMIRE2 confocal microscope. An exact similar method of staining and imaging technique was used for the human post-mortem PD brain samples. For the slice culture samples similar staining strategic method was employed, but with mild modifications in the methodology and experimental conditions as previously described in detail and illustrated by (Aguzzi and Falsig, 2012; Harischandra et al., 2014b; Kondru et al., 2017; Sonati et al., 2013).

Confocal imaging and Z stack image capturing and 3D reconstruction. Confocal imaging was performed at the Iowa State University Microscopy Facility, using a Leica DMIRE2 confocal microscope with the 63X oil objectives and Leica Confocal

Software. For the cells, one optical series of Z-stack covered 5-7 optical slices of 0.5 μm thickness each. For slices culture tissue sections, animals and human sections of midbrain region we had employed 12-15 optical slices of 0.5 μm thickness each. The IMARIS software 10.0 was used to analyze the Z stack images. The surface reconstruction wizard in the IMARIS software version 10.0 was used to make 3-D reconstructed images for seeing architectural changes and picture definition. Further details to the images marking topographic alterations were reconstructed using modules in IMARIS such as Normal Shading, Maximum Intensity Projections (MIP) and 3D surface developer.

Measurement of mitochondrial oxygen consumption by Seahorse XFe24 Bioanalyzer. Mitochondrial oxygen consumption was measured using a Seahorse XFe24 Extracellular Flux analyzer (Agilent Technologies (Santa Clara, CA) as described previously in detail by (Charli et al., 2015; Dranka et al., 2011; Dranka et al., 2012). The Seahorse XFe24 Extracellular Flux analyzer is a sensitive, high-throughput instrument that makes real-time measurements of respiration rates of cells with or without oxidative stress. In our studies, we employed two different strategies to monitor the effects of Control CRISPR/Cas9 and TFAM CRISPR/Cas9 stable knockdown N27 cells on oxygen consumption rates (OCR). The experimental strategy was to analyze the mitochondrial bioenergetics of Control CRISPR/Cas9 and TFAM CRISPR/Cas9 stable knockdown N27 cells by measuring the OCR and ECAR as a function of time. The cells were seeded at a density of 3 x 10^4 per well into a V7-PS culture plate and incubated overnight in 5% CO_2 at 37°C and the Seahorse Flux Pak cartridge was equilibrated using the equilibration buffer overnight at 37°C at 0% CO_2. Following this process, the next day, the V7-PS culture plate cover was replaced with

the Flux Pak cartridge with corresponding injection port loaded with the mito-stressor agents oligomycin (1 µg/ml). Once the mito-stressor was loaded in the corresponding position in the cartridge, the cell plate was introduced into the Seahorse analyzer covered with the Flux Pak cartridge. The analyzer was then programmed to measure the basal OCR and ECAR readouts in 3 specified time intervals before progressing to inject the mito-stressors. These stressor was injected after every three cycles of measuring OCR (Fig. 7A). Further calculations of basal acidification rate, glycolysis rate, basal respiration rate and ATP-linked respiration were performed as described (Charli et al., 2015; Dranka et al., 2011; Dranka et al., 2012; Langley et al., 2017).

Statistical data analysis. All in vitro data were determined from at least 2-3 biologically independent experiments, each done with a minimum of three biological replicates. Data analysis was performed using Prism 4.0 software (GraphPad Software, San Diego, CA). Data were analyzed using one-way ANOVA with the Tukey-Kramer post-test for comparing all treatment groups with that of the control. Differences with $p < 0.05$ were considered statistically significant.

Results

Pyridaben (3µM) induce dose and time – dependent histone H3 and H4 hyperacetylation in N27 dopaminergic cells

In our previous studies we have shown that exposure of N27 to pesticide compounds such as dieldrin and paraquat, induces hyperacetylation of histones H3 and H4 (Song et al., 2010; Song et al., 2011). Also, we have shown previously that pyridaben is a potent inhibitor of mitochondrial dynamics, functional and structural attributes when exposed to dopaminergic neuronal cells in culture (Charli et al., 2015). Therefore in our present study we have demonstrated the effect of pyridaben in modulating

hyperacetylation of H3 and H4 in the N27 cells. Here we had treated the N27 cells with 1-10 μM of pyridaben for 1-6 hr. Post the treatment, the cells were scraped and collected, and the histones fractions were extracted for further studies using western blot analysis. It was observed visually and using the statistical densitometeric analysis that pyridaben (3 μM) and at a 3 hr time point demonstrated promising potential in trigger hyperacetylation of H3 and H4 in the N27 cells (Fig. 1A and B). Adding the hyperacetylation of H3 and H4 was also noteworthily increased in a dose-dependent manner post exposure of pyridaben. Treatment of N27 cells with dieldrin (100 μM) for 25 minutes, was used as a positive control, in order to compare the effect of pyridaben to trigger histones acetylation.

Significant increase in Ac-H3(K23) and Ac-H4(K5) expression and altered nuclear morphology following pyridaben and rotenone treatments in N27 cells

To enable better understanding of the process of histones H3 and H4 acetylation, we had depicted this phenomena using immufluorescence staining and confocal microscopy. Previously we had shown dieldrin induces acetylation of H3 and H4 in the N27 cells post its exposure and hence in this dieldrin treatment was used as a positive control for comparative purposes. The N27 cells were treated with pyridaben and rotenone using a dose and time paradigm as mentioned above in the methods section. Prior to these treatments it was observed that there was siginificant increase in Ac-H3 (K23) and Ac-H4 (K5) expressions. This was visualized with the help of confocal microscopy and maximum intensity projection method of image representation. Further, these acquired images were quantified using ImageJ software and represented as line and 3D surface plots (Fig. 2A, B and C). Interestingly, one of the prominent observations using the confocal microscopy and IMARIS image

processing was the development of voids or architectural imperfections in the nucleus of the pyridaben and rotenone treated groups compared to the control. These morphological anomalies were depicted using a tool called Surface Shading in the IMARIS software. This enables the representation of topographical changes on a cell by aligning all the Z-Stack of images captured. These nuclear structural changes were surmised to be chromatin remodeling or fragmentation mark post exposure of pyridaben or rotenone to the N27 dopaminergic neuronal cells. Similar changes in nuclear structure and up-regulation of Ac-H3 (K23) and Ac-H4 (K5) were also observed after treatment with dieldrin (Fig. 2A, B and C).

TFAM knockdown CRISPR/Cas9 N27 exhibit reduced respiration rate and acidification rate and induces histones H3 and H4 acetylation

The TFAM knockdown CRISPR/Cas9 N27 cells is a transgenic *invitro* model of mitochondrial impairment, which we had created using the CRISPR/Cas9 system. Previously, we had shown and described that TFAM knockdown CRISPR/Cas9 N27 cells demonstrate an impaired system of mitochondrial respiration and structural damage (Langley et al., 2017). Similarly reiterating our findings, we have demonstrated that the TFAM knockdown CRISPS/Cas9 N27 cells express a reduced oxygen consumption rate depicting mitochondrial respiration deficit and loss in extra cellular acidification rate which represented the reduction in cellular metabolism compared to the Control CRISPR/Cas9 N27 cells (Fig. 3A). Further calculations from the Seahorse XFe24 bioanalyzer showed that there was also loss in ATP-Linked respiration and Glycolysis rates in the TFAM knockdown CRISPS/Cas9s compared to the Control CRISPS/Cas9 N27 cells (Fig. 3A). Since the TFAM knockdown CRISPR/Cas9 N27 cells are potentially exhibiting their mitochondria dysfunctional

qualities, we further tested this model for the expression of H3 and H4 acetylation. Our western blot analysis revealed a very fresh and new result that demonstrates the inherent quality of TFAM knockdown CRISPR/Cas9 N27 cells to express increased levels of H3 and H4 hyperacetylation comapred to the Control CRISPR/Cas9 N27 cells (Fig. 3B). This results suggests that mitochondrial dysfunction mediated stress might be a critical factor in triggering acetylation of H3 and H4 in the dopaminergic neuronal cells.

Pyridaben and rotenone exposure mediates loss of heterochormatin marker HP-1α in the nucleus of N27 cells

HP-1α (heterochromatin protein-1α) functions primarily as a regulator of the heterochromatin structure and is constitutively conserved in almost all eukaryotic cells (Dialynas et al., 2007; Singh et al., 1991). The HP family of protein usually are associated with the chromatin through the histones H3 (trimethylated at lysine 9) and functions as either a gene repressor or activator depending on the stress conditions and triggering causatives (de Wit et al., 2007; Eissenberg and Elgin, 2000; Hediger and Gasser, 2006). Considering these concrete evidences about HP-1α and it's important role in functioning as a marker of heterochromatin, we had tested to check the protein expression levels of HP-1α in the N27 cells post pyridaben or rotenone exposure. The N27 cells were firstly treated with pyridaben or rotenone for varying time interval points (1-3 hrs) and following this exposure the cells were collected and processed for further analysis using western blotting. It was observed that the protein level expression of HP-1α decreased significantly in a time-dependent manner (1-3 hrs) post the pyridaben or rotenone exposure on the N27 dopaminergic neuronal cells (Fig. 4 A and B). This results suggests that there might be possible propensity for the

nucleus of the dopaminergic neuronal cells to undergo a conformational change or structural alteration prior to treatment with pyridaben or rotenone, marked by a loss in HP-1α levels and as seen above using microscopic evidences.

Augmented HAT activity post pyridaben rotenone and TFAM knock down in the N27 cells

HATs are histone acteyltransferases that primarily function by modifying (promoting acetylation) chromatin histones and also have a pivotal role in modulation of transcription programs. HATs have also known to acetylate non-histone proteins in different cell systems and are divided into several sub-classes (Legube and Trouche, 2003). In our study HATs may play a promising role in accentuating the hyperacetylation of H3 and H4 post the mitochondrial inhibiting pesticides exposure. In order to test this surmise, we had treated the N27 cells with pyridaben and rotenone for 3 hrs and subjected the treated cells to measuring the HAT activity using the methodology and kit as mentioned in the methods section. We had also included the TFAM CRIPSR/Cas9 knockdown N27 cells for this spectro-photometric analysis and readout of measuring HAT activity. It was observed that the pyridaben, rotenone treated N27 cells have demonstrated quantitatively higher levels of H3 and H4 directed HAT activity. Similarily, TFAM CRIPSR/Cas9 knockdown N27 cells also shows an inherent higher expression of HAT activity. This HAT activity augmentation data implies that the mitochondrial stress and dysfunction induced by the pesticides exposure or by TFAM knockdown triggers HAT activity in the N27 cells compared to the corresponding controls.

HAT inhibitor anacardic acid attenuates pyridaben - and rotenone induced dopaminergic neurotoxicity

In the previous set of experiment we had shown the functional importance of HAT activity in triggering acetylation of histones H3 and H4, here we propounded to check for the functional intervention and role of HAT inhibitor to attenuate pyridaben or rotenone induced dopaminergic neuronal toxicities. Firstly, the cytoxicity leading to apoptotic cell death was measured as a function of caspase-3 activity post the pesticides treatment in the N27 cells. Anacardic acid, a very well studied HAT inhibitor was pre-treated and co-treated along with pyridaben or rotenone as explained comprehensibly in the methods section. It was observed that anacardic acid was significantly attenuating the caspase-3 activity induced by pyridaben or rotenone (Fig. 6A). Adding, another readout for neurotoxicity was performed as a function of DNA fragmentation quantification. Here too, anacardic acid proved to me a potent protector against pyridaben or rotenone induced neurotoxic cell death in the N27 dopaminergic neuronal cells (Fig. 6B). As a final point, the conformation of the caspase-3 activity and DNA fragmentation was reiterated and demonstrated using the SYTOX green dye that enables the measurement of cytotoxic cell death. SYTOX green cytotoxicity assay shows that the anacardic acid pre- and co-treatment significantly ameliorated the toxicity induced by pyridaben or rotenone exposure in the N27 cells. This was also visualized and depicted as fluorescence images that showed fewer green fluorescence spots in the anacardic acid pretreated groups compared to the pesticides exposed groups (Fig. 6C). Adding on, anacardic acid at 8.5 μM dose was not toxic, thus making re-emphasizing the usage was toxicologically relevant. Cumulatively, anacardic acid

functioning as a HAT inhibitor demonstrated creditably significant protection against pyridaben or rotenone toxicity in the N27 dopaminergic neuronal cells.

Organotypic slice culture of mouse midbrain demonstrates prominent increase in acetylation of H3 and H4 post pyridan and rotenone exposures

One of the impact creating tools that have been used in recent years for brain research is the organotypic slice culture. This technique although exists since the 1950s and 60s, started to attain traction in the past decade. Previously there have been many groups including us who have successfully employed this *exvivo* method for validating and proving hypotheses (Harischandra et al., 2014c; Humpel, 2015; Kondru et al., 2017; Testa et al., 2005; Ullrich and Humpel, 2009). We have employed the organotypic slice culture methodology in order to understand the expressional changes in histones H3 and H4 acetylation in the midbrain post exposure to mitochondrial inhibiting pesticides pyridaben or rotenone, translating the model system from *invitro* to *exvivo*. Here in our present study, we had prepared the organotypic slices (300 μm thickness) from the midbrain of 9-12 day old control mice pups as described in detail in the methods section above. These slices were treated with pyridaben or rotenone at a dose of 20 nM for 24 hrs. This resulting slices following treatment expressed note worthily increase in the levels of H3 and H4 acetylation of histones, which was demonstrated using the western blotting analysis (Fig. 7A). Furthermore, we had also tested for the site specific acetylation of H3 and H4 at K23 and K5 respectively in the organotypic brain slice culture model, using immuno-fluorescence staining and confocal microscopy. The images captured by the confocal microscope in a maximum intensity projection configuration revealed, appreciable increase in the levels of acetylated H3 (K23) and H4 (K5). Interestingly,

the nuclear structure on a topographic perspective was visualized to be damage or altered in the brain slices post treatment with pyridaben or rotenone compared to the control (Fig. 7 B and C). The suggestive images were processed using IMARIS by developing 3D-surfaces of the nucleus and by the surface shading tools. These mounting results with the mid-brain slice culture model illustrates a connection and similarity to our previous data with the immuno- fluorescence staining on the N27 cells (Fig. 2 A and B) in terms of the increased levels of H3 and H4 acetylation and also the conspicuous nuclear structural and architectural alterations. The nuclear structure damage seems a promising marker that occurs visually appealing along with the accentuated H3 (K23) and H4 (K5) hyperacetylation in the dopaminergic neuronal cells. These results suggests and throws the spot-light on details towards the further connection between histones acetylation and chromatin damage or nuclear damage in the dopaminergic neuronal cells post exposure to mitochondrial complex-1 inhibiting pesticides pyridaben and rotenone.

Progressive hyperacetylation of H3 and H4 in transgenic MITOPARK mouse model

The MitoPark model has been recently developed as an animal model of PD by conditional inactivation of TFAM specifically in dopaminergic neurons (Ekstrand et al., 2007). MitoPark mouse recapitulates several aspects of human PD, such as adult-onset, progressive degeneration of dopaminergic neurons, protein inclusion in nigral tissues, and responsiveness to levodopa (Galter et al., 2010). Thus making the MitoPark mouse a very useful model for further studying the molecular mechanism underlying and functioning as an important causative of the disease and also for testing potential neuroprotective agents/drugs for the treatment of PD. In our present

study the primary hypothesis overarches and encircles on mitochondrial dysfunction mediated histones H3 and H4 acetylation, hence testing this hypothesis using the mitochondrial defective mitopark transgenic mouse model would be a purposefully directed study. We have demonstrated progressive age (8 to 23 weeks) dependent acetylation of histones H3 and H4 in *substantia nigra* of the mitopark mice (Fig. 8A). This data provided the well suited impetus for the study as the mitopark mouse is a progressive age dependent animal model portraying the motor and non-motor symptoms of the disease. It has been previously demonstrated by number studies that the mitopark mice at 24 weeks of age suffers from severe motor and non-motor behavioral and neurochemical deficits, along with significant loss of TH positive neurons in the *substantia nigra* region of the mid brain (Branch et al., 2016; Cong et al., 2016; Ekstrand et al., 2007; Langley et al., 2017). Thus we checked site specific acetylation of H3 and H4 in the 24 week old mitopark mice. These animals exhibited significant increase in the acetylation of H3 (K23) and H4 (K5) (Fig. 8B) compared to the 24 week littermate age match control. Further analysis and visualization of the TH neurons and H3 and H4 components of the nucleus in the 24 week mitopark and littermate controls were performed using immuno-fluorescence staining and confocal microscopy. The 3D reconstructed images were generated using the IMARIS software prior to acquisition of the Z-stack series images from the confocal microscopy and post immuno-fluorescence staining with TH and AcH3 (K23) or AcH4 (K5). These final set of images revealed possible nuclear relaxation and nucleoplasmic declustering in the mitopark mice compared to the corresponding age matched controls. These topographically viewed and reconstructed structures looked similar and in trend with our previous finding of pyridaben and rotenone treated organotypic

slice culture and in the pesticides treated N27 cells. Thus these data together strongly suggests the occurrence of the nuclear architectural changes accompanying the process of histone H3 and H4 acetylation triggered by mitochondrial inhibition and dysfunction in the dopaminergic neuronal cells.

Hyperacetylation of H3 and H4 in the *substantia nigra* of postmortem Parkinson's disease brains

Histone acetylation phenomena has been observed recently in various brain disorders involving noteworthy loss of neurons and dysfunction. Also, these epigenetic modifications correlates to potential molecular and cellular alterations in the cell system (Habibi et al., 2011; Kwok, 2010; Marques et al., 2011). Despite many studies in the past and upcoming studies , the importance of hyperacetylation of histones H3 and H4 in the dopmainergic neuronal cells and its role in pathogenesis of PD has not been very well understood till date. In this current study, we have directed our interests in unravelling this novel epigenetic process in the post mortem PD brain *substantia nigra* tissues. Firstly, using western blot analysis and comparing 11 Control and 11 PD *substantia nigra* tissues (total of 22 samples), we have demonstrated significant hyperacetylation of histones H3 and H4 (Fig. 9A). This result implanted the impact of acetylation of histones H3 and H4 and propounded the importance of this particular epigenetic change in the apoptotic cell death of dopaminergic neurons. Additionally the immuno-histochemistry and confocal microscopy study of the sectioned control and PD *substantia nigra* region further revealed the up-regulation of acetylated H3(K23) and H4(K5) (Fig. 9B). Detailed additional microscopic analysis using IMARIS software creating 3D reconstructed images, we were able to demonstrate the nuclear declustering process in the PD brain

sections. These obtained results from the human post mortem brains follows similar trends with our previously tested data from mitopark mouse model, *exvivo* slice culture and pyridaben or rotenone treated N27 cells *invitro* model, in terms of up-regulation of AcH3(K23), AcH3(K23) and nuclear structural changes.

Discussion

The results of the present study addresses and provides novel evidences on mitochondria inhibiting pesticides induced histone hyperacetylation as a key neurotoxicological mechanism in environmentally-linked neurodegenerative processes of the dopaminergic neuronal cell system. We also show that there is conspicuous changes in the nuclear architecture or in other words nuclear declustering process that involves disturbing the chromatin structure, whose occurrence is accompanied along with the histone H3 and H4 acetylation.

Chronic exposure to mitochondria-impairing neurotoxic pesticides is a major public health problem around the world and has been linked to many disease conditions including Parkinson's disease. Despite the established link, the cellular and molecular mechanisms central to the role of mitochondria-impairing pesticide exposure in the pathogenesis of Parkinson's disease remain unidentified. We primarily focus our study on the exposure and effects of rotenone or pyridaben leading histones H3 and H4 acetylation and enabling the progression of dopaminergic neuronal apoptotic cell death.

In the current study firstly, we start by identifying the appropriate dose and time at which pyridaben causes significant appreciable histones acetylation. N27 cells treated with pyridaben (1-10 μM) for 1-6 hrs, showed noteworthy levels of histones H3 and H4 acetylation at the 3 μM for 3 hrs (Fig. 1 A and B). Also, the

immunocytochemistry analysis using immuno-fluorescence staining and confocal microscopy, revealed the significant site specific up-regulation of acetylated H3 (K23) and H4(K5), observed in the N27 cells post pyridaben or rotenone exposure for 3 hrs (Fig. 2 A and B). These results were compared to the positive control group treated with dieldrin, which has been previously shown by us as a potent contributor of hyperacetylation of H3 and H4 in the dopaminergic neuronal cells (Song et al., 2010). Further processing of the acquired images using 3D reconstruction and surface shading technique using the IMARIS software, unearthed a serendipitous observation. N27 cells treated with the mitochondrial inhibiting pesticides pyridaben or rotenone, demonstrated a disturbance in their nuclear structures. These nucleus seem to be declustered which is a chromatin dysregulation phenomena. This data suggests that there is subsequent nuclear chromatin dysrgulation and declustering occurring in consensus to the hyperacetylation histones H3(K23) and H4 (K5) in the N27 cells prior to the exposure of pyridaben or rotenone. Similar type of declustering process was also studied in the H2B-GFP expressing mice, revealing that accumulation of H2BGFP causes dramatic changes in the nuclear architecture of pyramidal neurons, including chromocenter declustering and loss of peripheral heterochromatin. Further this process lead to transcriptional defects and behavioural abnormalities in the animal, contributed by alerations associated with serotonin (5-HT) dysfunction (Ito et al., 2014). Rotenone in many cases proven to be potent contributors of neurotoxicity leading to neurological symptoms and neuro-pathological diseases. For example, a case-control study based on self-reported exposure to rotenone in an East Texas population reported a >10-fold increase in PD risk (Dhillon et al., 2008). More recently, another study carefully examined a large population (110 PD cases and 358

controls) and found that rotenone exposure is associated with a 2.5 times greater risk of PD (Spivey, 2011; Tanner et al., 2011). Like rotenone, pyridaben is highly lipophilic and can thus easily cross the blood-brain barrier (BBB). Considering the link between complex I dysfunction and PD, pyridaben likely poses a disease risk, but the epidemiological evidence is lacking. We and others have demonstrated that exposure to micromolar concentrations of pyridaben induces significant neurotoxicity in cultured neuronal cells and midbrain organotypic slices (Charli et al., 2015; Sherer et al., 2007). Another study of pyridaben-treated C57BL mice found a strong correlations between pyridaben exposure and both DAergic neuron loss and increased αSyn immunoreactivity (Gollamudi et al., 2012).

We were focused on creating a transgenic *invitro* model that posses an inherently altered dynamics in mitochondrial function, health and structure. This model could also potentially serve as a tool for studying mitochondrial dysfunction and for screening neuroprotective compounds. Thus this made us create the TFAM CRISPR/cas9 knock down stable N27 cells. TFAM was our target protein mainly because it is involved in a plethora of mitochondrial function and maintenance. Mitochondrial transcription factor A also known as TFAM, is a nuclear-encoded mitochondrial protein that promotes the production of mitochondrially encoded genes by regulating the mtDNA and ATP production maintenance (Alvarez et al., 2008; Duchen, 2004). Recent studies also indicate that TFAM-mediated mtDNA regulation places a crucial role in PD (Gaweda-Walerych et al., 2010; Gaweda-Walerych and Zekanowski, 2013). Another important role of TFAM is its ability to be an important aspect during mitochondrial biogenesis. In general mitochondrial biogenesis is regulated by the TFAM and mtDNA interactions, which is modulated by the

expression and binding of TFAM (Kanki et al., 2004; Picca and Lezza, 2015). It has been well noted and understood that mitochondrial biogenesis is down-regulated during the process of complex 1 inhibition driven PD (Thomas et al., 2012). We have previously shown that the TFAM CRISPR/cas9 knock down N27 cells exhibited a lowered mitochondrial function and significant mitochondria structural damage (Langley et al., 2017). In our present study we have shown using the seahorse XFe24 bioanalyzer that TFAM CRISPR/cas9 knock down N27 cells compared to the Control CRISPR/cas9 N27 cells inherently possessed an inhibited mitochondrial oxygen consumption rate, ATP-Linked respiration, glycolysis rate and basal acidification rates (Fig. 3A). Thereby demonstrates the incompetence of the TFAM CRISPR/cas9 knock down N27 cells to function as a regular control due to its defective mitochondrial function and altered respirational dynamics. Interestingly, we had observed that the TFAM CRISPR/cas9 knock down N27 cells also exhibits significant basal inherent histones H3 and H4 acetylation compared to the control CRISPR/cas9 N27 cells (Fig. 3B). Another interesting finding by using our N27 cells exposed to pyridaben and rotenone, was that a time dependent significant decrease in the hetereochromatin marker, HP-1α (Fig. 4 A and B). HP-1α is a very well known marker of heterchromatin that primarily functions as a vital component involved in the formation of transcriptionally inactive heterochromatin. In a precise context, HP-1α plays a role in chromatin packaging and gene regulation (Norwood et al., 2004). Hence our data suggesting time dependent reduction in the expression of HP-1α post pyridaben or rotenone treatments in the N27 cells, suggests a probable loss in the integrity of the heterochromatin structure, mediated through the acetylation of H3 and H4.

We have also shown that the HAT activity has a significant effect of increase in the N27 cells post the pesticides exposure and in the TFAM CRISPR/Cas9 knockdown N27 cells (Fig. 5). This rightfully suggests the pronounced impact of HAT activity leading to the acetylation of histones H3 and H4. Although we have not looked into the type of HATs that get regulated exclusively, the global HAT activity increase is definitely a good start in this study. We and many other groups have shown the potential role of anacardic acid and its function as a HAT inhibitor in a number of studies involving various cell types and disease models (Song et al., 2011; Sun et al., 2006; Sung et al., 2008; Yasutake et al., 2013). Here in our current study, we pre-treated and co-treated anacardic acid (8.5 μM) along with pyridaben or rotenone treatments in the N27 cells, to understand the protective role of anacardic acid against the neurotoxic effects of the two pesticides. Anacardic acid shows significant protection against the pesticides toxicity which was measured as a readout interns of caspase-3 activity, DNA fragmentation and SYTOX dye (Fig. 6 A, B and C).

Organotypic slice culture an *exvivo* study model was performed and was used as a translational model from the *invitro* N27 studies. In recent years, we and other research groups have demonstrated neurotoxic molecular studies by employing the slice culture technique. In this present study the midbrain slice were cultured in media for 10-14 days and finally were treated with pyridaben or rotenone (20 nM) for 24 hrs. Western blot analysis showed that there was appreciable histones acetylation in the pesticides treated slices compared to the control slices (Fig. 7 A). The immuno-histochemistry by fluorescence staining and confocal microscopy, vividly demonstrated the acetylation of H3(K23) and H4 (K5) in the pyridaben and rotenone

treated slices. Adding on, the IMARIS software generated 3D reconstructed images that depicts the nuclear declustering structures post pesticides treatment (Fig. 7 B and C). This data re-illustrates and confirms our findings from the nuclear imaging studies using the N27 cells.

Another highlight finding of this study is the mitopark mice age dependent increase in histones acetylation and also the acetylation of H3(K23) and H4 (K5) in the 24 week compared to the corresponding age match controls. In recent years, MitoPark animal model of PD, in which the TFAM is selectively removed in midbrain dopamine neurons has been developed for many studies especially involving neuroprotective drug discovery. This animal model recapitulates many of the hallmark features of PD, such as adult-onset progressive dopaminergic neurodegeneration, protein aggregation in nigral tissues, L-dopa responsive motor deficits and disease symptoms in an age progressive manner (Branch et al., 2016; Cong et al., 2016; Ekstrand and Galter, 2009; Ekstrand et al., 2007; Langley et al., 2017). We observed that in the *substantia nigra* region of the mitopark mice starting from an age of 8 weeks and until 24 weeks, there was increased hyperacetylation of histones H3 and H4 in an age progressive manner. Also the 24 week mitopark mice also showed significant H3(K23) and H4 (K5) acetylation compared to the age match littermate controls (Fig. 8 A and B). Further analysis immunohistochemical analysis and confocal microscopy also demonstrated the hyperacetylation of H3 (K23) and H4 (K5) in the 24 week old mitopark mice. Also, the alterations in the nuclear arhcitecture seen as declustered structures were also distinctly observed in the 24 week old mitoparks (Fig. 8 C), suggesting that a mitochondrial defective animal model can promote acetylation of histones H3 and H4.

Finally the study results were confirmed by analyzing human post mortem *substantia nigra* brain tissues. We had employed the use of 11 controls and 11 PD brain tissue samples for this study. We identified using western blotting and immuno-histochemical analysis that the PD brains had significant increase in H3 and H4 acetylation compared to the control patients brains (Fig. 9A and B). IHC studies also revealed the site specific hyperacetylation of H3(K23) and H4 (K5). Moreover, close obervation using confocal microscopy and IMARIS image 3D reconstruction, we were also able to unanimously commend on the formation of nuclear declustered structures in PD *substantia nigra* brains sections. This completely lies in trend with our above underlined findings in *invitro, exvivo* and *invivo* models of PD, suggesting the creditability of the occurrence of the nuclear structural alterations driven by the acetylation of histones in the dopaminergic neuronal cells.

In summary, the above findings obtained from neurotoxicity models of PD suggests that histone hyperacetylation is a key epigenetic mechanism in the nigral dopaminergic neruonal cells following pyridaben or rotenone-induced mitochondrial neurotoxicity. Overall, believe that further systematic characterization of specific histones acetylation sites and HAT regulators and identification of dysregulated genes in response to pesticides-induced histone modification in animal models will undoubtedly provide new insights into the molecular mechanism associated with environmentally-linked PD.

References

Adams, F.S., La Rosa, F.G., Kumar, S., Edwards-Prasad, J., Kentroti, S., Vernadakis, A., Freed, C.R., and Prasad, K.N. (1996). Characterization and transplantation of two neuronal cell lines with dopaminergic properties. Neurochem Res 21, 619-627.

Aguzzi, A., and Falsig, J. (2012). Prion propagation, toxicity and degradation. Nat Neurosci 15, 936-939.

Alvarez, V., Corao, A.I., Sánchez-Ferrero, E., De Mena, L., Alonso-Montes, C., Huerta, C., Blázquez, M., Ribacoba, R., Guisasola, L.M., Salvador, C., *et al.* (2008). Mitochondrial transcription factor A (TFAM) gene variation in Parkinson's disease. Neurosci Lett 432, 79-82.

Anantharam, V., Kitazawa, M., Wagner, J., Kaul, S., and Kanthasamy, A.G. (2002). Caspase-3-dependent proteolytic cleavage of protein kinase Cdelta is essential for oxidative stress-mediated dopaminergic cell death after exposure to methylcyclopentadienyl manganese tricarbonyl. J Neurosci 22, 1738-1751.

Ay, M., Luo, J., Langley, M., Jin, H., Anantharam, V., Kanthasamy, A., and Kanthasamy, A.G. (2017). Molecular mechanisms underlying protective effects of quercetin against mitochondrial dysfunction and progressive dopaminergic neurodegeneration in cell culture and MitoPark transgenic mouse models of Parkinson's Disease. J Neurochem 141, 766-782.

Benedetto, A., Au, C., and Aschner, M. (2009). Manganese-induced dopaminergic neurodegeneration: insights into mechanisms and genetics shared with Parkinson's disease. Chemical reviews 109, 4862-4884.

Betarbet, R., Sherer, T.B., MacKenzie, G., Garcia-Osuna, M., Panov, A.V., and Greenamyre, J.T. (2000). Chronic systemic pesticide exposure reproduces features of Parkinson's disease. Nature neuroscience 3, 1301-1306.

Bonifati, V. (2014). Genetics of Parkinson's disease--state of the art, 2013. Parkinsonism & related disorders 20 Suppl 1, S23-28.

Branch, S.Y., Chen, C., Sharma, R., Lechleiter, J.D., Li, S., and Beckstead, M.J. (2016). Dopaminergic Neurons Exhibit an Age-Dependent Decline in Electrophysiological Parameters in the MitoPark Mouse Model of Parkinson's Disease. J Neurosci 36, 4026-4037.

Calvert, G.M., Rodriguez, L., Prado, J.B., and (CDC), C.f.D.C.a.P. (2015). Worker illness related to newly marketed pesticides--Douglas County, Washington, 2014. MMWR Morb Mortal Wkly Rep 64, 42-44.

Cannon, J.R., Tapias, V., Na, H.M., Honick, A.S., Drolet, R.E., and Greenamyre, J.T. (2009). A highly reproducible rotenone model of Parkinson's disease. Neurobiology of disease 34, 279-290.

Charli, A., Jin, H., Anantharam, V., Kanthasamy, A., and Kanthasamy, A.G. (2015). Alterations in mitochondrial dynamics induced by tebufenpyrad and pyridaben in a dopaminergic neuronal cell culture model. Neurotoxicology.

Cong, L., Muir, E.R., Chen, C., Qian, Y., Liu, J., Biju, K.C., Clark, R.A., Li, S., and Duong, T.Q. (2016). Multimodal MRI Evaluation of the MitoPark Mouse Model of Parkinson's Disease. PLoS One 11, e0151884.

de Wit, E., Greil, F., and van Steensel, B. (2007). High-resolution mapping reveals links of HP1 with active and inactive chromatin components. PLoS Genet 3, e38.

Dhillon, A.S., Tarbutton, G.L., Levin, J.L., Plotkin, G.M., Lowry, L.K., Nalbone, J.T., and Shepherd, S. (2008). Pesticide/environmental exposures and Parkinson's disease in East Texas. Journal of agromedicine 13, 37-48.

Dialynas, G.K., Terjung, S., Brown, J.P., Aucott, R.L., Baron-Luhr, B., Singh, P.B., and Georgatos, S.D. (2007). Plasticity of HP1 proteins in mammalian cells. J Cell Sci 120, 3415-3424.

Dranka, B.P., Benavides, G.A., Diers, A.R., Giordano, S., Zelickson, B.R., Reily, C., Zou, L., Chatham, J.C., Hill, B.G., Zhang, J., *et al.* (2011). Assessing bioenergetic function in response to oxidative stress by metabolic profiling. Free Radic Biol Med 51, 1621-1635.

Dranka, B.P., Zielonka, J., Kanthasamy, A.G., and Kalyanaraman, B. (2012). Alterations in bioenergetic function induced by Parkinson's disease mimetic compounds: lack of correlation with superoxide generation. Journal of neurochemistry 122, 941-951.

Drolet, R.E., Cannon, J.R., Montero, L., and Greenamyre, J.T. (2009). Chronic rotenone exposure reproduces Parkinson's disease gastrointestinal neuropathology. Neurobiology of disease 36, 96-102.

Duchen, M.R. (2004). Mitochondria in health and disease: perspectives on a new mitochondrial biology. Mol Aspects Med 25, 365-451.

Eissenberg, J.C., and Elgin, S.C. (2000). The HP1 protein family: getting a grip on chromatin. Curr Opin Genet Dev 10, 204-210.

Ekstrand, M.I., and Galter, D. (2009). The MitoPark Mouse - an animal model of Parkinson's disease with impaired respiratory chain function in dopamine neurons. Parkinsonism Relat Disord 15 Suppl 3, S185-188.

Ekstrand, M.I., Terzioglu, M., Galter, D., Zhu, S., Hofstetter, C., Lindqvist, E., Thams, S., Bergstrand, A., Hansson, F.S., Trifunovic, A., *et al.* (2007). Progressive parkinsonism in mice with respiratory-chain-deficient dopamine neurons. Proceedings of the National Academy of Sciences of the United States of America 104, 1325-1330.

Falsig, J., and Aguzzi, A. (2008). The prion organotypic slice culture assay--POSCA. Nat Protoc 3, 555-562.

Galter, D., Pernold, K., Yoshitake, T., Lindqvist, E., Hoffer, B., Kehr, J., Larsson, N.G., and Olson, L. (2010). MitoPark mice mirror the slow progression of key symptoms and L-DOPA response in Parkinson's disease. Genes, brain, and behavior 9, 173-181.

Gaweda-Walerych, K., Safranow, K., Maruszak, A., Bialecka, M., Klodowska-Duda, G., Czyzewski, K., Slawek, J., Rudzinska, M., Styczynska, M., Opala, G., *et al.* (2010). Mitochondrial transcription factor A variants and the risk of Parkinson's disease. Neurosci Lett 469, 24-29.

Gaweda-Walerych, K., and Zekanowski, C. (2013). The impact of mitochondrial DNA and nuclear genes related to mitochondrial functioning on the risk of Parkinson's disease. Curr Genomics 14, 543-559.

Ghosh, A., Saminathan, H., Kanthasamy, A., Anantharam, V., Jin, H., Sondarva, G., Harischandra, D.S., Qian, Z., Rana, A., and Kanthasamy, A.G. (2013). The peptidyl-prolyl isomerase Pin1 up-regulation and proapoptotic function in dopaminergic neurons: relevance to the pathogenesis of Parkinson disease. The Journal of biological chemistry 288, 21955-21971.

Goldman, S.M. (2014). Environmental toxins and Parkinson's disease. Annual review of pharmacology and toxicology 54, 141-164.

Gollamudi, S., Johri, A., Calingasan, N.Y., Yang, L., Elemento, O., and Beal, M.F. (2012). Concordant signaling pathways produced by pesticide exposure in mice correspond to pathways identified in human Parkinson's disease. PloS one 7, e36191.

Gordon, R., Hogan, C.E., Neal, M.L., Anantharam, V., Kanthasamy, A.G., and Kanthasamy, A. (2011). A simple magnetic separation method for high-yield isolation of pure primary microglia. Journal of neuroscience methods 194, 287-296.

Gordon, R., Neal, M.L., Luo, J., Langley, M.R., Harischandra, D.S., Panicker, N., Charli, A., Jin, H., Anantharam, V., Woodruff, T.M., *et al.* (2016). Prokineticin-2 upregulation during neuronal injury mediates a compensatory protective response against dopaminergic neuronal degeneration. Nat Commun 7, 12932.

Greenamyre, J.T., Betarbet, R., and Sherer, T.B. (2003). The rotenone model of Parkinson's disease: genes, environment and mitochondria. Parkinsonism & related disorders 9 Suppl 2, S59-64.

Greenamyre, J.T., Cannon, J.R., Drolet, R., and Mastroberardino, P.G. (2010). Lessons from the rotenone model of Parkinson's disease. Trends in pharmacological sciences 31, 141-142; author reply 142-143.

Greenamyre, J.T., Sherer, T.B., Betarbet, R., and Panov, A.V. (2001). Complex I and Parkinson's disease. IUBMB life 52, 135-141.

Habibi, E., Masoudi-Nejad, A., Abdolmaleky, H.M., and Haggarty, S.J. (2011). Emerging roles of epigenetic mechanisms in Parkinson's disease. Functional & integrative genomics 11, 523-537.

Harischandra, D.S., Kondru, N., Martin, D.P., Kanthasamy, A., Jin, H., Anantharam, V., and Kanthasamy, A.G. (2014a). Role of proteolytic activation of protein kinase Cdelta in the pathogenesis of prion disease. Prion 8, 143-153.

Harischandra, D.S., Kondru, N., Martin, D.P., Kanthasamy, A., Jin, H., Anantharam, V., and Kanthasamy, A.G. (2014b). Role of proteolytic activation of protein kinase Cδ in the pathogenesis of prion disease. Prion 8, 143-153.

Hediger, F., and Gasser, S.M. (2006). Heterochromatin protein 1: don't judge the book by its cover! Curr Opin Genet Dev 16, 143-150.

Humpel, C. (2015). Organotypic brain slice cultures: A review. Neuroscience 305, 86-98.

Inden, M., Kitamura, Y., Abe, M., Tamaki, A., Takata, K., and Taniguchi, T. (2011). Parkinsonian rotenone mouse model: reevaluation of long-term administration of rotenone in C57BL/6 mice. Biological & pharmaceutical bulletin 34, 92-96.

Inden, M., Kitamura, Y., Takeuchi, H., Yanagida, T., Takata, K., Kobayashi, Y., Taniguchi, T., Yoshimoto, K., Kaneko, M., Okuma, Y., *et al.* (2007). Neurodegeneration of mouse nigrostriatal dopaminergic system induced by repeated oral administration of rotenone is prevented by 4-phenylbutyrate, a chemical chaperone. Journal of neurochemistry 101, 1491-1504.

Ito, S., Magalska, A., Alcaraz-Iborra, M., Lopez-Atalaya, J.P., Rovira, V., Contreras-Moreira, B., Lipinski, M., Olivares, R., Martinez-Hernandez, J., Ruszczycki, B., *et al.* (2014). Loss of neuronal 3D chromatin organization causes transcriptional and behavioural deficits related to serotonergic dysfunction. Nat Commun 5, 4450.

Jin, H., Kanthasamy, A., Anantharam, V., Rana, A., and Kanthasamy, A.G. (2011a). Transcriptional regulation of pro-apoptotic protein kinase Cdelta: implications for oxidative stress-induced neuronal cell death. J Biol Chem 286, 19840-19859.

Jin, H., Kanthasamy, A., Ghosh, A., Yang, Y., Anantharam, V., and Kanthasamy, A.G. (2011b). alpha-Synuclein negatively regulates protein kinase Cdelta expression to suppress apoptosis in dopaminergic neurons by reducing p300 histone acetyltransferase activity. The Journal of neuroscience : the official journal of the Society for Neuroscience 31, 2035-2051.

Jin, H., Kanthasamy, A., Ghosh, A., Yang, Y., Anantharam, V., and Kanthasamy, A.G. (2011c). α-Synuclein negatively regulates protein kinase Cδ expression to suppress apoptosis in dopaminergic neurons by reducing p300 histone acetyltransferase activity. J Neurosci 31, 2035-2051.

Johnson, M.E., and Bobrovskaya, L. (2015). An update on the rotenone models of Parkinson's disease: their ability to reproduce the features of clinical disease and model gene-environment interactions. Neurotoxicology 46, 101-116.

Johri, A., and Beal, M.F. (2012). Mitochondrial dysfunction in neurodegenerative diseases. The Journal of pharmacology and experimental therapeutics 342, 619-630.

Kanki, T., Ohgaki, K., Gaspari, M., Gustafsson, C.M., Fukuoh, A., Sasaki, N., Hamasaki, N., and Kang, D. (2004). Architectural role of mitochondrial transcription factor A in maintenance of human mitochondrial DNA. Mol Cell Biol 24, 9823-9834.

Kanthasamy, A., Anantharam, V., Ali, S.F., and Kanthasamy, A.G. (2006a). Methamphetamine induces autophagy and apoptosis in a mesencephalic dopaminergic neuronal culture model: role of cathepsin-D in methamphetamine-induced apoptotic cell death. Ann N Y Acad Sci 1074, 234-244.

Kanthasamy, A.G., Anantharam, V., Zhang, D., Latchoumycandane, C., Jin, H., Kaul, S., and Kanthasamy, A. (2006b). A novel peptide inhibitor targeted to caspase-3 cleavage site of a proapoptotic kinase protein kinase C delta (PKCdelta) protects against dopaminergic neuronal degeneration in Parkinson's disease models. Free Radic Biol Med 41, 1578-1589.

Kanthasamy, A.G., Kitazawa, M., Yang, Y., Anantharam, V., and Kanthasamy, A. (2008). Environmental neurotoxin dieldrin induces apoptosis via caspase-3-dependent proteolytic activation of protein kinase C delta (PKCdelta): Implications for neurodegeneration in Parkinson's disease. Mol Brain 1, 12.

Kieburtz, K., and Wunderle, K.B. (2013). Parkinson's disease: evidence for environmental risk factors. Movement disorders : official journal of the Movement Disorder Society 28, 8-13.

Kitazawa, M., Wagner, J.R., Kirby, M.L., Anantharam, V., and Kanthasamy, A.G. (2002). Oxidative stress and mitochondrial-mediated apoptosis in dopaminergic cells exposed to methylcyclopentadienyl manganese tricarbonyl. J Pharmacol Exp Ther 302, 26-35.

Kondru, N., Manne, S., Greenlee, J., West Greenlee, H., Anantharam, V., Halbur, P., and Kanthasamy, A. (2017). Integrated Organotypic Slice Cultures and RT-QuIC (OSCAR) Assay: Implications for Translational Discovery in Protein Misfolding Diseases. Sci Rep 7, 43155.

Kwok, J.B. (2010). Role of epigenetics in Alzheimer's and Parkinson's disease. Epigenomics 2, 671-682.

Langley, M., Ghosh, A., Charli, A., Sarkar, S., Ay, M., Luo, J., Zielonka, J., Brenza, T., Bennett, B., Jin, H., et al. (2017). Mito-Apocynin Prevents Mitochondrial Dysfunction, Microglial Activation, Oxidative Damage, and Progressive

Neurodegeneration in MitoPark Transgenic Mice. Antioxid Redox Signal 27, 1048-1066.

Latchoumycandane, C., Anantharam, V., Jin, H., and Kanthasamy, A. (2011a). Dopaminergic neurotoxicant 6-OHDA induces oxidative damage through proteolytic activation of PKCδ in cell culture and animal models of Parkinson's disease. Toxicol Appl Pharmacol 256, 314-323.

Latchoumycandane, C., Anantharam, V., Jin, H., Kanthasamy, A., and Kanthasamy, A. (2011b). Dopaminergic neurotoxicant 6-OHDA induces oxidative damage through proteolytic activation of PKCdelta in cell culture and animal models of Parkinson's disease. Toxicol Appl Pharmacol 256, 314-323.

Legube, G., and Trouche, D. (2003). Regulating histone acetyltransferases and deacetylases. EMBO Rep 4, 944-947.

Lin, M.T., and Beal, M.F. (2006). Mitochondrial dysfunction and oxidative stress in neurodegenerative diseases. Nature 443, 787-795.

Lubbe, S., and Morris, H.R. (2014). Recent advances in Parkinson's disease genetics. Journal of neurology 261, 259-266.

Marques, S.C., Oliveira, C.R., Pereira, C.M., and Outeiro, T.F. (2011). Epigenetics in neurodegeneration: a new layer of complexity. Prog Neuropsychopharmacol Biol Psychiatry 35, 348-355.

Mullin, S., and Schapira, A.H. (2015). Pathogenic mechanisms of neurodegeneration in Parkinson disease. Neurologic clinics 33, 1-17.

Norwood, L.E., Grade, S.K., Cryderman, D.E., Hines, K.A., Furiasse, N., Toro, R., Li, Y., Dhasarathy, A., Kladde, M.P., Hendrix, M.J., *et al.* (2004). Conserved properties of HP1(Hsalpha). Gene 336, 37-46.

Obeso, J.A., Rodriguez-Oroz, M.C., Goetz, C.G., Marin, C., Kordower, J.H., Rodriguez, M., Hirsch, E.C., Farrer, M., Schapira, A.H., and Halliday, G. (2010). Missing pieces in the Parkinson's disease puzzle. Nat Med 16, 653-661.

Pan-Montojo, F., Anichtchik, O., Dening, Y., Knels, L., Pursche, S., Jung, R., Jackson, S., Gille, G., Spillantini, M.G., Reichmann, H., and Funk, R.H. (2010). Progression of Parkinson's disease pathology is reproduced by intragastric administration of rotenone in mice. PloS one 5, e8762.

Panov, A., Dikalov, S., Shalbuyeva, N., Taylor, G., Sherer, T., and Greenamyre, J.T. (2005). Rotenone model of Parkinson disease: multiple brain mitochondria dysfunctions after short term systemic rotenone intoxication. The Journal of biological chemistry 280, 42026-42035.

Picca, A., and Lezza, A.M. (2015). Regulation of mitochondrial biogenesis through TFAM-mitochondrial DNA interactions: Useful insights from aging and calorie restriction studies. Mitochondrion 25, 67-75.

Prasad, K.N., Clarkson, E.D., La Rosa, F.G., Edwards-Prasad, J., and Freed, C.R. (1998). Efficacy of grafted immortalized dopamine neurons in an animal model of parkinsonism: a review. Mol Genet Metab 65, 1-9.

Reyland, M.E., Anderson, S.M., Matassa, A.A., Barzen, K.A., and Quissell, D.O. (1999). Protein kinase C delta is essential for etoposide-induced apoptosis in salivary gland acinar cells. J Biol Chem 274, 19115-19123.

Sarkar, S., Malovic, E., Harishchandra, D.S., Ghaisas, S., Panicker, N., Charli, A., Palanisamy, B.N., Rokad, D., Jin, H., Anantharam, V., *et al.* (2017). Mitochondrial impairment in microglia amplifies NLRP3 inflammasome proinflammatory signaling in cell culture and animal models of Parkinson's disease. NPJ Parkinsons Dis 3, 30.

Sherer, T.B., Betarbet, R., Testa, C.M., Seo, B.B., Richardson, J.R., Kim, J.H., Miller, G.W., Yagi, T., Matsuno-Yagi, A., and Greenamyre, J.T. (2003). Mechanism of toxicity in rotenone models of Parkinson's disease. The Journal of neuroscience : the official journal of the Society for Neuroscience 23, 10756-10764.

Sherer, T.B., Richardson, J.R., Testa, C.M., Seo, B.B., Panov, A.V., Yagi, T., Matsuno-Yagi, A., Miller, G.W., and Greenamyre, J.T. (2007). Mechanism of toxicity of pesticides acting at complex I: relevance to environmental etiologies of Parkinson's disease. Journal of neurochemistry 100, 1469-1479.

Singh, P.B., Miller, J.R., Pearce, J., Kothary, R., Burton, R.D., Paro, R., James, T.C., and Gaunt, S.J. (1991). A sequence motif found in a Drosophila heterochromatin protein is conserved in animals and plants. Nucleic Acids Res 19, 789-794.

Sonati, T., Reimann, R.R., Falsig, J., Baral, P.K., O'Connor, T., Hornemann, S., Yaganoglu, S., Li, B., Herrmann, U.S., Wieland, B., *et al.* (2013). The toxicity of antiprion antibodies is mediated by the flexible tail of the prion protein. Nature 501, 102-106.

Song, C., Kanthasamy, A., Anantharam, V., Sun, F., and Kanthasamy, A.G. (2010). Environmental neurotoxic pesticide increases histone acetylation to promote apoptosis in dopaminergic neuronal cells: relevance to epigenetic mechanisms of neurodegeneration. Mol Pharmacol 77, 621-632.

Song, C., Kanthasamy, A., Jin, H., Anantharam, V., and Kanthasamy, A.G. (2011). Paraquat induces epigenetic changes by promoting histone acetylation in cell culture models of dopaminergic degeneration. Neurotoxicology 32, 586-595.

Spivey, A. (2011). Rotenone and paraquat linked to Parkinson's disease: human exposure study supports years of animal studies. Environmental health perspectives 119, A259.

Sun, Y., Jiang, X., Chen, S., and Price, B.D. (2006). Inhibition of histone acetyltransferase activity by anacardic acid sensitizes tumor cells to ionizing radiation. FEBS Lett 580, 4353-4356.

Sung, B., Pandey, M.K., Ahn, K.S., Yi, T., Chaturvedi, M.M., Liu, M., and Aggarwal, B.B. (2008). Anacardic acid (6-nonadecyl salicylic acid), an inhibitor of histone acetyltransferase, suppresses expression of nuclear factor-kappaB-regulated gene products involved in cell survival, proliferation, invasion, and inflammation through inhibition of the inhibitory subunit of nuclear factor-kappaBalpha kinase, leading to potentiation of apoptosis. Blood 111, 4880-4891.

Tanner, C.M., Kamel, F., Ross, G.W., Hoppin, J.A., Goldman, S.M., Korell, M., Marras, C., Bhudhikanok, G.S., Kasten, M., Chade, A.R., *et al.* (2011). Rotenone, paraquat, and Parkinson's disease. Environmental health perspectives 119, 866-872.

Testa, C.M., Sherer, T.B., and Greenamyre, J.T. (2005). Rotenone induces oxidative stress and dopaminergic neuron damage in organotypic substantia nigra cultures. Brain Res Mol Brain Res 134, 109-118.

Thomas, R.R., Keeney, P.M., and Bennett, J.P. (2012). Impaired complex-I mitochondrial biogenesis in Parkinson disease frontal cortex. J Parkinsons Dis 2, 67-76.

Trinh, J., and Farrer, M. (2013). Advances in the genetics of Parkinson disease. Nature reviews Neurology 9, 445-454.

Ullrich, C., and Humpel, C. (2009). Rotenone induces cell death of cholinergic neurons in an organotypic co-culture brain slice model. Neurochem Res 34, 2147-2153.

Yasutake, T., Wada, H., Higaki, M., Nakamura, M., Honda, K., Watanabe, M., Ishii, H., Kamiya, S., Takizawa, H., and Goto, H. (2013). Anacardic acid, a histone acetyltransferase inhibitor, modulates LPS-induced IL-8 expression in a human alveolar epithelial cell line A549. F1000Res 2, 78.

Zhang, D., Kanthasamy, A., Yang, Y., Anantharam, V., and Kanthasamy, A. (2007). Protein kinase C delta negatively regulates tyrosine hydroxylase activity and dopamine synthesis by enhancing protein phosphatase-2A activity in dopaminergic neurons. The Journal of neuroscience : the official journal of the Society for Neuroscience 27, 5349-5362.
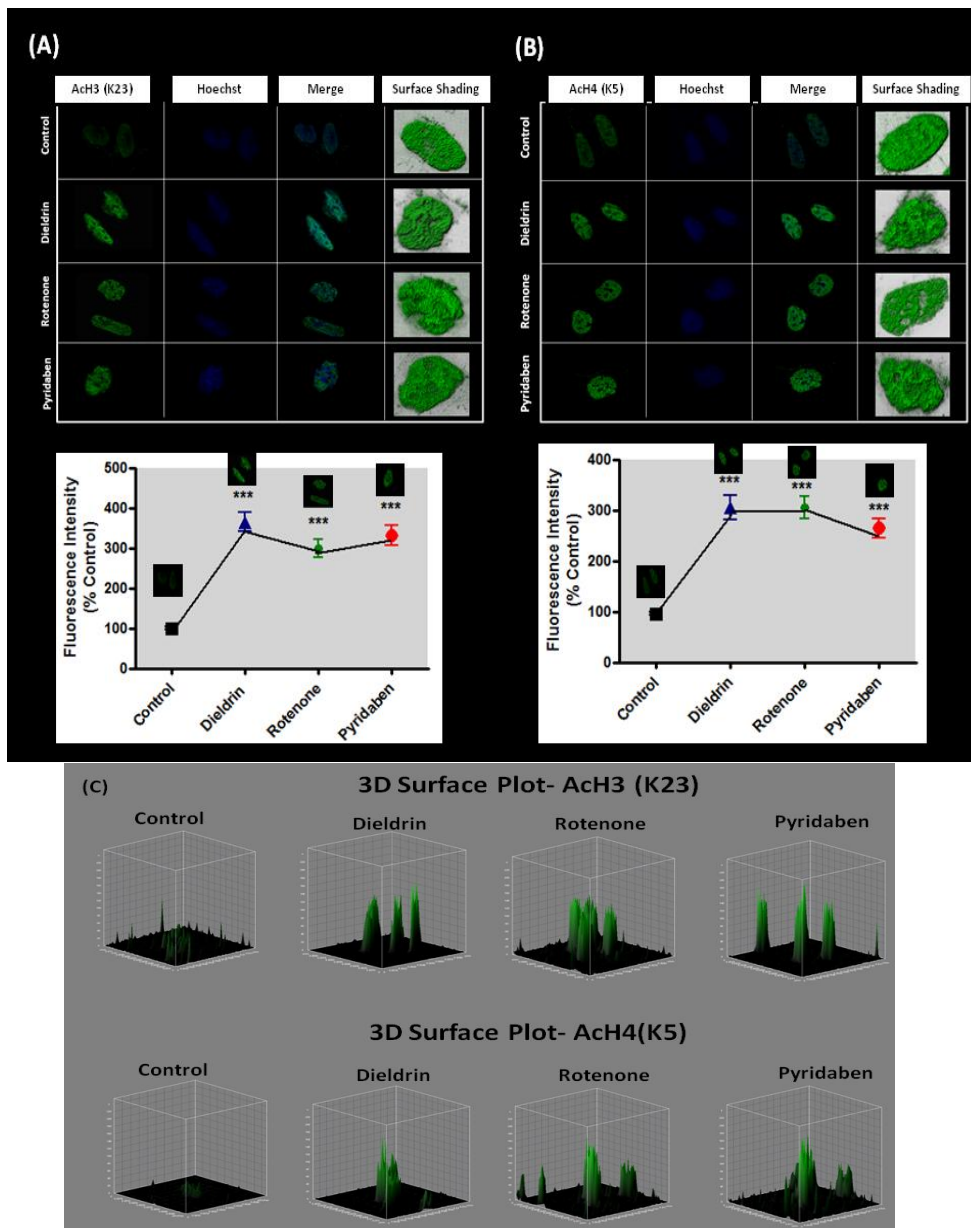
Figures
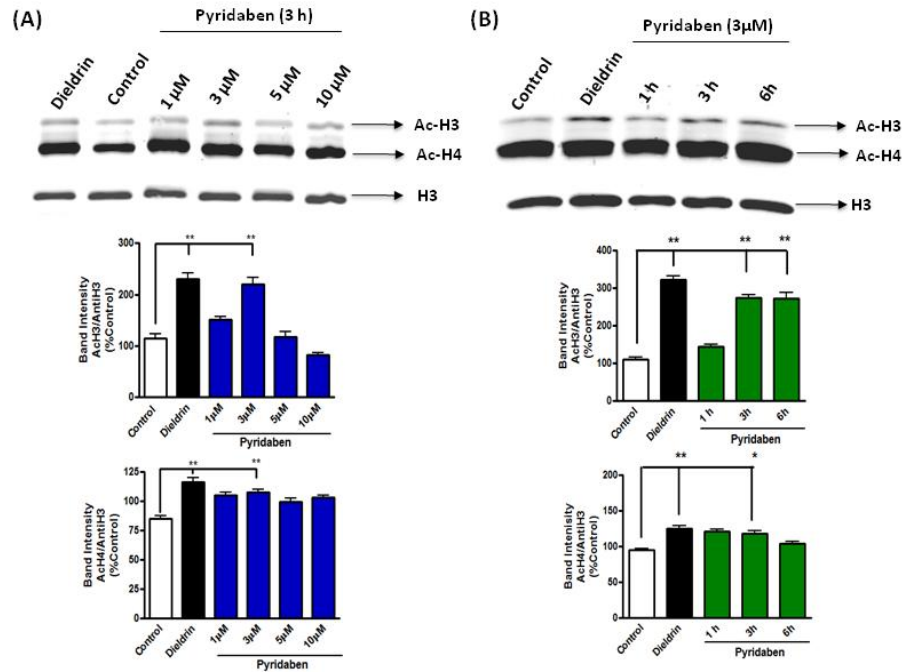
**Figure 1: Pyridaben induce dose and time – dependent histone H3 and H4 hyperacetylation in N27 dopaminergic cells**
(A) Dose dependent histones H3 and H4 hyperacetylation - N27 cells were treated with pyridaben (1-10 μM) for 3 hr and histones extracted lysates and subjected to Western blot analysis. Representative immunoblots of anti-acety lysine as shown above in section A. (B) Time dependent histones H3 and H4 hyperacetylation - N27 cells were treated with pyridaben (3 μM) for 1-6 hr and histones extracted lysates and subjected to Western blot analysis. Representative immunoblots of anti-acety lysine as shown above in section B. Anti-H3 was used as a loading control in sections A and B. Dieldrin (100μM-25 mins) was used as the assay positive control for sections A and B. Data shown represent mean ± SEM from two independent experiments performed in triplicate (*$p<0.05$ and **$p<0.01$).

Figure 2: Immunocytochemistry shows increased Ac-H3(K23) and Ac-H4(K5) immunoreactivty and altered nuclear morphology following pyridaben and rotenone treatments in N27 cells

N27 cells were treated with pyridaben (3 μM) or rotenone (1 μM) for 3 hr. (A) Acetylation of H3(K23) fluorescently stained for AcH3(K23) (green) and Hoechst (blue). (B) Acetylation of H4(K5) fluorescently stained for AcH4(K5) (green) and Hoechst (blue). (C) 3D surface plots representing the increase in hyperacetylation. The z-stack images were captured on using a 63X oil immersion lens of the Leica Confocal Microscopy system and the processing of images were performed using IMARIS 10.0 software. Dieldrin (100μM-25 mins) was used as the assay positive control. Data shown represent mean ± SEM from three independent experiments performed in triplicate (***$p<0.001$).
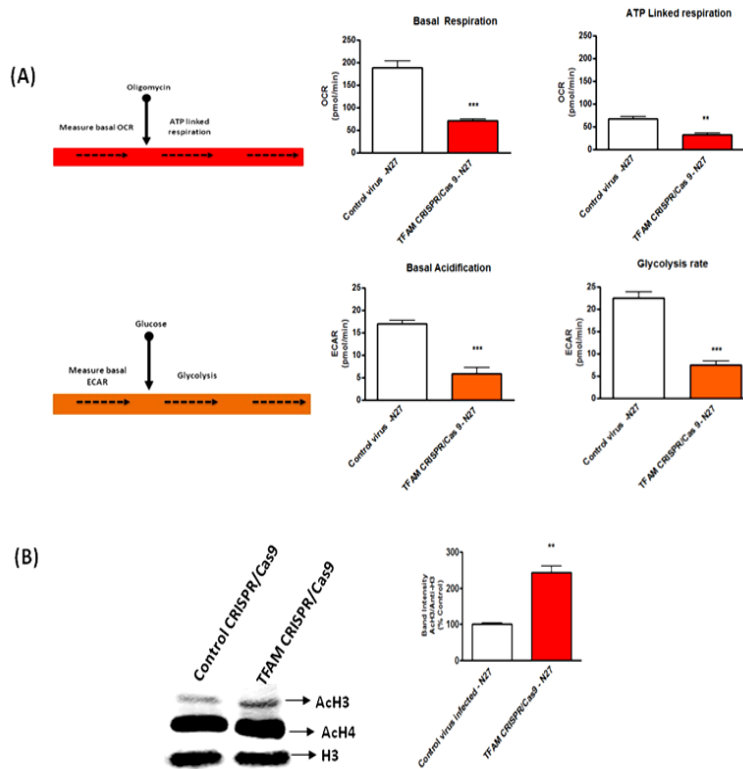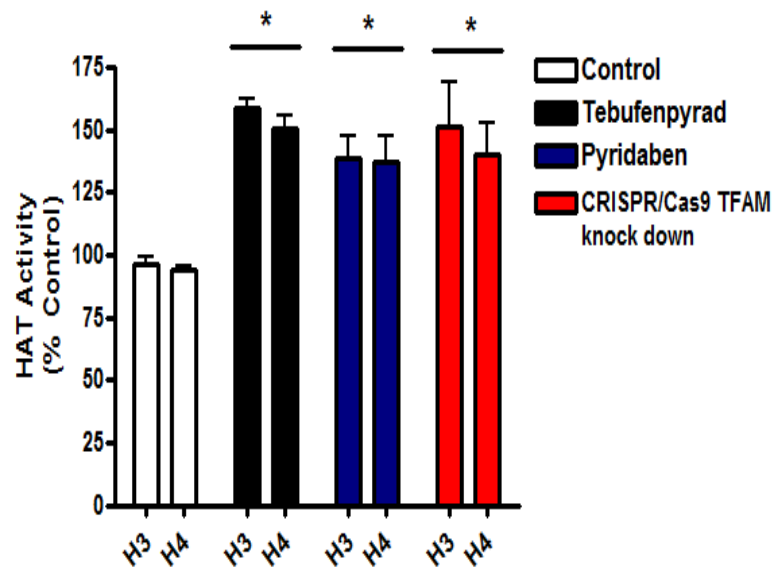
Figure 3 : TFAM knockdown CRISPS/Cas9 N27 cells demonstrates an impaired mitochondria and induces histones acetylation

(A) A bioenergetic scheme of the Seahorse XFe24 Bioanalyzer illustrating the injection method employed for comparing the mitochondrial dynamic difference between Control and TFAM knockdown CRISPR/Cas9 N27 cells. Mitochondrial dynamics were measured using one-stage injection of mito-stressors. Injected 1 µg/ml oligomycin and the analyzer continuously measures OCR and ECAR. (A) Different parameters like basal respiration and ATP-Linked respiration, basal acidification rates and glycolysis rates were estimated from the output OCR and ECAR values respectively after completion. Data shown represent mean ± SEM from two independent experiments performed in quadruplicate (**$p < 0.01$ and ***$p<0.001$). (B) Histones lysates were extracted from Control and TFAM knockdown CRISPR/Cas9 N27 cells and were subjected to Western blot analysis. Representative immunoblots of anti-acety lysine as shown above in section B. Anti-H3 was used as a loading control in section B. Data shown represent mean ± SEM from three independent experiments performed in triplicate (**$p<0.01$).
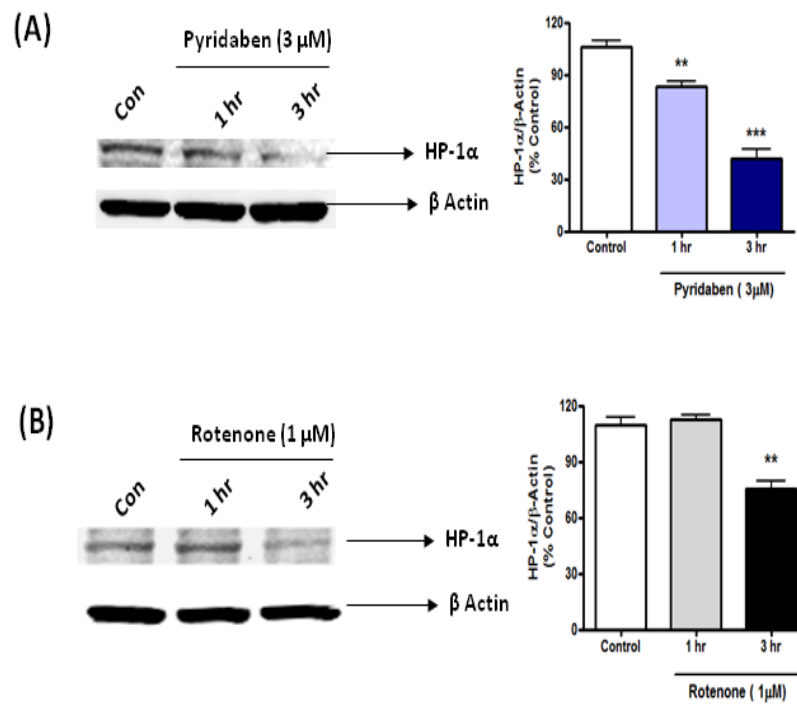
Figure 4 : Pyridaben and rotenone exposure mediate loss of heterochormatin marker HP-1α in the N27 cells
N27 cells were treated with (A) pyridaben (3 μM) or (B) rotenone (1 μM) for 1-3 hr and cell lysates were prepared and subjected to Western blot analysis. Representative immunoblots of HP-1α and β-Actin was used as a loading control for all the western blot analysis. Data shown represent mean ± SEM from three independent experiments performed in triplicate (**$p<0.01$ and ***$p<0.001$).

Figure 5 : Pyridaben or rotenone treatment and TFAM knockdown augment HAT activity in the dopaminergic neuronal cells
Pyridaben (3 µM for 3 hr) or rotenone (1 µM for 3 hr) were treated to the N27 cells and TFAM knockdown CRISPR/Cas9 N27 cells, were lysed and the assay was run in accordance to the HAT Assay kit's protocol and manufacturer's instructions from Millipore (Billerica, MA). The resulting HAT activity was calculated and presented as percentage of Control. Data shown represent mean ± SEM from two independent experiments performed in quadruplicate (*$p<0.05$).
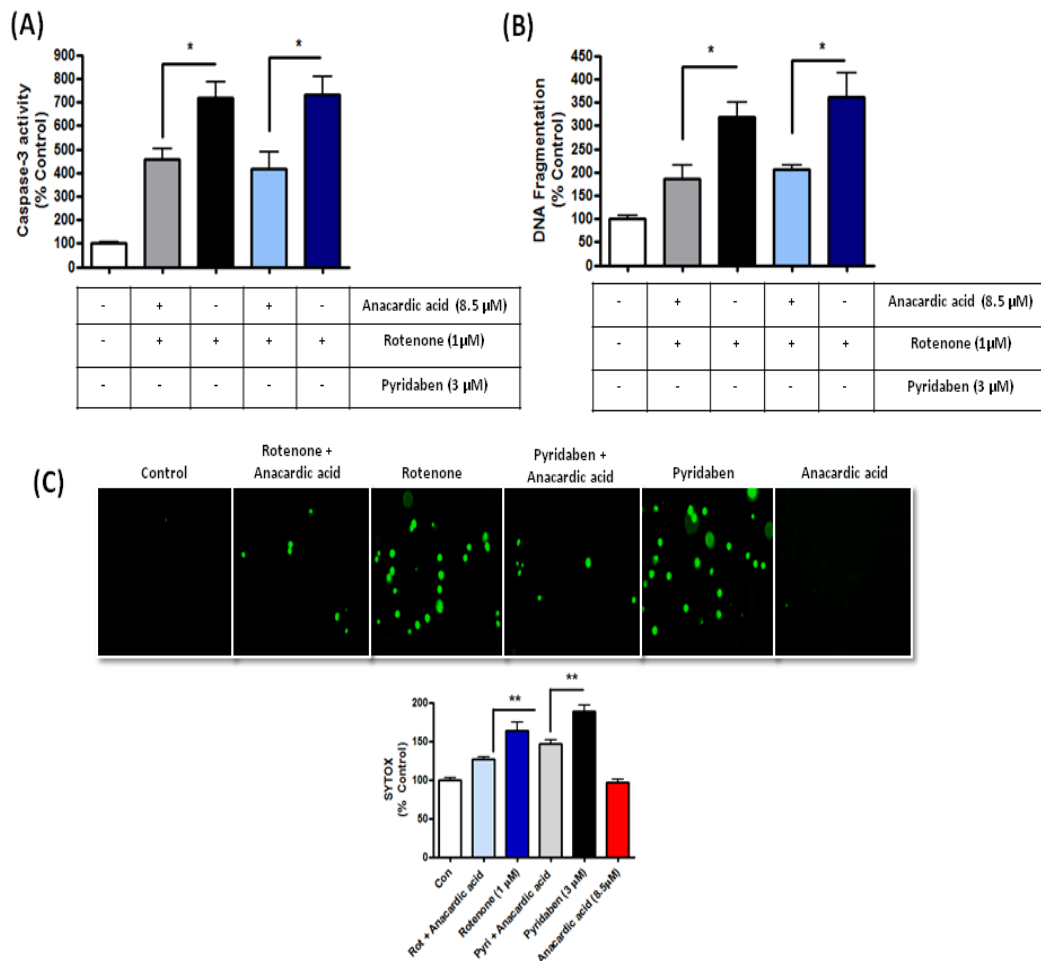
Figure 6 : HAT inhibitor anacardic acid attenuates pyridaben - and rotenone induced dopaminergic neurotoxicity

N27 cells were treated with pyridaben (3 µM for 3 hr) or rotenone (1 µM for 3 hr).Along with the treated anacardic acid was pre-treated (1 hr) and co-treated (8.5 µM for 3 hr) with the pesticides treatment. (A) Cells were collected and assayed for caspase-3 activity using the Ac-DEVD-AMC caspase-3 substrate. (B) Cells were collected post treatments and then assayed for DNA fragmentation using a quantitative ELISA technique. (C) Cytoxicity post treatments was measured using SYTOX Green assay. Representative SYTOX Green staining images are shown. The resulting cytotoxicity parameters correspondingly were calculated and presented as percentage of Control. Data shown represent mean ± SEM from three independent experiments performed in quadruplicate (*$p < 0.05$ and **$p < 0.01$).
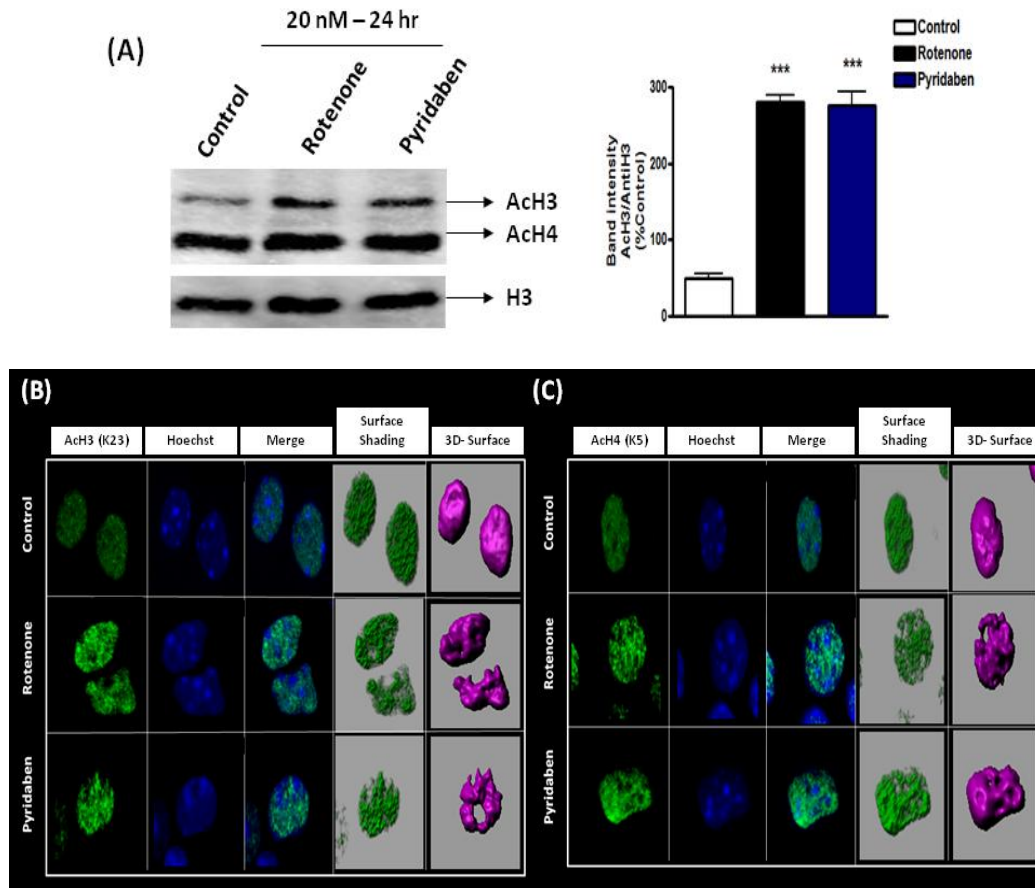
Figure 7 : Acetylation of histones post treatment with pyridaben and rotenone in the organotypic slice culture of midbrain
The organotypic slices were sectioned (300 μm thickness) and were maintained for 10-14 days and were treated with pyridaben or rotenone (20 nM for 24 hr). (A) Histones lysates were extracted and subjected to Western blot analysis. Representative immunoblots of anti-acetyl lysine as shown in section A. Anti-H3 was used as a loading control. (B-C) Post treatments the slices were fixed and processed for immuno-histochemistry analysis and microscopy.(B) Acetylation of H3(K23) fluorescently stained for AcH3(K23) (green) and Hoechst (blue). (C) Acetylation of H4(K5) fluorescently stained for AcH4(K5) (green) and Hoechst (blue). The z-stack images were captured on using a 63X oil immersion lens of the Leica Confocal Microscopy system and the processing of images were performed using IMARIS 10.0 software. Data shown represent mean ± SEM from two independent experiments performed in quadruplicate (***$p<0.001$).
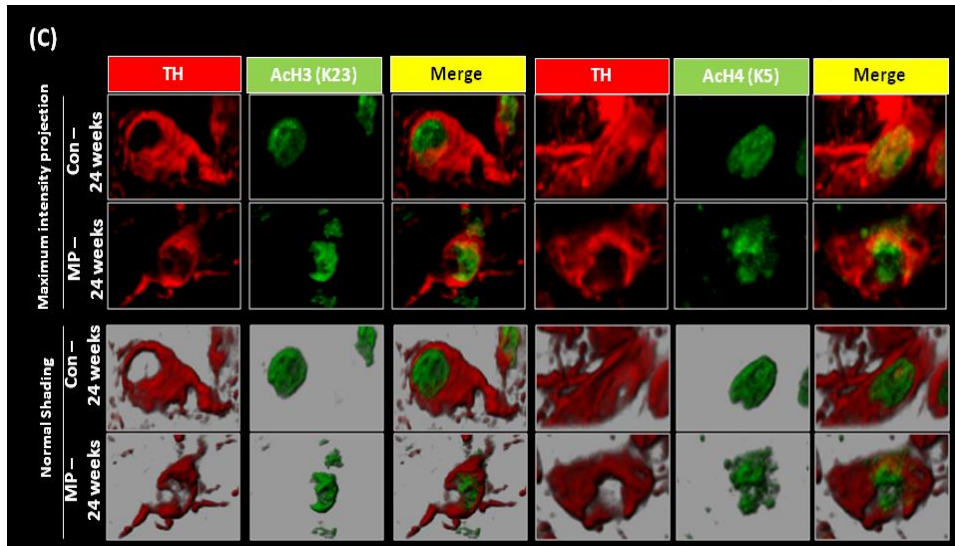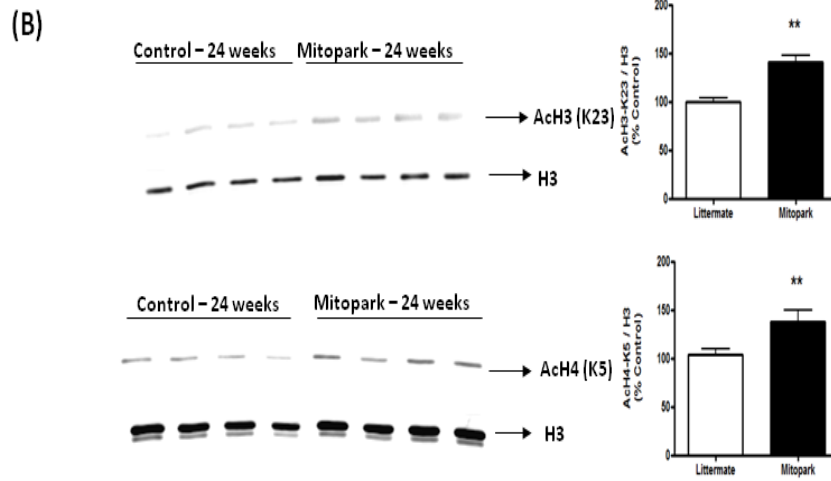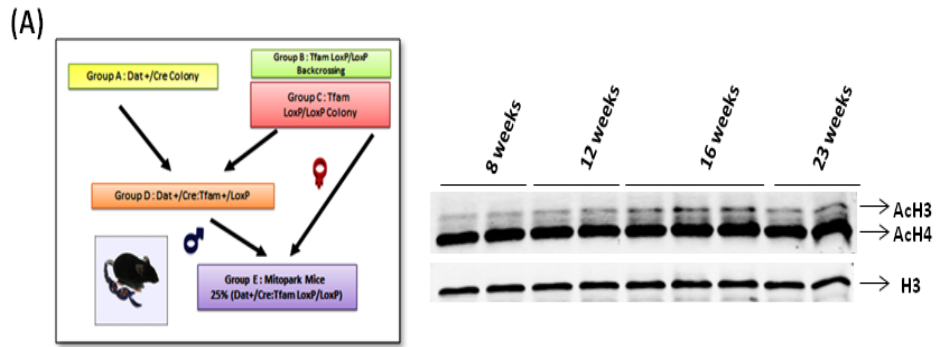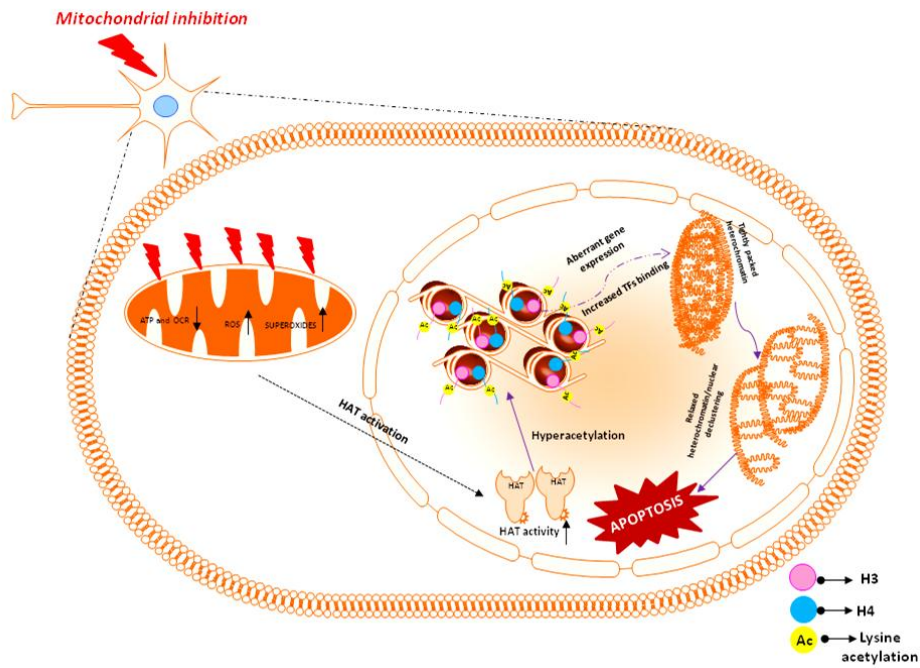
Figure 8 : Age dependent progress of hyperacetylation of H3 and H4 in transgenic mitopark mouse. (A) Mitopark mice of age 8-24 weeks were euthanized and the *substantia nigra* tissues were dissected for biochemical analysis. Histones lysates were prepared from the *substantia nigra* tissues and subjected to Western blot analysis. Representative immunoblots of anti-acetyl lysine as shown in section A. Anti-H3 was used as a loading control. (B) 24 week mitopark and littermate control mice were euthanized and the *substantia nigra* tissues were dissected for biochemical analysis. Histones lysates were prepared from the *substantia nigra* tissues and subjected to Western blot analysis. Representative immunoblots of AcH3(K23) or AcH4(K5) as shown in section B. Anti-H3 was used as a loading control. (C) 24 week mitopark and littermate control mice were euthanized and the *substantia nigra* tissues were dissected, fixed and were sectioned (30 μm) for immunohistochemical staining. The fluorescent staining was performed for AcH3(K23) or AcH4(K5) (green) and anti-TH (red). The z-stack images were captured on using a 63X oil immersion lens of the Leica Confocal Microscopy system and the processing of images were performed using IMARIS 10.0 software (Images depicted in maximum intensity projection and normal shading formats one below the other respectively). Data shown represent mean ± SEM from animals four individual animals in total for each group (**$p<0.01$).
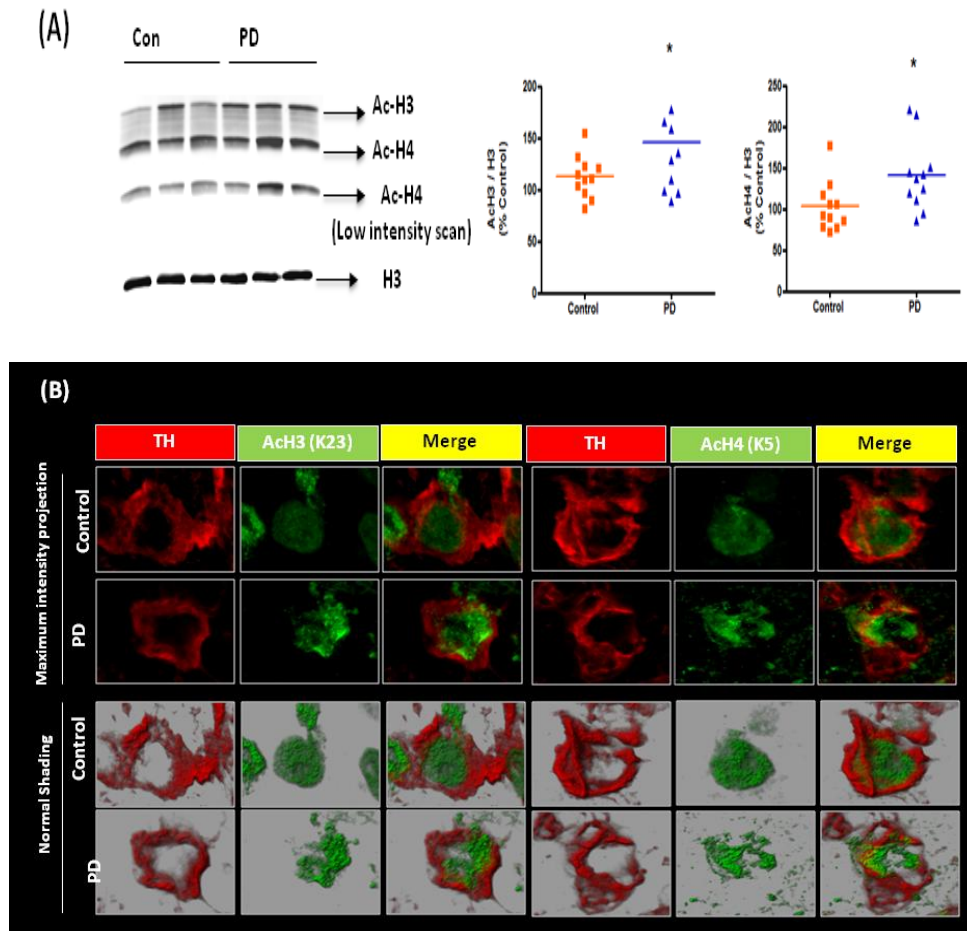
Figure 9 : H3 and H4 hyperacetylation in the *substantia nigra* of postmortem PD brains

(A) *Substantia nigra* of postmortem control and PD brain tissues were obtained from the brain bank at Miller School of Medicine, University of Miami, FL. Histones lysates were extracted from these tissues and subjected to Western blot analysis. Representative immunoblots of anti-acetyl lysine as shown in section A. Anti-H3 was used as a loading control. (B) Sections of *Substantia nigra* from postmortem control and PD brains were obtained from the brain bank at Banner Sun Health Research Institute, AZ. The fluorescent staining was performed for AcH3(K23) or AcH4(K5) (green) and anti-TH (red). The z-stack images were captured on using a 63X oil immersion lens of the Leica Confocal Microscopy system and the processing of images were performed using IMARIS 10.0 software (Images depicted in maximum intensity projection and normal shading formats one below the other respectively). Data shown represent mean ± SEM from 11 control and 11 PD individual humans post mortem in total for each group (*$p<0.05$).

Figure 10 : A schematic illustrating the effect of mitochondrial inhibition and dysfunction mediated H3 and H4 acetylation and nuclear declustering and architectural loss leading to DNA fragmentation and apoptotuc cell death. Drawing was created by A.Charli using biomedical PowerPoint toolkit from Motifolio.

CHAPTER V: GENERAL CONCLUSIONS

This section presents an detailed overview of the results and findings of this dissertation, with a exclusive emphasis and spotlight on overall findings regarding the functional role mitochondrial complex I inhibiting pesticides in its potential in triggering mechanistic epigenetic alterations   and pro-apoptotic kinase signalling action that possess potential influences in development of pathology and symptoms of Parkinson's disease. The major findings of each research chapter included in this dissertation are covered in the discussion section of the relevant chapter.

Alterations of mitochondrial dynamics in the dopaminergic neurons post exposure to mitochondrial complex i inhibiting pesticides.

Previous studies in the past decade have shown the effect of mitochondrial complex I inhibiting pesticides such as MPTP and rotenone in triggering mitochondrial dysfunction in dopamingeric neurons and their association with PD (Betarbet and Greenamyre, 2004; Choi et al., 2011; Greenamyre et al., 2001; Przedborski and Jackson-Lewis, 1998; Przedborski and Vila, 2003). In the present study, we sought to analyze the toxicological effects of two newly classified mitochondrial complex I inhibitors, tebufenpyrad and pyridaben on the dopaminergic neuronal cells with respect to the alterations and changes in mitochondrial function and structural dynamics. Pyridaben accidental off-target exposure has been recently reported , causing neurological and respiratory disorders in the farmers in the field during this exposure (Calvert et al., 2015). But than this, there have not been major studies to understand the effects of exposure to tebufenpyrad and pyridaben. Another special interest of ours with tebufenpyrad and pyridaben specifically is because of their primary functional use as a greenhouse pesticides. This makes the exposure rates

and routes to the workers in the greenhouse a lot higher and further increases the rate of incessant exposure to these mitochondrial complex I inhibitors. We have demonstrated that exposure of the N27 dopaminergic neuronal cells to tebufenpyrad and pyridaben lead to a dose dependent cell death, marked by calculation of the EC50 (Tebufenpyrad - 3.98±0.21 µM (95% CI) and Pyridaben - 3.77±0.21 µM (95% CI)). Tebufenpyrad and pyridaben exposure to the N27 cells also lead to significant oxidative damage marked by the augmented increase in ROS, superoxides generation and dramatic reduction in the intracellular ATP production. We also shows mitochondrial dysfunction and structural morphological impairment in the N27 cells exposed to tebufenpyrad and pyridaben. Another important functional role of tebufepyrad and pyridaben that we demonstrated was using the Seahorse XF bioanlayzer. Both the greenhouse pesticides induced mitochondrial respiration inhibition marked by loss of basal, ATP-Linked respiration and maximum respiratory capacity. Adding on, in order to validate and compare the mitochondrial toxicity and dysfunction potentiated by tebufenpyrad and pyridaben, we had employed the use of rotenone as a positive control for all our studies. there are numerous animal models and epidemiological studies that demonstrate the potent effect of rotenone on dopaminergic neurons and its association to PD (Betarbet et al., 2000; Choi et al., 2011; Greenamyre et al., 2001; Perier et al., 2003; Richardson et al., 2005; Testa et al., 2005). Hence using rotenone as a positive control enabled us to develop a comparative correlation between these two different complex I inhibiting pesticides and their effects on the mitochondria of dopaminergic neurons.

Cumulatively, from this study we have underlined the toxicological impact and effect of tebufenpyrad and pyridaben in the *invitro* dopaminergic neuronal cell

system. Further studies in animal models and epidemiological studies in greenhouse workers will clarify the potential risk of tebufenpyrad and pyridaben greenhouse pesticides in the etiology of PD. Also, such studies might open newer avenues of pathways related to the role of mitochondrial complex I inhibitors contributing to the pathology and symptoms of PD.

Activated PKCδ functions as a LaminB1 kinase and induce nuclear membrane damage.

We have shown recently that tebufenpyrad induces alterations in mitochondrial functional and structural morphological dynamics in the dopaminergic neuronal cell culture model (Charli et al., 2016). In this current study, we further extended to understand the potential role of tebufenpyrad mediated mitochondrial dysfunction and oxidative stress in terms of its ability to trigger PKCδ kinase activity and nuclear membrane damage. Our previous studies in the past couple decades of research, has clearly demonstrated the role of PKCδ as kinase, which upon activation in an caspase-3 dependent manner functions as a pro-apoptotic signalling factor mediating an avalanche of downstream cascades leading to the death of dopamingeric neurons (Gordon et al., 2012; Harischandra et al., 2014c; Jin et al., 2011a; Jin et al., 2011c; Jin et al., 2014c; Kanthasamy et al., 2008; Latchoumycandane et al., 2011a; Saminathan et al., 2011). Keeping in mind our expertise in PKCδ characterization, we explored the efficiency of tebufenpyrad to trigger PKCδ activation in a caspase-3 dependent process and its downstream targets leading to the apoptotic cell death of dopamingeric neurons.

We in this study show that tebufenpyrad (3 μM -3 hrs) induces PKCδ activation in a caspase-3 dependent mechanism. The PKCδ activation is marked

vividly by the formation of cleavage of PKCδ into its catalytic and regulatory domain and also by the upregulation of p-PKCδ (T505). Furthermore, using *insilico* system of analysis and online tools, we identified LaminB1 as a potential downstream target for the activated PKCδ. Also, we identified that T575 on LaminB1 is susceptible to phosphorylation modification induced by the activated PKCδ. This suggested the potential role of PKCδ as a LaminB1 kinase. Previously it has been shown in an oncogenic *invitro* system of study that PKCδ functions as a LaminB1 kinase initiating nuclear membrane damage and cell death (Cross et al., 2000). But the exact mechanism and essential initiating events of this phenomena is not been well characterised or studied. To support and prove this functional role of PKCδ as a LaminB1 kinase in the dopaminergic neurons, we had employed several *invitro* model systems. Our studies performed using the PKCδ-CRM and PKCδ CRISPR/Cas9 knockdown stable N27 cells vividly demonstrated that post exposure to tebufenpyrad, these PKCδ dysfunctional and knockdown systems respectively, show protection against PKCδ activation, phosphorylation of LaminB1 at T575 and loss of nuclear membrane structure. Thus suggesting a protective mechanism in the absence of PKCδ, against tebufenpyrad induced mitochondrial toxicity in N27 dopaminergic neuronal cells. Moreover, our site-directed mutagenesis study involving the replacement of threonine at 575 with glycine in the LaminB1, also validated the site specific importance of LaminB1 T575 phosphorylation and LaminB1 loss. Mutant N27 cells treated with tebufenpyrad exhibited absence of LaminB1 phosphorylation and loss of LaminB1, compared to their corresponding control wildtype N27 cells. Adding on, evidences from the organotypic slice culture studies from the PKCδ+/+ and PKCδ-/- pup midbrains (9-12 days old pups) and from the control and PD post

mortem *substantia nigra* tissues analyzes, demonstrated the function of activated PKCδ as a LaminB1 kinase. These results translated the concept of PKCδ functioning as a LaminB1 kinase from an *invitro* finding to an *exvivo* and also onto a human model system.

Suggesting with these results together, we show that activated PKCδ functions as a kinase phosphorylating LaminB1 at T575 and causing the loss of LaminB1 and hence initiating nuclear membrane damage, resulting in the apoptotic cell death of the dopaminergic neuronal cells. The underlying hot point of take from this study is that the T575 site on LaminB1, has the potential to serve as a promising target for creating pharmacological drug targets, to study neurotoxicity induced by mitochondrial inhibiting pesticides leading the apoptotic dopaminergic neuronal cell death.

Hyperacetylation of histones H3 and H4 induced by mitochondrial inhibiting pesticides.

Linking the interplay between mitochondrial dysfunction induced by the complex I inhibiting pesticides and epigenetic dysregulation such as H3 and H4 hyeracetylation opens a novel pathway involving prominent nuclear architectural changes leading to the death of dopamingeric neuronal cells. We have previously shown that environmental pesticides, paraquat and dieldrin induces histones H3 and H4 hyperacetylation in the dopaminergic neurons mediating the apoptotic cell death (Song et al., 2010; Song et al., 2011). We have also shown previously that pyridaben pronounces significant mitochondrial dysfunction and damage post its exposure to dopaminergic neuronal cells (Charli et al., 2016). Hence in this present study we have identified a novel mechanism bridging the connection of mitochondrial dysfunction mediated trigger of histones acetylation. Here we show that pyridaben induces a dose

and time dependent increase in H3 and H4 hyperacetylation observed in the N27 cells. Analysis by immuno-fluorescence staining study using confocal microscopy unravelled a preferential acetylation at lysine sites K23 and K5 on H3 and H4, respectively. More detailed analysis using the confocal microscopy and image processing software IMARIS, revealed the formation of a nuclear declustered structure post pyridaben exposure to the N27 dopamingeric neuronal cells compared to the control. Dieldrin and rotenone were used as controls for this findings to validate the results of pyridaben exposure induced histones acetylation in the N27 cells. Moreover, post pyridaben or rotenone exposure in the N27 cells, HP-1α, a marker of heterochromatin, significant decreased in a time dependent manner. Thus suggesting there is a topological architectural or remodelling of chromatin induced by the H3 and H4 acetylation post exposure to the mitochondrial targeted pesticides. We have shown previously that the TFAM CRISPR/Cas9 knockdown exhibited a defective mitochondrial structure and function compared to the control CRISPR/Cas9 N27 cells (Langley et al., 2017). Since the TFAM CRISPR/Cas9 knockdown N27 cells possess a inherently defective mitochondria, we had employed it in our present study to understand role of mitochondrial dysfunction in triggering histones acetylation. This present study revealed that the TFAM CRISPR/Cas9 knockdown demonstrate up-regulated levels of H3 and H4 histones acetylation compared to the control CRISPR/Cas9 N27 cells.

Adding on, we demonstrated that pre-treating the N27 cells with anacardic acid (HAT inhibitor), protected against its toxicity induced by pyridaben or rotenone. This suggests the functional role of HAT activity during the process of histones acetylation mediated cell apoptotic cell death. Organotypic brain slice culture of the

midbrain, post pyridaben or rotenone exposure revealed histones acetylation and also the confocal microscopy analysis show-cased the formation of nuclear declustering topological structures in the treated slices of midbrain.

Next we moved the study onto an *invivo* transgenic model of PD called the mitopark mouse model. It has been previously shown by us and other groups that the mitopark mouse model recapitulates the pathological, motor and non-motor symptoms and the age progression deficits that are well associated and studied in PD. These mice exhibit mitochondrial dysfunction and respiration loss due to the specific conditional knockout of TFAM (mitochondrial transcription factor, a regulator of mtDNA) in the dopaminergic neurons in the midbrain of these mice (Ay et al., 2017; Branch et al., 2016; Cong et al., 2016; Ekstrand et al., 2007; Gordon et al., 2016; Langley et al., 2017). We in this current study demonstrated age progressive increase in histones acetylation in the mitopark mice (8 to 24 weeks of age). Also, the 24 week old mitopark compared to the littermate age controls, exhibited site specific significant increase in H3(K23) and H4(K5) acetylation, and nuclear declustering was observed using the confocal microscopy analysis. Similar noteworthy trend of H3 and H4 acetylation and the nuclear topological surface changes were also observed in the human post mortem PD brain tissues and sections respectively.

Collectively, our study enables the understanding of a novel mechanism highlighting the phenomena of mitochondrial dysfunction triggering epigenetic dysregulation of core histones H3 and H4 acetylation, which together may play a critical role in the etiopathology of environmentally pesticides exposure triggering - linked PD.

In summary, our findings suggests the connective novel interplay between mitochondrial dysfunction process and epigenetic dysregulation, triggered by the exposure to mitochondrial complex I inhibiting pesticides on the dopamingeric neuronal cells. These molecular pathway paves way for discovery of new targets for understanding environmentally linked etiopathogenesis of PD.
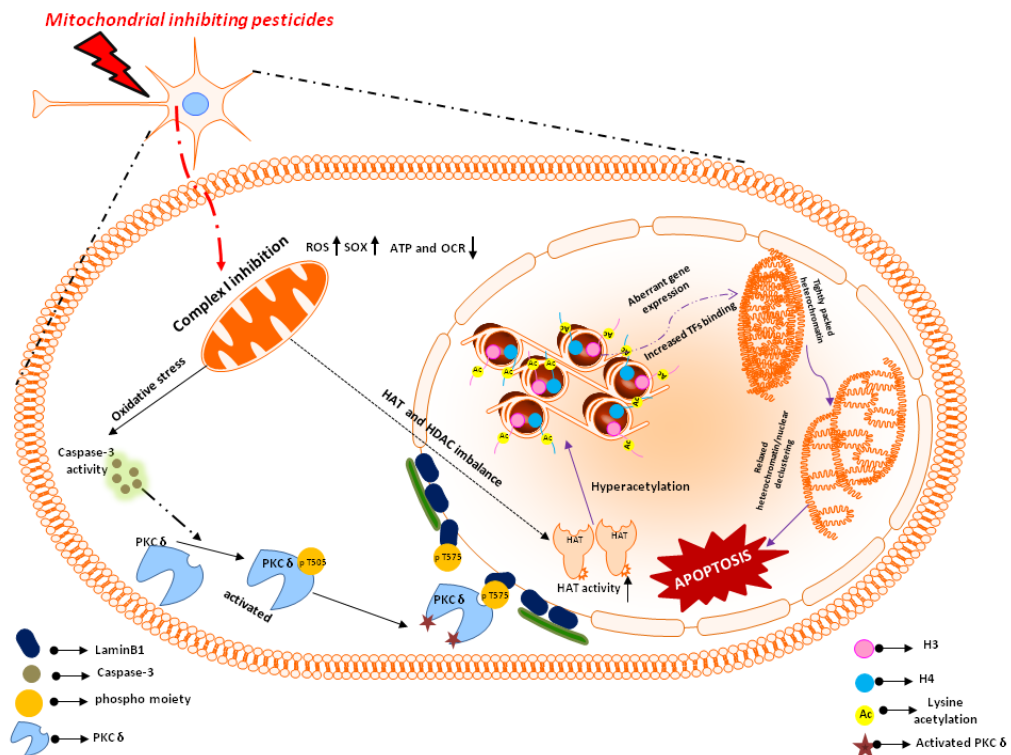
Figure 5.1 Scheme illustrating the integrated mechanisms triggered by mitochondrial complex I inhibiting pesticides

REFERENCES

Abeliovich, A., Schmitz, Y., Fariñas, I., Choi-Lundberg, D., Ho, W.H., Castillo, P.E., Shinsky, N., Verdugo, J.M., Armanini, M., Ryan, A.*, et al.* (2000). Mice lacking alpha-synuclein display functional deficits in the nigrostriatal dopamine system. Neuron 25, 239-252.

Abou-Sleiman, P.M., Muqit, M.M., and Wood, N.W. (2006). Expanding insights of mitochondrial dysfunction in Parkinson's disease. Nature reviews 7, 207-219.

Alam, M., and Schmidt, W.J. (2002). Rotenone destroys dopaminergic neurons and induces parkinsonian symptoms in rats. Behav Brain Res 136, 317-324.

Alam, Z.I., Jenner, A., Daniel, S.E., Lees, A.J., Cairns, N., Marsden, C.D., Jenner, P., and Halliwell, B. (1997). Oxidative DNA damage in the parkinsonian brain: an apparent selective increase in 8-hydroxyguanine levels in substantia nigra. Journal of neurochemistry 69, 1196-1203.

Anantharam, V., Kaul, S., Song, C., Kanthasamy, A., and Kanthasamy, A.G. (2007). Pharmacological inhibition of neuronal NADPH oxidase protects against 1-methyl-4-phenylpyridinium (MPP+)-induced oxidative stress and apoptosis in mesencephalic dopaminergic neuronal cells. Neurotoxicology 28, 988-997.

Anantharam, V., Kitazawa, M., Wagner, J., Kaul, S., and Kanthasamy, A.G. (2002). Caspase-3-dependent proteolytic cleavage of protein kinase Cdelta is essential for oxidative stress-mediated dopaminergic cell death after exposure to methylcyclopentadienyl manganese tricarbonyl. J Neurosci 22, 1738-1751.

Ares-Santos, S., Granado, N., and Moratalla, R. (2013). The role of dopamine receptors in the neurotoxicity of methamphetamine. J Intern Med 273, 437-453.

Ay, M., Luo, J., Langley, M., Jin, H., Anantharam, V., Kanthasamy, A., and Kanthasamy, A.G. (2017). Molecular mechanisms underlying protective effects of quercetin against mitochondrial dysfunction and progressive dopaminergic neurodegeneration in cell culture and MitoPark transgenic mouse models of Parkinson's Disease. J Neurochem 141, 766-782.

Baldereschi, M., Di Carlo, A., Rocca, W.A., Vanni, P., Maggi, S., Perissinotto, E., Grigoletto, F., Amaducci, L., and Inzitari, D. (2000). Parkinson's disease and parkinsonism in a longitudinal study: two-fold higher incidence in men. ILSA Working Group. Italian Longitudinal Study on Aging. Neurology 55, 1358-1363.

Ballard, P.A., Tetrud, J.W., and Langston, J.W. (1985). Permanent human parkinsonism due to 1-methyl-4-phenyl-1,2,3,6-tetrahydropyridine (MPTP): seven cases. Neurology 35, 949-956.

Banerjee, R., Starkov, A.A., Beal, M.F., and Thomas, B. (2009). Mitochondrial dysfunction in the limelight of Parkinson's disease pathogenesis. Biochim Biophys Acta 1792, 651-663.

Barroso, N., Campos, Y., Huertas, R., Esteban, J., Molina, J.A., Alonso, A., Gutierrez-Rivas, E., and Arenas, J. (1993). Respiratory chain enzyme activities in lymphocytes from untreated patients with Parkinson disease. Clinical chemistry 39, 667-669.

Beitz, J.M. (2014). Parkinson's disease: a review. Front Biosci (Schol Ed) 6, 65-74.

Bereczki, E., Bogstedt, A., Höglund, K., Tsitsi, P., Brodin, L., Ballard, C., Svenningsson, P., and Aarsland, D. (2017). Synaptic proteins in CSF relate to Parkinson's disease stage markers. NPJ Parkinsons Dis 3, 7.

Betarbet, R., and Greenamyre, J.T. (2004). Regulation of dopamine receptor and neuropeptide expression in the basal ganglia of monkeys treated with MPTP. Exp Neurol 189, 393-403.

Betarbet, R., Sherer, T.B., MacKenzie, G., Garcia-Osuna, M., Panov, A.V., and Greenamyre, J.T. (2000). Chronic systemic pesticide exposure reproduces features of Parkinson's disease. Nat Neurosci 3, 1301-1306.

Blesa, J., Phani, S., Jackson-Lewis, V., and Przedborski, S. (2012). Classic and new animal models of Parkinson's disease. J Biomed Biotechnol 2012, 845618.

Boehm, E., Zornoza, M., Jourdain, A.A., Delmiro Magdalena, A., García-Consuegra, I., Torres Merino, R., Orduña, A., Martín, M.A., Martinou, J.C., De la Fuente, M.A., and Simarro, M. (2016). Role of FAST Kinase Domains 3 (FASTKD3) in Post-transcriptional Regulation of Mitochondrial Gene Expression. J Biol Chem 291, 25877-25887.

Bonifati, V., Rizzu, P., Squitieri, F., Krieger, E., Vanacore, N., van Swieten, J.C., Brice, A., van Duijn, C.M., Oostra, B., Meco, G., and Heutink, P. (2003a). DJ-1(PARK7), a novel gene for autosomal recessive, early onset parkinsonism. Neurol Sci 24, 159-160.

Bonifati, V., Rizzu, P., van Baren, M.J., Schaap, O., Breedveld, G.J., Krieger, E., Dekker, M.C., Squitieri, F., Ibanez, P., Joosse, M., *et al.* (2003b). Mutations in the DJ-1 gene associated with autosomal recessive early-onset parkinsonism. Science 299, 256-259.

Bose, A., and Beal, M.F. (2016). Mitochondrial dysfunction in Parkinson's disease. J Neurochem 139 Suppl 1, 216-231.

Branch, S.Y., Chen, C., Sharma, R., Lechleiter, J.D., Li, S., and Beckstead, M.J. (2016). Dopaminergic Neurons Exhibit an Age-Dependent Decline in Electrophysiological Parameters in the MitoPark Mouse Model of Parkinson's Disease. J Neurosci 36, 4026-4037.

Branco, D.M., Arduino, D.M., Esteves, A.R., Silva, D.F., Cardoso, S.M., and Oliveira, C.R. (2010). Cross-talk between mitochondria and proteasome in Parkinson's disease pathogenesis. Frontiers in aging neuroscience 2, 17.

Cabeza-Arvelaiz, Y., and Schiestl, R.H. (2012). Transcriptome analysis of a rotenone model of parkinsonism reveals complex I-tied and -untied toxicity mechanisms common to neurodegenerative diseases. PLoS One 7, e44700.

Calvert, G.M., Rodriguez, L., Prado, J.B., and (CDC), C.f.D.C.a.P. (2015). Worker illness related to newly marketed pesticides--Douglas County, Washington, 2014. MMWR Morb Mortal Wkly Rep 64, 42-44.

Cantu, D., Schaack, J., and Patel, M. (2009). Oxidative inactivation of mitochondrial aconitase results in iron and H_2O_2-mediated neurotoxicity in rat primary mesencephalic cultures. PLoS One 4, e7095.

Caudle, W.M., Guillot, T.S., Lazo, C.R., and Miller, G.W. (2012). Industrial toxicants and Parkinson's disease. Neurotoxicology 33, 178-188.

Chang, L., Alicata, D., Ernst, T., and Volkow, N. (2007). Structural and metabolic brain changes in the striatum associated with methamphetamine abuse. Addiction 102 Suppl 1, 16-32.

Charli, A., Jin, H., Anantharam, V., Kanthasamy, A., and Kanthasamy, A.G. (2015). Alterations in mitochondrial dynamics induced by tebufenpyrad and pyridaben in a dopaminergic neuronal cell culture model. Neurotoxicology.

Charli, A., Jin, H., Anantharam, V., Kanthasamy, A., and Kanthasamy, A.G. (2016). Alterations in mitochondrial dynamics induced by tebufenpyrad and pyridaben in a dopaminergic neuronal cell culture model. Neurotoxicology 53, 302-313.

Chaudhuri, K.R., and Schapira, A.H. (2009). Non-motor symptoms of Parkinson's disease: dopaminergic pathophysiology and treatment. Lancet neurology 8, 464-474.

Choi, W.S., Palmiter, R.D., and Xia, Z. (2011). Loss of mitochondrial complex I activity potentiates dopamine neuron death induced by microtubule dysfunction in a Parkinson's disease model. J Cell Biol 192, 873-882.

Chou, A.P., Li, S., Fitzmaurice, A.G., and Bronstein, J.M. (2010). Mechanisms of rotenone-induced proteasome inhibition. Neurotoxicology 31, 367-372.

Chu, C.T., Bayır, H., and Kagan, V.E. (2014). LC3 binds externalized cardiolipin on injured mitochondria to signal mitophagy in neurons: implications for Parkinson disease. Autophagy 10, 376-378.

Chu, C.T., Ji, J., Dagda, R.K., Jiang, J.F., Tyurina, Y.Y., Kapralov, A.A., Tyurin, V.A., Yanamala, N., Shrivastava, I.H., Mohammadyani, D., *et al.* (2013).

Cardiolipin externalization to the outer mitochondrial membrane acts as an elimination signal for mitophagy in neuronal cells. Nat Cell Biol 15, 1197-1205.

Cong, L., Muir, E.R., Chen, C., Qian, Y., Liu, J., Biju, K.C., Clark, R.A., Li, S., and Duong, T.Q. (2016). Multimodal MRI Evaluation of the MitoPark Mouse Model of Parkinson's Disease. PLoS One 11, e0151884.

Cross, T., Griffiths, G., Deacon, E., Sallis, R., Gough, M., Watters, D., and Lord, J.M. (2000). PKC-delta is an apoptotic lamin kinase. Oncogene 19, 2331-2337.

Dauer, W., and Przedborski, S. (2003). Parkinson's disease: mechanisms and models. Neuron 39, 889-909.

Davey, G.P., and Clark, J.B. (1996). Threshold effects and control of oxidative phosphorylation in nonsynaptic rat brain mitochondria. J Neurochem 66, 1617-1624.

Dehay, B., Bové, J., Rodríguez-Muela, N., Perier, C., Recasens, A., Boya, P., and Vila, M. (2010). Pathogenic lysosomal depletion in Parkinson's disease. J Neurosci 30, 12535-12544.

Deng, H., Dodson, M.W., Huang, H., and Guo, M. (2008). The Parkinson's disease genes pink1 and parkin promote mitochondrial fission and/or inhibit fusion in Drosophila. Proceedings of the National Academy of Sciences of the United States of America 105, 14503-14508.

Deng, H., Le, W., Guo, Y., Hunter, C.B., Xie, W., and Jankovic, J. (2005). Genetic and clinical identification of Parkinson's disease patients with LRRK2 G2019S mutation. Annals of neurology 57, 933-934.

Dexter, D.T., Wells, F.R., Lees, A.J., Agid, F., Agid, Y., Jenner, P., and Marsden, C.D. (1989). Increased nigral iron content and alterations in other metal ions occurring in brain in Parkinson's disease. Journal of neurochemistry 52, 1830-1836.

Dick, F.D., De Palma, G., Ahmadi, A., Scott, N.W., Prescott, G.J., Bennett, J., Semple, S., Dick, S., Counsell, C., Mozzoni, P., *et al.* (2007). Environmental risk factors for Parkinson's disease and parkinsonism: the Geoparkinson study. Occup Environ Med 64, 666-672.

Dranka, B.P., Hill, B.G., and Darley-Usmar, V.M. (2010). Mitochondrial reserve capacity in endothelial cells: The impact of nitric oxide and reactive oxygen species. Free Radic Biol Med 48, 905-914.

Duchen, M.R. (2004). Mitochondria in health and disease: perspectives on a new mitochondrial biology. Mol Aspects Med 25, 365-451.

Díez-Guerra, F.J. (2010). Neurogranin, a link between calcium/calmodulin and protein kinase C signaling in synaptic plasticity. IUBMB Life 62, 597-606.

Ekstrand, M.I., Terzioglu, M., Galter, D., Zhu, S., Hofstetter, C., Lindqvist, E., Thams, S., Bergstrand, A., Hansson, F.S., Trifunovic, A.*, et al.* (2007). Progressive parkinsonism in mice with respiratory-chain-deficient dopamine neurons. Proc Natl Acad Sci U S A 104, 1325-1330.

Foroud, T., Pankratz, N., Martinez, M., and Consortium, P.G.-E. (2006). Chromosome 5 and Parkinson disease. Eur J Hum Genet 14, 1106-1110.

Fountaine, T.M., Venda, L.L., Warrick, N., Christian, H.C., Brundin, P., Channon, K.M., and Wade-Martins, R. (2008). The effect of alpha-synuclein knockdown on MPP+ toxicity in models of human neurons. Eur J Neurosci 28, 2459-2473.

Fountaine, T.M., and Wade-Martins, R. (2007). RNA interference-mediated knockdown of alpha-synuclein protects human dopaminergic neuroblastoma cells from MPP(+) toxicity and reduces dopamine transport. J Neurosci Res 85, 351-363.

Gandhi, S., and Abramov, A.Y. (2012). Mechanism of oxidative stress in neurodegeneration. Oxid Med Cell Longev 2012, 428010.

Gao, H., Yang, W., Qi, Z., Lu, L., Duan, C., Zhao, C., and Yang, H. (2012). DJ-1 protects dopaminergic neurons against rotenone-induced apoptosis by enhancing ERK-dependent mitophagy. J Mol Biol 423, 232-248.

Gendelman, H.E., Anantharam, V., Bronich, T., Ghaisas, S., Jin, H., Kanthasamy, A.G., Liu, X., McMillan, J., Mosley, R.L., Narasimhan, B., and Mallapragada, S.K. (2015). Nanoneuromedicines for degenerative, inflammatory, and infectious nervous system diseases. Nanomedicine 11, 751-767.

Ghosh, A., Chandran, K., Kalivendi, S.V., Joseph, J., Antholine, W.E., Hillard, C.J., Kanthasamy, A., and Kalyanaraman, B. (2010). Neuroprotection by a mitochondria-targeted drug in a Parkinson's disease model. Free Radic Biol Med 49, 1674-1684.

Gispert, S., Kurz, A., Brehm, N., Rau, K., Walter, M., Riess, O., and Auburger, G. (2015). Complexin-1 and Foxp1 Expression Changes Are Novel Brain Effects of Alpha-Synuclein Pathology. Mol Neurobiol 52, 57-63.

Gollamudi, S., Johri, A., Calingasan, N.Y., Yang, L., Elemento, O., and Beal, M.F. (2012). Concordant signaling pathways produced by pesticide exposure in mice correspond to pathways identified in human Parkinson's disease. PLoS One 7, e36191.

Gong, X., Wang, H., Ye, Y., Shu, Y., Deng, Y., He, X., Lu, G., and Zhang, S. (2016). miR-124 regulates cell apoptosis and autophagy in dopaminergic neurons and protects them by regulating AMPK/mTOR pathway in Parkinson's disease. Am J Transl Res 8, 2127-2137.

Gordon, R., Anantharam, V., Kanthasamy, A.G., and Kanthasamy, A. (2012). Proteolytic activation of proapoptotic kinase protein kinase Cδ by tumor necrosis factor α death receptor signaling in dopaminergic neurons during neuroinflammation. J Neuroinflammation 9, 82.

Gordon, R., Neal, M.L., Luo, J., Langley, M.R., Harischandra, D.S., Panicker, N., Charli, A., Jin, H., Anantharam, V., Woodruff, T.M.*, et al.* (2016). Prokineticin-2 upregulation during neuronal injury mediates a compensatory protective response against dopaminergic neuronal degeneration. Nat Commun 7, 12932.

Goulet, M., and Madras, B.K. (2000). D(1) dopamine receptor agonists are more effective in alleviating advanced than mild parkinsonism in 1-methyl-4-phenyl-1,2,3, 6-tetrahydropyridine-treated monkeys. J Pharmacol Exp Ther 292, 714-724.

Gourie-Devi, M., Ramu, M.G., and Venkataram, B.S. (1991). Treatment of Parkinson's disease in 'Ayurveda' (ancient Indian system of medicine): discussion paper. J R Soc Med 84, 491-492.

Grandy, D.K., Litt, M., Allen, L., Bunzow, J.R., Marchionni, M., Makam, H., Reed, L., Magenis, R.E., and Civelli, O. (1989). The human dopamine D2 receptor gene is located on chromosome 11 at q22-q23 and identifies a TaqI RFLP. Am J Hum Genet 45, 778-785.

Grandy, D.K., Zhou, Q.Y., Allen, L., Litt, R., Magenis, R.E., Civelli, O., and Litt, M. (1990). A human D1 dopamine receptor gene is located on chromosome 5 at q35.1 and identifies an EcoRI RFLP. Am J Hum Genet 47, 828-834.

Greenamyre, J.T., Cannon, J.R., Drolet, R., and Mastroberardino, P.G. (2010). Lessons from the rotenone model of Parkinson's disease. Trends in pharmacological sciences 31, 141-142; author reply 142-143.

Greenamyre, J.T., Sherer, T.B., Betarbet, R., and Panov, A.V. (2001). Complex I and Parkinson's disease. IUBMB Life 52, 135-141.

Haas, R.H., Nasirian, F., Nakano, K., Ward, D., Pay, M., Hill, R., and Shults, C.W. (1995). Low platelet mitochondrial complex I and complex II/III activity in early untreated Parkinson's disease. Annals of neurology 37, 714-722.

Halliwell, B. (2006). Oxidative stress and neurodegeneration: where are we now? J Neurochem 97, 1634-1658.

Harischandra, D.S., Kondru, N., Martin, D.P., Kanthasamy, A., Jin, H., Anantharam, V., and Kanthasamy, A.G. (2014). Role of proteolytic activation of protein kinase Cδ in the pathogenesis of prion disease. Prion 8, 143-153.

Hastings, T.G. (2009). The role of dopamine oxidation in mitochondrial dysfunction: implications for Parkinson's disease. Journal of bioenergetics and biomembranes 41, 469-472.

Hatano, Y., Li, Y., Sato, K., Asakawa, S., Yamamura, Y., Tomiyama, H., Yoshino, H., Asahina, M., Kobayashi, S., Hassin-Baer, S.*, et al.* (2004). Novel PINK1 mutations in early-onset parkinsonism. Ann Neurol 56, 424-427.

Hatcher, J.M., Richardson, J.R., Guillot, T.S., McCormack, A.L., Di Monte, D.A., Jones, D.P., Pennell, K.D., and Miller, G.W. (2007). Dieldrin exposure induces oxidative damage in the mouse nigrostriatal dopamine system. Exp Neurol 204, 619-630.

Hattori, N., Kitada, T., Matsumine, H., Asakawa, S., Yamamura, Y., Yoshino, H., Kobayashi, T., Yokochi, M., Wang, M., Yoritaka, A.*, et al.* (1998). Molecular genetic analysis of a novel Parkin gene in Japanese families with autosomal recessive juvenile parkinsonism: evidence for variable homozygous deletions in the Parkin gene in affected individuals. Ann Neurol 44, 935-941.

Hernán, M.A., Takkouche, B., Caamaño-Isorna, F., and Gestal-Otero, J.J. (2002). A meta-analysis of coffee drinking, cigarette smoking, and the risk of Parkinson's disease. Ann Neurol 52, 276-284.

Higuchi, S., Muramatsu, T., Arai, H., Hayashida, M., Sasaki, H., and Trojanowski, J.Q. (1995). Polymorphisms of dopamine receptor and transporter genes and Parkinson's disease. J Neural Transm Park Dis Dement Sect 10, 107-113.

Hisahara, S., and Shimohama, S. (2011). Dopamine receptors and Parkinson's disease. Int J Med Chem 2011, 403039.

Hoglinger, G.U., Carrard, G., Michel, P.P., Medja, F., Lombes, A., Ruberg, M., Friguet, B., and Hirsch, E.C. (2003). Dysfunction of mitochondrial complex I and the proteasome: interactions between two biochemical deficits in a cellular model of Parkinson's disease. Journal of neurochemistry 86, 1297-1307.

Hu, K., Carroll, J., Rickman, C., and Davletov, B. (2002). Action of complexin on SNARE complex. J Biol Chem 277, 41652-41656.

Hulihan, M.M., Ishihara-Paul, L., Kachergus, J., Warren, L., Amouri, R., Elango, R., Prinjha, R.K., Upmanyu, R., Kefi, M., Zouari, M.*, et al.* (2008). LRRK2 Gly2019Ser penetrance in Arab-Berber patients from Tunisia: a case-control genetic study. Lancet neurology 7, 591-594.

Jenner, P. (2003). Oxidative stress in Parkinson's disease. Annals of neurology 53 Suppl 3, S26-36; discussion S36-28.

Jin, H., Kanthasamy, A., Anantharam, V., Rana, A., and Kanthasamy, A.G. (2011a). Transcriptional regulation of pro-apoptotic protein kinase Cdelta: implications for oxidative stress-induced neuronal cell death. J Biol Chem 286, 19840-19859.

Jin, H., Kanthasamy, A., Ghosh, A., Yang, Y., Anantharam, V., and Kanthasamy, A.G. (2011b). α-Synuclein negatively regulates protein kinase Cδ expression to

suppress apoptosis in dopaminergic neurons by reducing p300 histone acetyltransferase activity. J Neurosci 31, 2035-2051.

Jin, H., Kanthasamy, A., Harischandra, D.S., Anantharam, V., and Rana, A. (2015). Targeted toxicants to dopaminergic neuronal cell death. Methods Mol Biol 1254, 239-252.

Jin, H., Kanthasamy, A., Harischandra, D.S., Kondru, N., Ghosh, A., Panicker, N., Anantharam, V., Rana, A., and Kanthasamy, A.G. (2014). Histone Hyperacetylation Upregulates PKCδ in Dopaminergic Neurons to Induce Cell Death: Relevance to Epigenetic Mechanisms of Neurodegeneration in Parkinson's Disease. J Biol Chem.

Johnson, M.E., and Bobrovskaya, L. (2015). An update on the rotenone models of Parkinson's disease: their ability to reproduce the features of clinical disease and model gene-environment interactions. Neurotoxicology 46, 101-116.

Kalia, L.V., and Lang, A.E. (2015). Parkinson's disease. Lancet 386, 896-912.

Kanthasamy, A.G., Kanthasamy, A., Matsumoto, R.R., Vu, T.Q., and Truong, D.D. (1997). Neuroprotective effects of the strychnine-insensitive glycine site NMDA antagonist (R)-HA-966 in an experimental model of Parkinson's disease. Brain Res 759, 1-8.

Kanthasamy, A.G., Kitazawa, M., Kanthasamy, A., and Anantharam, V. (2005). Dieldrin-induced neurotoxicity: relevance to Parkinson's disease pathogenesis. Neurotoxicology 26, 701-719.

Kanthasamy, A.G., Kitazawa, M., Yang, Y., Anantharam, V., and Kanthasamy, A. (2008). Environmental neurotoxin dieldrin induces apoptosis via caspase-3-dependent proteolytic activation of protein kinase C delta (PKCdelta): Implications for neurodegeneration in Parkinson's disease. Mol Brain 1, 12.

Kaul, S., Kanthasamy, A., Kitazawa, M., Anantharam, V., and Kanthasamy, A.G. (2003). Caspase-3 dependent proteolytic activation of protein kinase C delta mediates and regulates 1-methyl-4-phenylpyridinium (MPP+)-induced apoptotic cell death in dopaminergic cells: relevance to oxidative stress in dopaminergic degeneration. Eur J Neurosci 18, 1387-1401.

Kitazawa, M., Anantharam, V., and Kanthasamy, A.G. (2001). Dieldrin-induced oxidative stress and neurochemical changes contribute to apoptopic cell death in dopaminergic cells. Free Radic Biol Med 31, 1473-1485.

Klein, C., and Westenberger, A. (2012). Genetics of Parkinson's disease. Cold Spring Harb Perspect Med 2, a008888.

Klionsky, D.J., Abdelmohsen, K., Abe, A., Abedin, M.J., Abeliovich, H., Acevedo Arozena, A., Adachi, H., Adams, C.M., Adams, P.D., Adeli, K., *et al.* (2016).

Guidelines for the use and interpretation of assays for monitoring autophagy (3rd edition). Autophagy 12, 1-222.

Koob, A.O., Shaked, G.M., Bender, A., Bisquertt, A., Rockenstein, E., and Masliah, E. (2014). Neurogranin binds α-synuclein in the human superior temporal cortex and interaction is decreased in Parkinson's disease. Brain Res 1591, 102-110.

Kowall, N.W., Hantraye, P., Brouillet, E., Beal, M.F., McKee, A.C., and Ferrante, R.J. (2000). MPTP induces alpha-synuclein aggregation in the substantia nigra of baboons. Neuroreport 11, 211-213.

Krishnakumar, S.S., Radoff, D.T., Kümmel, D., Giraudo, C.G., Li, F., Khandan, L., Baguley, S.W., Coleman, J., Reinisch, K.M., Pincet, F., and Rothman, J.E. (2011). A conformational switch in complexin is required for synaptotagmin to trigger synaptic fusion. Nat Struct Mol Biol 18, 934-940.

Kruger, R., Kuhn, W., Muller, T., Woitalla, D., Graeber, M., Kosel, S., Przuntek, H., Epplen, J.T., Schols, L., and Riess, O. (1998). Ala30Pro mutation in the gene encoding alpha-synuclein in Parkinson's disease. Nature genetics 18, 106-108.

Lahut, S., Gispert, S., Ömür, Ö., Depboylu, C., Seidel, K., Domínguez-Bautista, J.A., Brehm, N., Tireli, H., Hackmann, K., Pirkevi, C., *et al.* (2017). Blood RNA biomarkers in prodromal PARK4 and rapid eye movement sleep behavior disorder show role of complexin 1 loss for risk of Parkinson's disease. Dis Model Mech 10, 619-631.

Langley, M., Ghosh, A., Charli, A., Sarkar, S., Ay, M., Luo, J., Zielonka, J., Brenza, T., Bennett, B., Jin, H., *et al.* (2017). Mito-Apocynin Prevents Mitochondrial Dysfunction, Microglial Activation, Oxidative Damage, and Progressive Neurodegeneration in MitoPark Transgenic Mice. Antioxid Redox Signal 27, 1048-1066.

Langston, J.W. (2017). The MPTP Story. J Parkinsons Dis 7, S11-S22.

Langston, J.W., Ballard, P., Tetrud, J.W., and Irwin, I. (1983). Chronic Parkinsonism in humans due to a product of meperidine-analog synthesis. Science 219, 979-980.

Langston, J.W., and Ballard, P.A. (1983). Parkinson's disease in a chemist working with 1-methyl-4-phenyl-1,2,5,6-tetrahydropyridine. N Engl J Med 309, 310.

Latchoumycandane, C., Anantharam, V., Jin, H., and Kanthasamy, A. (2011). Dopaminergic neurotoxicant 6-OHDA induces oxidative damage through proteolytic activation of PKCδ in cell culture and animal models of Parkinson's disease. Toxicol Appl Pharmacol 256, 314-323.

Lees, A.J., Hardy, J., and Revesz, T. (2009). Parkinson's disease. Lancet 373, 2055-2066.

Leroy, E., Boyer, R., Auburger, G., Leube, B., Ulm, G., Mezey, E., Harta, G., Brownstein, M.J., Jonnalagada, S., Chernova, T.*, et al.* (1998). The ubiquitin pathway in Parkinson's disease. Nature 395, 451-452.

Lewin, R. (1984). Trail of ironies to Parkinson's disease. Science 224, 1083-1085.

Lin, M.T., and Beal, M.F. (2006). Mitochondrial dysfunction and oxidative stress in neurodegenerative diseases. Nature 443, 787-795.

Lohmann, E., Periquet, M., Bonifati, V., Wood, N.W., De Michele, G., Bonnet, A.M., Fraix, V., Broussolle, E., Horstink, M.W., Vidailhet, M.*, et al.* (2003). How much phenotypic variation can be attributed to parkin genotype? Ann Neurol 54, 176-185.

Lotharius, J., and Brundin, P. (2002). Pathogenesis of Parkinson's disease: dopamine, vesicles and alpha-synuclein. Nat Rev Neurosci 3, 932-942.

Lümmen, P. (1998). Complex I inhibitors as insecticides and acaricides. Biochim Biophys Acta 1364, 287-296.

Malkus, K.A., Tsika, E., and Ischiropoulos, H. (2009). Oxidative modifications, mitochondrial dysfunction, and impaired protein degradation in Parkinson's disease: how neurons are lost in the Bermuda triangle. Molecular neurodegeneration 4, 24.

Mata, I.F., Wedemeyer, W.J., Farrer, M.J., Taylor, J.P., and Gallo, K.A. (2006). LRRK2 in Parkinson's disease: protein domains and functional insights. Trends Neurosci 29, 286-293.

Mattson, M.P. (2003). Methylation and acetylation in nervous system development and neurodegenerative disorders. Ageing Res Rev 2, 329-342.

Meredith, G.E., and Rademacher, D.J. (2011). MPTP mouse models of Parkinson's disease: an update. J Parkinsons Dis 1, 19-33.

Migliore, L., and Coppedè, F. (2009). Environmental-induced oxidative stress in neurodegenerative disorders and aging. Mutat Res 674, 73-84.

Miller, G.W. (2007). Paraquat: the red herring of Parkinson's disease research. Toxicol Sci 100, 1-2.

Miller, R.L., James-Kracke, M., Sun, G.Y., and Sun, A.Y. (2009). Oxidative and inflammatory pathways in Parkinson's disease. Neurochemical research 34, 55-65.

Mizuno, Y., Ohta, S., Tanaka, M., Takamiya, S., Suzuki, K., Sato, T., Oya, H., Ozawa, T., and Kagawa, Y. (1989). Deficiencies in complex I subunits of the respiratory chain in Parkinson's disease. Biochemical and biophysical research communications 163, 1450-1455.

Mounsey, R.B., and Teismann, P. (2010). Mitochondrial dysfunction in Parkinson's disease: pathogenesis and neuroprotection. Parkinson's disease 2011, 617472.

Murphy, D.D., Rueter, S.M., Trojanowski, J.Q., and Lee, V.M. (2000). Synucleins are developmentally expressed, and alpha-synuclein regulates the size of the presynaptic vesicular pool in primary hippocampal neurons. J Neurosci 20, 3214-3220.

Narendra, D., Tanaka, A., Suen, D.F., and Youle, R.J. (2008). Parkin is recruited selectively to impaired mitochondria and promotes their autophagy. The Journal of cell biology 183, 795-803.

Nicklas, W.J., Youngster, S.K., Kindt, M.V., and Heikkila, R.E. (1987). MPTP, MPP+ and mitochondrial function. Life Sci 40, 721-729.

Nixon, R.A. (2013). The role of autophagy in neurodegenerative disease. Nat Med 19, 983-997.

Onyango, I.G. (2008). Mitochondrial dysfunction and oxidative stress in Parkinson's disease. Neurochemical research 33, 589-597.

Orr-Urtreger, A., Shifrin, C., Rozovski, U., Rosner, S., Bercovich, D., Gurevich, T., Yagev-More, H., Bar-Shira, A., and Giladi, N. (2007). The LRRK2 G2019S mutation in Ashkenazi Jews with Parkinson disease: is there a gender effect? Neurology 69, 1595-1602.

Ovallath, S., and Deepa, P. (2013). The history of parkinsonism: descriptions in ancient Indian medical literature. Mov Disord 28, 566-568.

Pankratz, N., and Foroud, T. (2007). Genetics of Parkinson disease. Genet Med 9, 801-811.

Park, J., Kim, Y., and Chung, J. (2009). Mitochondrial dysfunction and Parkinson's disease genes: insights from Drosophila. Disease models & mechanisms 2, 336-340.

Parker, W.D., Boyson, S.J., and Parks, J.K. (1989). Abnormalities of the electron transport chain in idiopathic Parkinson's disease. Ann Neurol 26, 719-723.

Paul, J., Nandhu, M.S., Kuruvilla, K.P., and Paulose, C.S. (2010). Dopamine D_1 and D_2 receptor subtypes functional regulation in corpus striatum of unilateral rotenone lesioned Parkinson's rat model: effect of serotonin, dopamine and norepinephrine. Neurol Res 32, 918-924.

Perier, C., Bové, J., Vila, M., and Przedborski, S. (2003). The rotenone model of Parkinson's disease. Trends Neurosci 26, 345-346.

Petit, A., Kawarai, T., Paitel, E., Sanjo, N., Maj, M., Scheid, M., Chen, F., Gu, Y., Hasegawa, H., Salehi-Rad, S., *et al.* (2005). Wild-type PINK1 prevents basal

and induced neuronal apoptosis, a protective effect abrogated by Parkinson disease-related mutations. The Journal of biological chemistry 280, 34025-34032.

Polymeropoulos, M.H., Lavedan, C., Leroy, E., Ide, S.E., Dehejia, A., Dutra, A., Pike, B., Root, H., Rubenstein, J., Boyer, R., *et al.* (1997). Mutation in the alpha-synuclein gene identified in families with Parkinson's disease. Science (New York, NY 276, 2045-2047.

Priyadarshi, A., Khuder, S.A., Schaub, E.A., and Priyadarshi, S.S. (2001). Environmental risk factors and Parkinson's disease: a metaanalysis. Environ Res 86, 122-127.

Przedborski, S., and Ischiropoulos, H. (2005). Reactive oxygen and nitrogen species: weapons of neuronal destruction in models of Parkinson's disease. Antioxid Redox Signal 7, 685-693.

Przedborski, S., and Jackson-Lewis, V. (1998). Mechanisms of MPTP toxicity. Mov Disord 13 Suppl 1, 35-38.

Przedborski, S., Jackson-Lewis, V., Djaldetti, R., Liberatore, G., Vila, M., Vukosavic, S., and Almer, G. (2000). The parkinsonian toxin MPTP: action and mechanism. Restor Neurol Neurosci 16, 135-142.

Przedborski, S., and Vila, M. (2003). The 1-methyl-4-phenyl-1,2,3,6-tetrahydropyridine mouse model: a tool to explore the pathogenesis of Parkinson's disease. Ann N Y Acad Sci 991, 189-198.

Reim, K., Mansour, M., Varoqueaux, F., McMahon, H.T., Südhof, T.C., Brose, N., and Rosenmund, C. (2001). Complexins regulate a late step in Ca2+-dependent neurotransmitter release. Cell 104, 71-81.

Richardson, J.R., Caudle, W.M., Wang, M., Dean, E.D., Pennell, K.D., and Miller, G.W. (2006). Developmental exposure to the pesticide dieldrin alters the dopamine system and increases neurotoxicity in an animal model of Parkinson's disease. FASEB J 20, 1695-1697.

Richardson, J.R., Quan, Y., Sherer, T.B., Greenamyre, J.T., and Miller, G.W. (2005). Paraquat neurotoxicity is distinct from that of MPTP and rotenone. Toxicol Sci 88, 193-201.

Rothfuss, O., Fischer, H., Hasegawa, T., Maisel, M., Leitner, P., Miesel, F., Sharma, M., Bornemann, A., Berg, D., Gasser, T., and Patenge, N. (2009). Parkin protects mitochondrial genome integrity and supports mitochondrial DNA repair. Human molecular genetics 18, 3832-3850.

Saminathan, H., Asaithambi, A., Anantharam, V., Kanthasamy, A.G., and Kanthasamy, A. (2011). Environmental neurotoxic pesticide dieldrin activates a

non receptor tyrosine kinase to promote PKCδ-mediated dopaminergic apoptosis in a dopaminergic neuronal cell model. Neurotoxicology 32, 567-577.

Schapira, A.H. (2007). Mitochondrial dysfunction in Parkinson's disease. Cell Death Differ 14, 1261-1266.

Schapira, A.H., Cooper, J.M., Dexter, D., Clark, J.B., Jenner, P., and Marsden, C.D. (1990a). Mitochondrial complex I deficiency in Parkinson's disease. J Neurochem 54, 823-827.

Schapira, A.H., Cooper, J.M., Dexter, D., Jenner, P., Clark, J.B., and Marsden, C.D. (1989). Mitochondrial complex I deficiency in Parkinson's disease. Lancet 1, 1269.

Schapira, A.H., Mann, V.M., Cooper, J.M., Dexter, D., Daniel, S.E., Jenner, P., Clark, J.B., and Marsden, C.D. (1990b). Anatomic and disease specificity of NADH CoQ1 reductase (complex I) deficiency in Parkinson's disease. J Neurochem 55, 2142-2145.

Schmidt, N., and Ferger, B. (2001). Neurochemical findings in the MPTP model of Parkinson's disease. J Neural Transm 108, 1263-1282.

Schmutz, J., Martin, J., Terry, A., Couronne, O., Grimwood, J., Lowry, S., Gordon, L.A., Scott, D., Xie, G., Huang, W.*, et al.* (2004). The DNA sequence and comparative analysis of human chromosome 5. Nature 431, 268-274.

Schuler, F., Yano, T., Di Bernardo, S., Yagi, T., Yankovskaya, V., Singer, T.P., and Casida, J.E. (1999). NADH-quinone oxidoreductase: PSST subunit couples electron transfer from iron-sulfur cluster N2 to quinone. Proc Natl Acad Sci U S A 96, 4149-4153.

Selnes, P., Stav, A.L., Johansen, K.K., Bjørnerud, A., Coello, C., Auning, E., Kalheim, L., Almdahl, I.S., Hessen, E., Zetterberg, H.*, et al.* (2017). Impaired synaptic function is linked to cognition in Parkinson's disease. Ann Clin Transl Neurol 4, 700-713.

Shamoto-Nagai, M., Maruyama, W., Kato, Y., Isobe, K., Tanaka, M., Naoi, M., and Osawa, T. (2003). An inhibitor of mitochondrial complex I, rotenone, inactivates proteasome by oxidative modification and induces aggregation of oxidized proteins in SH-SY5Y cells. Journal of neuroscience research 74, 589-597.

Sherer, T.B., Betarbet, R., Testa, C.M., Seo, B.B., Richardson, J.R., Kim, J.H., Miller, G.W., Yagi, T., Matsuno-Yagi, A., and Greenamyre, J.T. (2003). Mechanism of toxicity in rotenone models of Parkinson's disease. J Neurosci 23, 10756-10764.

Sherer, T.B., Richardson, J.R., Testa, C.M., Seo, B.B., Panov, A.V., Yagi, T., Matsuno-Yagi, A., Miller, G.W., and Greenamyre, J.T. (2007). Mechanism of

toxicity of pesticides acting at complex I: relevance to environmental etiologies of Parkinson's disease. Journal of neurochemistry 100, 1469-1479.

Shimura, H., Hattori, N., Kubo, S., Mizuno, Y., Asakawa, S., Minoshima, S., Shimizu, N., Iwai, K., Chiba, T., Tanaka, K., and Suzuki, T. (2000). Familial Parkinson disease gene product, parkin, is a ubiquitin-protein ligase. Nature genetics 25, 302-305.

Shulman, J.M., De Jager, P.L., and Feany, M.B. (2011). Parkinson's disease: genetics and pathogenesis. Annual review of pathology 6, 193-222.

Silva, B.A., Einarsdóttir, O., Fink, A.L., and Uversky, V.N. (2013). Biophysical Characterization of α-Synuclein and Rotenone Interaction. Biomolecules 3, 703-732.

Simarro, M., Gimenez-Cassina, A., Kedersha, N., Lazaro, J.B., Adelmant, G.O., Marto, J.A., Rhee, K., Tisdale, S., Danial, N., Benarafa, C., *et al.* (2010). Fast kinase domain-containing protein 3 is a mitochondrial protein essential for cellular respiration. Biochem Biophys Res Commun 401, 440-446.

Smeyne, R.J., and Jackson-Lewis, V. (2005). The MPTP model of Parkinson's disease. Brain Res Mol Brain Res 134, 57-66.

Smith, W.W., Pei, Z., Jiang, H., Moore, D.J., Liang, Y., West, A.B., Dawson, V.L., Dawson, T.M., and Ross, C.A. (2005). Leucine-rich repeat kinase 2 (LRRK2) interacts with parkin, and mutant LRRK2 induces neuronal degeneration. Proc Natl Acad Sci U S A 102, 18676-18681.

Song, C., Kanthasamy, A., Anantharam, V., Sun, F., and Kanthasamy, A.G. (2010). Environmental neurotoxic pesticide increases histone acetylation to promote apoptosis in dopaminergic neuronal cells: relevance to epigenetic mechanisms of neurodegeneration. Mol Pharmacol 77, 621-632.

Song, C., Kanthasamy, A., Jin, H., Anantharam, V., and Kanthasamy, A.G. (2011). Paraquat induces epigenetic changes by promoting histone acetylation in cell culture models of dopaminergic degeneration. Neurotoxicology 32, 586-595.

Sonia Angeline, M., Chaterjee, P., Anand, K., Ambasta, R.K., and Kumar, P. (2012). Rotenone-induced parkinsonism elicits behavioral impairments and differential expression of parkin, heat shock proteins and caspases in the rat. Neuroscience 220, 291-301.

Spivey, A. (2011). Rotenone and paraquat linked to Parkinson's disease: human exposure study supports years of animal studies. Environmental health perspectives 119, A259.

Stern, Y., Tetrud, J.W., Martin, W.R., Kutner, S.J., and Langston, J.W. (1990). Cognitive change following MPTP exposure. Neurology 40, 261-264.

Tanner, C.M. (1992). Epidemiology of Parkinson's disease. Neurol Clin 10, 317-329.

Tanner, C.M., Kamel, F., Ross, G.W., Hoppin, J.A., Goldman, S.M., Korell, M., Marras, C., Bhudhikanok, G.S., Kasten, M., Chade, A.R.*, et al.* (2011). Rotenone, paraquat, and Parkinson's disease. Environmental health perspectives 119, 866-872.

Taylor, T.D., Noguchi, H., Totoki, Y., Toyoda, A., Kuroki, Y., Dewar, K., Lloyd, C., Itoh, T., Takeda, T., Kim, D.W.*, et al.* (2006). Human chromosome 11 DNA sequence and analysis including novel gene identification. Nature 440, 497-500.

Testa, C.M., Sherer, T.B., and Greenamyre, J.T. (2005). Rotenone induces oxidative stress and dopaminergic neuron damage in organotypic substantia nigra cultures. Brain Res Mol Brain Res 134, 109-118.

Thomas, B., and Beal, M.F. (2007). Parkinson's disease. Human molecular genetics 16 Spec No. 2, R183-194.

Tsang, A.H., and Chung, K.K. (2009). Oxidative and nitrosative stress in Parkinson's disease. Biochimica et biophysica acta 1792, 643-650.

Valente, E.M., Abou-Sleiman, P.M., Caputo, V., Muqit, M.M., Harvey, K., Gispert, S., Ali, Z., Del Turco, D., Bentivoglio, A.R., Healy, D.G.*, et al.* (2004). Hereditary early-onset Parkinson's disease caused by mutations in PINK1. Science 304, 1158-1160.

Van Den Eeden, S.K., Tanner, C.M., Bernstein, A.L., Fross, R.D., Leimpeter, A., Bloch, D.A., and Nelson, L.M. (2003). Incidence of Parkinson's disease: variation by age, gender, and race/ethnicity. American journal of epidemiology 157, 1015-1022.

Wang, H., Ye, Y., Zhu, Z., Mo, L., Lin, C., Wang, Q., Gong, X., He, X., Lu, G., Lu, F., and Zhang, S. (2016). MiR-124 Regulates Apoptosis and Autophagy Process in MPTP Model of Parkinson's Disease by Targeting to Bim. Brain Pathol 26, 167-176.

Werner, C.J., Heyny-von Haussen, R., Mall, G., and Wolf, S. (2008). Proteome analysis of human substantia nigra in Parkinson's disease. Proteome Sci 6, 8.

West, A.B., Moore, D.J., Biskup, S., Bugayenko, A., Smith, W.W., Ross, C.A., Dawson, V.L., and Dawson, T.M. (2005). Parkinson's disease-associated mutations in leucine-rich repeat kinase 2 augment kinase activity. Proc Natl Acad Sci U S A 102, 16842-16847.

Winklhofer, K.F., and Haass, C. (2010). Mitochondrial dysfunction in Parkinson's disease. Biochim Biophys Acta 1802, 29-44.

Winterbourn, C.C. (2008). Reconciling the chemistry and biology of reactive oxygen species. Nature chemical biology 4, 278-286.

Wooten, G.F., Currie, L.J., Bovbjerg, V.E., Lee, J.K., and Patrie, J. (2004). Are men at greater risk for Parkinson's disease than women? Journal of neurology, neurosurgery, and psychiatry 75, 637-639.

Youle, R.J., and Narendra, D.P. (2011). Mechanisms of mitophagy. Nature reviews 12, 9-14.

Yuan, Y.H., Yan, W.F., Sun, J.D., Huang, J.Y., Mu, Z., and Chen, N.H. (2015). The molecular mechanism of rotenone-induced α-synuclein aggregation: emphasizing the role of the calcium/GSK3β pathway. Toxicol Lett 233, 163-171.

Zarranz, J.J., Alegre, J., Gomez-Esteban, J.C., Lezcano, E., Ros, R., Ampuero, I., Vidal, L., Hoenicka, J., Rodriguez, O., Atares, B., *et al.* (2004). The new mutation, E46K, of alpha-synuclein causes Parkinson and Lewy body dementia. Annals of neurology 55, 164-173.

Zhang, T., Hong, J., Di, T., and Chen, L. (2016). MPTP Impairs Dopamine D1 Receptor-Mediated Survival of Newborn Neurons in Ventral Hippocampus to Cause Depressive-Like Behaviors in Adult Mice. Front Mol Neurosci 9, 101.

Zhang, Y., Dawson, V.L., and Dawson, T.M. (2000). Oxidative stress and genetics in the pathogenesis of Parkinson's disease. Neurobiology of disease 7, 240-250.